

The mystery of missing heritability: Genetic interactions create phantom heritability

Or Zuk^a, Eliana Hechter^a, Shamil R. Sunyaev^{a,b}, and Eric S. Lander^{a,1}

Broad Institute of MIT and Harvard, Cambridge, MA 02142; and ^bGenetics Division, Brigham and Women's Hospital, Harvard Medical School, Boston, MA 02115

Contributed by Eric S. Lander, December 5, 2011 (sent for review October 9, 2011)

Human genetics has been haunted by the mystery of “missing heritability” of common traits. Although studies have discovered >1,200 variants associated with common diseases and traits, these variants typically appear to explain only a minority of the heritability. The proportion of heritability explained by a set of variants is the ratio of (*i*) the heritability due to these variants (numerator), estimated directly from their observed effects, to (*ii*) the total heritability (denominator), inferred indirectly from population data. The prevailing view has been that the explanation for missing heritability lies in the numerator—that is, in as-yet undiscovered variants. While many variants surely remain to be found, we show here that a substantial portion of missing heritability could arise from overestimation of the denominator, creating “phantom heritability.” Specifically, (*i*) estimates of total heritability implicitly assume the trait involves no genetic interactions (epistasis) among loci; (*ii*) this assumption is not justified, because models with interactions are also consistent with observable data; and (*iii*) under such models, the total heritability may be much smaller and thus the proportion of heritability explained much larger. For example, 80% of the currently missing heritability for Crohn’s disease could be due to genetic interactions, if the disease involves interaction among three pathways. In short, missing heritability need not directly correspond to missing variants, because current estimates of total heritability may be significantly inflated by genetic interactions. Finally, we describe a method for estimating heritability from isolated populations that is not inflated by genetic interactions.

genome-wide association studies | statistical genetics

A continuing mystery in human genetics is the so-called missing heritability of common traits. Genome-wide association studies (GWAS) have led to the identification of >1,200 loci harboring genetic variants associated with >165 common human diseases and traits, revealing previously unknown roles for scores of biological pathways (1–3). However, early GWAS were puzzling because they appeared to explain only a small proportion of the “heritability” of the traits. With larger GWAS, the proportion of heritability apparently explained has grown (to 20–30% in some well-studied cases and >50% in a few), but, for most traits, the majority of the heritability remains unexplained (1).

This is our first in a series of papers exploring the explanations for missing heritability. Geneticists define the proportion of (narrow-sense) heritability of a trait explained by a set of known genetic variants to be the ratio $\pi_{\text{explained}} = h^2_{\text{known}}/h^2_{\text{all}}$, where (*i*) the numerator h^2_{known} is the proportion of the phenotypic variance explained by the additive effects of known variants and (*ii*) the denominator h^2_{all} is the proportion of the phenotypic variance attributable to the additive effects of all variants, including those not yet discovered. The numerator can be calculated directly from the measured effects of the variants, but the denominator must be inferred indirectly from population data.

The prevailing view among human geneticists has been that the explanation for missing heritability lies in the numerator, that is, in additional variants remaining to be discovered. Much debate has focused on whether these additional variants are common alleles (frequency $\geq 1\%$) with moderate-to-small effects or rare alleles

(frequency <1%) with large effects (3–9). We will discuss the frequency spectrum of disease-related variants in our second paper in this series.

Here we explore the possibility that a significant portion of the missing heritability might not reflect missing variants at all. The basic idea is easy to state: Current studies use estimators of h^2_{all} that are not consistent (that is, converge to the wrong answer); they may seriously overestimate the denominator h^2_{all} and thus underestimate $\pi_{\text{explained}}$. As a result, even when all variants affecting the trait are discovered, $\pi_{\text{explained}}$ may fall far short of 100%. We refer to this gap as “phantom heritability.”

Quantitative geneticists have long known that genetic interactions can affect heritability calculations (10). However, human genetic studies of missing heritability have paid little attention to the potential impact of genetic interactions. A few authors have constructed mathematical examples (11, 12), but these abstract models have not been related to biologically plausible mechanisms, and the studies have not considered whether the presence of genetic interactions would be readily detected, thereby preventing geneticists from being fooled by phantom heritability. The prevailing view among human geneticists appears to be that interactions play at most a minor part in explaining missing heritability.

Here we show that simple and plausible models can give rise to substantial phantom heritability. Biological processes often depend on the rate-limiting value among multiple inputs, such as the levels of components of a molecular complex required in stoichiometric ratios, reactants required in a biochemical pathway, or proteins required for transcription of a gene. We thus introduce the limiting pathway (LP) model, in which a trait depends on the rate-limiting value of k inputs, each of which is a strictly additive trait that depends on a set of variants (that may be common or rare). When $k = 1$, the LP model is simply a standard additive trait. For $k > 1$, we show that $LP(k)$ traits can have substantial phantom heritability.

The potential magnitude of phantom heritability can be illustrated by considering Crohn’s disease, for which GWAS have so far identified 71 risk associated loci (13). Under the usual assumption that the disease arises from a strictly additive genetic architecture, these loci explain only 21.5% of the estimated heritability. However, if Crohn’s disease instead follows an $LP(3)$ model, the phantom heritability is 62.8%, thus genetic interactions could account for 80% of the currently missing heritability.

To avoid being fooled by phantom heritability, one might hope to be able to recognize when traits involve genetic interactions, for example, based on population data (such as phenotypic correlations among close relatives) or genetic data (such as pairwise tests

Author contributions: O.Z. and E.S.L. designed research; O.Z., E.H., S.R.S., and E.S.L. performed research; O.Z., E.H., S.R.S., and E.S.L. analyzed data; and O.Z. and E.S.L. wrote the paper.

The authors declare no conflict of interest.

Freely available online through the PNAS open access option.

¹To whom correspondence should be addressed. E-mail: lander@broadinstitute.org.

This article contains supporting information online at www.pnas.org/lookup/suppl/doi:10.1073/pnas.1119675109/-DCSupplemental.

of epistasis). We show, however, that this task may be difficult. For the case of Crohn's disease above, detecting the genetic interactions may require sample sizes in the range of 500,000.

In short, genetic interactions may greatly inflate the apparent heritability without being readily detectable by standard methods. Thus, current estimates of missing heritability are not meaningful, because they ignore genetic interactions.

Finally, we present a method to estimate h^2_{all} that is consistent not only for additive traits but for any genetic architecture. The method involves the study of isolated populations. It may provide a path forward for accurately measuring explained and missing heritability.

Extensive mathematical details and extensions are provided in *SI Appendix*. A Matlab software package used for the mathematical calculations is available at <http://www.broadinstitute.org/mpg/hc>.

Results

Quantitative and Disease Traits. Quantitative traits are assumed to depend on genotype G and environment E , according to a function $P = \Psi(G, E)$. Here, $G = (g_1, g_2, \dots, g_n)$ is the diploid genotype at n biallelic variant sites across the genome, g_i is the number of copies (0, 1, or 2) of a designated allele at the i th site, and f_i is the frequency of the designated allele. The variant sites are assumed to be in linkage equilibrium. The environment E may involve both a “shared” environment that is shared among pairs of relatives and a “unique” environment that is specific to each individual, which includes stochastic noise.

Disease traits are given by a binary function $\Delta(G, E)$ that is assumed to arise from a liability threshold model. Specifically, there is an underlying (and unobserved) quantitative trait $P = \Psi(G, E)$, called a “liability.” For a specified threshold τ , individuals are affected ($\Delta = 1$) if $\Psi(G, E) \leq \tau$ and unaffected ($\Delta = 0$) otherwise. (This condition is often equivalently defined as $\Delta = 1$ if $\Psi(G, E) \geq \tau$.)

For convenience, we assume throughout that P has been normalized to have mean 0 and variance 1. With $Var(P) = 1$, the amount of variance explained by a factor is equal to the proportion of variance explained.

Broad-Sense vs. Narrow-Sense Heritability. Heritability is measured in two ways: broad-sense heritability H^2 and narrow-sense heritability h^2 .

Broad-sense heritability H^2 measures the full contribution of genes. It is defined as $H^2 = V_G/Var(P)$, where V_G is the total variance due to genes. [Specifically, $V_G = Var(P) - Var(P|G)$, where $Var(P|G)$ is the phenotypic variance between genetically identical individuals.] H^2 is the relevant quantity for clinical risk assessment, because it measures our ultimate ability to predict phenotype from genotype.

By contrast, narrow-sense (or additive) heritability h^2 is meant to capture the “additive” contribution of genes to the trait: It is the maximum variance that can be explained by a linear combination of the allele counts, g_i . Although h^2 is a less intuitive concept, it is routinely used to measure progress toward explaining the genetic basis of a trait because one can readily calculate the contribution of individual loci to h^2 , as described below.

Explained, Missing, and Phantom Heritability. We next define “explained” and “missing” heritability, focusing on narrow-sense heritability h^2 . Let h^2_S (or h^2_{known}) denote the proportion of the phenotypic variance explained by a set S of known variants, and h^2_{all} ($= h^2$) denote the proportion of the phenotypic variance explained by all variants that affect the trait. For the variants in S , the proportion of “explained heritability” is $\pi_{explained} = h^2_{known}/h^2_{all}$ and “missing heritability” is $\pi_{missing} = 1 - \pi_{explained}$. When all trait-associated variants have been found, $\pi_{missing} = 0$.

Human geneticists typically use a “bottom-up” approach to estimate the numerator and a “top-down” approach to estimate the denominator.

Bottom-up. The numerator h^2_{known} is straightforward to estimate, based on the effects of the individual variants. The variance explained by the i th variant is $V_i = 2f_i(1-f_i)\beta_i^2$, where f_i is the frequency and β_i is the additive effect of the locus (defined as the regression coefficient of the phenotype P on the single-locus genotype g_i). Under linkage equilibrium, the variance explained by a set S of variants is the sum over the individual loci: $V_{known} = V_S = \sum_{i \in S} V_i$. Because $Var(P) = 1$, we have $h^2_{known} = V_{known}$ and $h^2_{all} = V_{all}$. We can thus estimate $h^2_{known} = \sum_i 2f_i(1-f_i)\beta_i^2$ from the allele frequencies and effect sizes estimated in a genome-wide association study.

Top-down. The problem comes in estimating the denominator h^2_{all} . Because not all variants are known, human geneticists must infer their total contributions indirectly, typically via a top-down quantity based on phenotypic correlations in a population. We refer to such quantities as “apparent heritability” and denote them by such symbols as h^2_{pop} .

Missing heritability is then estimated by assuming that $h^2_{all} = h^2_{pop}$ and obtaining an estimate of h^2_{pop} . The problem is that h^2_{all} and h^2_{pop} are not guaranteed to be equal unless the trait is strictly additive, that is, involves neither gene–gene (G–G) nor gene–environment (G–E) interactions. For traits with genetic interactions, h^2_{pop} may significantly exceed h^2_{all} . If so, even when all variants have been discovered, the estimate of $\pi_{missing}$ will not converge to zero with increasing sample size. Instead, it converges to $1 - (h^2_{all}/h^2_{pop})$, which we call the phantom heritability, $\pi_{phantom}$.

The term heritability and the symbol h^2 are often used in the literature to refer to the true heritability h^2_{all} and to several definitions of apparent heritability h^2_{pop} , despite the fact that these various quantities need not be equal (*SI Appendix*, section 1.5). We have introduced distinct terminology and notation to avoid confusion about these important differences.

Analogous definitions can be made for broad-sense heritability H^2 . In this case, it is easy to estimate the top-down quantity, but there is currently no practical way to estimate the bottom-up quantity (*SI Appendix*, section 12). As a result, human geneticists rarely attempt to estimate the proportion of the broad-sense heritability explained by a set of loci.

Assuming Additivity. We next describe the typical framework for analyzing human traits, noting why the equality $h^2_{all} = h^2_{pop}$ depends on the assumption of additivity. We focus on one measure of apparent heritability, $h^2_{pop}(ACE)$, which considers additive genetic, common environmental and unique environmental variance components, but discuss alternative measures in *SI Appendix*, section 1.3.

Quantitative traits. A commonly used definition for apparent heritability is $h^2_{pop}(ACE) = 2(r_{MZ} - r_{DZ})$, where r_{MZ} and r_{DZ} are the phenotypic correlations between monozygotic twins and dizygotic twins, respectively (14). (The measure is based on the ACE model of twin studies.) One can show that

$$h^2_{pop}(ACE) = h^2_{all} + W, \text{ with} \\ W = \left[\sum_{(i,j) \neq (1,0)} 2 \left(1 - 2^{-(i+2j)} \right) V_{A'D'} \right] \geq 0, \quad [1]$$

where $V_{A'D'}$ denotes the (nonnegative) variances due to all possible i th-order additive interactions and j th-order dominance interactions among loci (*SI Appendix*, section 1). The key point is that, if there are any genetic interactions, then $W > 0$, and $h^2_{pop}(ACE)$ overestimates h^2_{all} . Unfortunately, there has been no way to estimate W from population data. In most human genetic studies, the “solution” has been simply to make the (usually unstated) assumption that there is no genetic interaction, that is, that $W = 0$. Typically, the studies assume a strictly additive model. (Some studies allow dominance terms at each locus, but they invariably assume additivity across loci, that is, no genetic interactions.)

Assuming a strictly additive model, the genetic architecture takes the form

$$\Psi(G, E) = \left[\alpha + \sum_i \beta_i g_i \right] + \epsilon, \quad [2]$$

with the two terms each being roughly normally distributed with mean 0 and with Ψ being normalized to have variance 1. Under this model, the variance of the first term is the narrow-sense heritability h^2_{all} . The environmental noise ϵ consists of shared and nonshared environments, with a vector c_R denoting the proportion of the environmental variance $Var(\epsilon) = 1 - h^2_{all}$ that is shared between relatives of type R. (For example, c_{sib} is the proportion of environment shared among sibs.) We will refer to this additive model as $A(h^2, c_R)$.

The additive model has many elegant properties. If $\rho(R)$ denotes the phenotypic correlation between relatives of type R, then

$$\rho(R) = h^2 \gamma_R + (1 - h^2) c_R. \quad [3]$$

Here, γ_R is the genetic relatedness between relatives of type R ($\gamma_R = 1, 1/2, 1/4$, and $1/8$ for MZ twins, sibs, grandparent-grandchild, and first cousins). The phenotypic correlation is proportional to genetic relatedness under the additive model with no shared environmental variance.

Disease traits. Disease traits are traditionally assumed to follow a liability threshold model, where the unseen liability Ψ follows the additive model above and disease occurs if $\Psi \leq \tau$. We will refer to this additive disease model as $A_\Delta(h^2, c_R, \mu)$, where $\mu = Prob(\Psi \leq \tau)$ denotes the disease prevalence. The model parameters (h^2, c_R, μ) completely determine the epidemiologically observable quantities ($\mu, \lambda_{MZ}, \lambda_{sib}, \dots$), where μ is the disease prevalence and λ_R is the increased risk to relatives of type R (15).

To apply the model to a disease, one fits the model parameters based on observable quantities. (Geneticists often assume that $c_R = 0$, in which case the remaining two parameters can be fit based on μ and λ_{MZ} .) For genetic variants associated with the disease, one then uses the model to convert an observed increase in disease risk to an inferred additive effect on the liability scale. Heritability calculations are performed not on the observed disease status but on the unseen liability scale. One advantage of using the liability scale is that heritability calculations tend to be robust to uncertainty about disease prevalence. (See *SI Appendix*, section 2 for details, including the use of both λ_{MZ} and λ_{sib} to deal with shared environment.)

Genetic Interactions Create Phantom Heritability. What will happen if a geneticist analyzes a trait that involves genetic interactions under the erroneous assumption that it is additive? To explore this question, we introduce a simple and biologically plausible class of models.

Quantitative traits. Biological processes often depend on the rate-limiting value among multiple inputs, such as the levels of components of a molecular complex required in stoichiometric ratios, reactants required in a biochemical pathway, or proteins required for transcription of a gene. We thus define a limiting pathway model, in which a trait P depends on the rate-limiting input from $k \geq 1$ biological processes. For simplicity, we will assume that the inputs, $\Psi_1, \Psi_2, \dots, \Psi_k$, all follow the standard additive model in Eq. 2 above, each with exactly the same parameters, $h^2_{pathway}$, and c_R . Apart from the fact that the Ψ_i are roughly normal, we place no restrictions on the number or allele frequencies of the causal variants.

We define the trait $LP(k, h^2_{pathway}, c_R)$ to be the minimum value of the Ψ_i . For a single pathway ($k = 1$), the definition reduces to the simple additive model. What happens for $k > 1$?

Let us consider a specific example: $P^* = LP(4, 50\%, c_R)$, with $c_{sib} = 50\%$ (yielding shared environmental variance $V_c = 27\%$) and $c_R = 0$ for other relatives. Suppose that a geneticist analyzes P^* under the standard (but erroneous) assumption that it is

additive. Because we know the true genetic architecture (although the geneticist does not), we can calculate the exact value of all relevant parameters (*SI Appendix*, section 3). Because we are interested in asymptotic bias, we ignore sampling variation.

The geneticist would start by estimating the apparent heritability to be explained. The observed phenotypic correlation among twins is $(r_{MZ}, r_{DZ}) = (62.4\%, 35.4\%)$, yielding $h^2_{pop} = 2(r_{MZ} - r_{DZ}) = 54.0\%$. The geneticist would then conduct a genetic study, identify variants associated with the trait, estimate their effect sizes, estimate the heritability h^2_{known} explained by the variants, and compare it to the estimated value of h^2_{pop} . Assuming the sample is so large that all variants are identified (although the geneticist does not know this), h^2_{known} will be the true heritability, $h^2_{all} = 25.4\%$.

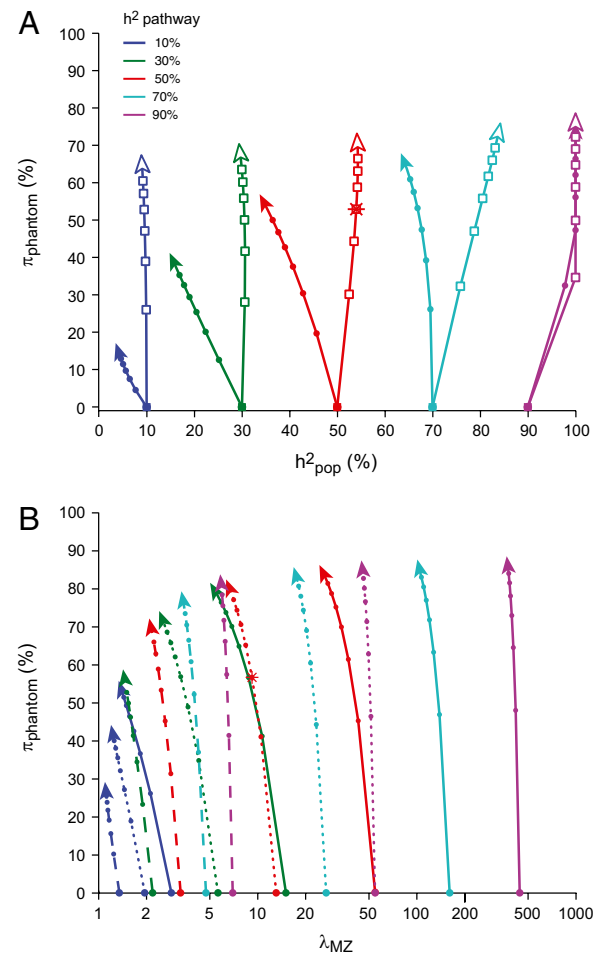


Fig. 1. Phantom heritability under the limiting pathway model. (A) Quantitative trait model $LP(k, h^2_{pathway}, c_R)$. For various parameters, curves show apparent heritability $h^2_{pop}(ACE)$ and phantom heritability $\pi_{phantom}$. Curves connect points with various values of k (1, 2, 3, 4, 5, 6, 7, 10, with tip of arrow at $k = 10$), and for specific values of $h^2_{pathway}$ (10, 30, 50, 70, and 90%, indicated by color of the curve) and c_R (0% filled circles and arrows, 50% open boxes and arrows). The red asterisk indicates example P^* referred to in the text. (The quantity h^2_{pop} can exceed 100%, as seen for some models with high heritability and for some real traits. In such cases, we set $h^2_{pop} = 100\%$.) Raw data are in *SI Appendix*, Table 6. (B) Disease model $LP_\Delta(k, h^2_{pathway}, 0\%, \mu)$. For various parameters, curves show value of λ_{MZ} and phantom heritability $\pi_{phantom}$. Values of k and $h^2_{pathway}$ are as in A. Values of prevalence μ are 0.1% (solid), 1% (dotted), and 10% (dashed). The red asterisk indicates example Δ^* referred to in the text. In both A and B, as k increases, the trait becomes more nonlinear; phantom heritability increases to 50% and beyond. Raw data are in *SI Appendix*, Table 7.

Even though all variants have been discovered, they will appear to explain only 47% ($=25.4/54.0$) of the apparent heritability, h^2_{pop} . The remaining 53% is phantom heritability, which will never be explained by additional variants. It is the result of analyzing the data under an erroneous model.

Similar results are obtained for a wide range of parameters. Fig. 1A shows results for $k = 1\text{--}10$, $h^2_{pathway} = 10\text{--}90\%$, and $c_R = 0$ or 50%. The phantom heritability grows steadily with k . A mathematical theorem (16) implies that $\pi_{phantom} \rightarrow 100\%$ as k grows (*SI Appendix, section 3.4*).

Disease traits. We can similarly define a limiting pathway model for disease traits by applying a threshold to the LP model for quantitative traits. Specifically, we define the disease trait $LP_\Delta(k, h^2_{pathway}, c_R, \mu)$ as occurring if and only if $LP(k, h^2_{pathway}, c_R) \leq \tau$, with μ denoting the disease prevalence. The case $k = 1$ again reduces to the additive model. What happens for $k > 1$?

Again, let us consider a specific case: $\Delta^* = LP_\Delta(3, 50\%, c_R, 1\%)$, with $c_R = 0\%$ for all relatives. Based on the observed relative risks to MZ and DZ twins, a geneticist would calculate that $h^2_{pop} = 49.0\%$. However, an infinitely large genetic mapping study would yield $h^2_{known} (=h^2_{all}) = 21.2\%$. Even though all variants had been identified, they would appear to explain only 43.2% ($=21.2/49.0$) of the apparent heritability h^2_{pop} . The remaining 56.8% is phantom heritability. Similar results are obtained for a wide range of parameters. Fig. 1B shows results for $k = 1\text{--}10$, $h^2_{pathway} = 10\text{--}90\%$, and $c = 0.1, 1$, and 10%.

Epistasis Is Common. The results show that mistakenly assuming that a trait is additive can seriously distort inferences about missing heritability. From a biological standpoint, there is no a priori reason to expect that traits should be additive. Biology is filled with nonlinearity: The saturation of enzymes with substrate concentration and receptors with ligand concentration yields sigmoid response curves; cooperative binding of proteins gives rise to sharp transitions; the outputs of pathways are constrained by rate-limiting inputs; and genetic networks exhibit bistable states.

Genetic studies in model organisms have long identified specific instances of interacting genes (17). Important examples include synthetic traits (e.g., 18), which occur only when multiple loci or pathways are all disrupted. With the advent of genome-wide mapping in controlled genetic backgrounds in model organisms, studies have begun to reveal that epistasis is pervasive. In the yeast *Saccharomyces cerevisiae*, Brem et al. (19) analyzed quantitative traits the levels of gene transcripts in segregants of a cross between two strains. For each transcript, they found the strongest quantitative trait locus (QTL) in the cross and then, conditional on the genotype at this locus, identified the strongest remaining QTL. In 67% of cases, these two QTLs demonstrated epistatic interactions. In bacteria, Khan et al. (20) and Chou et al. (21) have recently demonstrated clear epistasis among collections of five mutations that increase growth rate. In mouse and rat, Shao et al. (22) analyzed a panel of chromosome substitution strains, with each strain carrying a different chromosome from a donor strain on a common recipient genetic background. For dozens of quantitative traits, the sum of the effect attributable to the individual donor chromosomes far exceeds (median eightfold) the total effect of the donor genome, indicating strong epistasis. Although genetic interactions are hard to detect in humans (see below), several cases involving variants with large marginal effects have been recently reported in Hirschsprung's disease, ankylosing spondylitis, psoriasis, and type I diabetes (*SI Appendix, section 7.1*).

Several arguments are sometimes offered in support of the assumption of additivity (e.g., linearity of responses to selection). We discuss the flaws in such reasoning (*SI Appendix, section 11*).

Can We Detect Genetic Interactions by Comparisons Across Relatives?

Can a geneticist avoid being fooled by phantom heritability by detecting a priori that a trait involves genetic interactions, based

on the phenotypic correlations between close relatives? The task turns out to be difficult even if we restrict attention only to LP models.

Phenotypic distribution. The phenotypic distribution of a quantitative trait would not reveal the presence of genetic interactions. The distribution for $LP(k)$ traits with modest values of k (say, $k \leq 10$) is reasonably similar to the normal distribution in the additive model (*SI Appendix, Fig. 1*). Moreover, deviations from perfect normality are common in real traits and are typically resolved by applying a transformation to the distribution.

Sib correlations. Phenotypic correlations among sibs would not reveal that a trait involves genetic interactions. For quantitative traits, the correlations (r_{MZ}, r_{DZ}) for the LP models above are similar to those seen for real traits: They fit comfortably within the range of values recently reported by Hill et al. (23) for 86 traits (*SI Appendix, section 5.1*). For disease traits, the relative risks ($\lambda_{MZ}, \lambda_{sib}$) for various LP models similarly resemble those seen for real traits, for example, those reported for 15 actual diseases by Wray et al. (24) (*SI Appendix, section 5.2*).

Correlations among extended relatives. That sib correlations alone do not distinguish between additive and nonadditive LP models is not surprising: For either model, one can select parameters that largely fit the observed correlations. One might expand the analysis by considering additional relatives. For a trait with no shared environment, the phenotypic correlation between relatives should decrease linearly with genetic relatedness (γ_R) if the trait is additive (by Eq. 3), but should be concave up if the trait involves genetic interactions. In theory, one could test for genetic interactions by fitting different genetic models to the curve of phenotypic correlations among relatives. In practice, it is difficult to draw strong conclusions from such analysis. First, such tests essentially depend on fitting a handful of values (e.g., correlations for individuals with $\gamma_R = 1, 1/2, 1/4$, and $1/8$) with limited precision. Second, differences in the degree of shared environmental variance between relative types can substantially alter the shape of the curve (*SI Appendix, section 6*).

Examples: Crohn's disease and schizophrenia. The problem of discerning genetic architecture from a few parameters can be illustrated by considering alternative models for real diseases.

For Crohn's disease, current GWAS have identified 71 risk loci. Assuming the disease follows an additive model, these known loci explain $h^2_{known} = 10.8\%$ of the total phenotypic variance, or $\pi_{explained} = 21.5\%$ of the heritability (assuming $h^2_{all} = h^2_{pop} = 50\%$). Alternatively, one can define an $LP(3)$ model that is consistent with the prevalence and sib risks. Under this model, the phantom heritability is $\pi_{phantom} = 62.8\%$. Genetic interactions would account for 80% [$=62.8/(1 - 0.215)$] of the currently missing heritability. The known variants would account for $\pi_{explained} = 57.5\%$ [$=21.5/(1 - 0.628)$] of the true heritability $h^2_{all} = 18.6\%$ (*SI Appendix, section 6*).

For schizophrenia, Risch (15) presented recurrence risks for various relative types ($\gamma_R = 1, 1/2, 1/4$, and $1/8$). We fit an additive model and an $LP(2)$ model to the data (*SI Appendix, section 6*). Both models fit well, yet the former has no phantom heritability, whereas the latter has phantom heritability of 46%.

Can We Detect Genetic Interactions from Pairwise Epistasis? Even though it is difficult to detect genetic interactions a priori based on population data such as sib correlations, one might still hope to detect epistasis among variants a posteriori once they have been mapped. Indeed, geneticists have tested for pairwise epistasis between loci, but have found few significant signals. Should failure to detect pairwise epistasis allay our concerns about phantom heritability? Unfortunately, the answer is no.

The reason is that individual interaction effects are expected to be much smaller than linear effects, and the sample size required to detect an effect scales inversely with the square of the effect size. If n loci had equivalent effects, the sample size to

detect the n loci would thus scale with n^2 , whereas the sample size to detect their $\sim n^2$ interactions scales with n^4 .

Consider the $LP(3)$ disease model Δ^* discussed above, with phantom heritability of 56.8%. Suppose that we consider two variants with frequency 20% that contribute to different pathways and increase risk by 1.3-fold (which is a large effect relative to those typically seen in GWAS). The sample size required to detect the variants is $\sim 4,900$ (with 50% power and genome-wide significance level of $\alpha = 5 \times 10^{-8}$ in a genome-wide association study with an equal number of cases and controls), whereas the sample size required to detect their pairwise interaction is roughly 450,000 (at 50% power and an appropriate significance level to account for multiple hypothesis testing). A researcher who studied 100,000 samples would likely discover all of the loci but would find little evidence of epistatic interactions. The researcher might conclude that the genetic architecture is additive, although the phantom heritability is actually $>50\%$. In short, the failure to detect epistasis does not rule out the presence of genetic interactions sufficient to cause substantial phantom heritability. (We discuss other ways to potentially detect epistasis in *SI Appendix, section 7.5*.)

Consistent Top-Down Estimator of h^2_{all} . What we need is a top-down estimator h^2_{all} that is consistent not simply for additive traits but for any genetic architecture. Traditional approaches fail because they focus on phenotypic correlations between close relatives; this creates two problems: (i) Extensive allele sharing between close relatives makes it difficult to disentangle the effects of genetic interactions; and (ii) differences of shared environment between different relative types make it difficult to disentangle the effects of environment.

We can eliminate these problems by studying nearly unrelated individuals in a population. Specifically, one can (i) identify pairs of individuals whose probability of allele sharing at the causal loci differs slightly from the population average, and (ii) measure how their phenotypic similarity depends on their genotypic similarity.

This goal can be accomplished by studying recent genetically isolated populations (such as Iceland, Finland, the Hutterites, or the Amish), in which one can use dense genotyping to reliably detect large segments shared identical-by-descent (IBD) between individuals (*SI Appendix, section 8*). We have the following theorem.

Theorem 1. Consider a population in which one can detect large segments shared IBD between individuals. Given two individuals I_i and I_j , let $\kappa_{i,j} = \kappa(I_i, I_j)$ denote the proportion of their genomes shared in large IBD segments. Let κ_0 denote the average value of κ across the pairs in the population.

Given a trait, let $\rho(\kappa)$ denote the average phenotypic correlation between pairs of individuals who share proportion κ of their genomes in large IBD blocks. Regardless of the genetic architecture of the trait, the true heritability h^2_{all} equals $h^2_{slope(\kappa_0)} = (1 - \kappa_0)\rho'(\kappa_0)$, where $\rho'(\kappa_0)$ is the rate of change of phenotypic correlation around the average sharing level of large IBD segments. Accordingly, $\widehat{h^2_{slope(\kappa_0)}}$ provides a consistent top-down estimator for h^2_{all} .

The theorem applies to both quantitative traits and disease traits [with heritability measured on the disease (0,1) scale] with individuals sampled from the general population. The proof appears in *SI Appendix, section 8*, along with a version for individuals ascertained in a case-control study.

To apply this result in practice, one would (i) take a collection of individuals from the population; (ii) for each pair of individuals, calculate the product Q of the phenotype and the degree κ of IBD sharing; and (iii) estimate $\rho'(\kappa_0)$ as the regression coefficient of Q on κ , for pairs with κ in a neighborhood around κ_0 .

Fig. 2 illustrates the approach on simulated data for the quantitative trait P^* above, where $h^2_{all} = 25.4\%$ and $h^2_{pop} =$

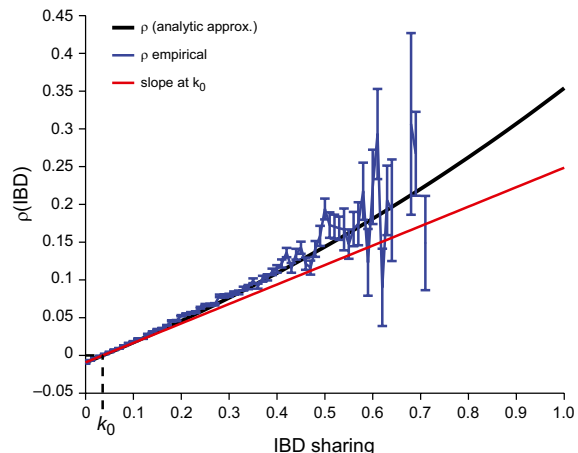


Fig. 2. Estimating additive heritability from the slope of phenotypic correlation around mean IBD sharing. We performed simulations of the estimator in theorem 1. Genotype and phenotype data were generated for samples of 1,000 individuals chosen from an isolated population (mean IBD sharing $\kappa_0 = 3.5\%$, SD 5.7%) and the limiting pathway trait P^* (described in text) with 1,000 causal loci (see *SI Appendix, section 9* for details); results were averaged over 100 simulations. For each pair of individuals, we computed the product Z_1Z_2 and the IBD sharing (*SI Appendix*). Blue error bars show mean and SD of expectation of Z_1Z_2 for pairs in each 1% bin of IBD sharing, estimated from all such pairs across all 100 simulations. The black curve shows an analytic approximation for the mean phenotypic similarity r_R (*SI Appendix, section 3.3, Eq. 3.12*). The red line shows a least-squares linear regression line fitted using all pairs with IBD sharing in the interval $[0, 2\kappa_0]$. The average estimated slope (multiplied by $1 - \kappa_0$) was 0.258 ± 0.082 ; as expected from theorem 1, this is very close to the true heritability $h^2_{all} = 0.254$ (and different from the apparent heritability, $h^2_{pop} = 0.54$).

54%. With simulated data for 1,000 individuals with IBD sharing similar to that seen in Qatar (25), we estimate $\widehat{h^2_{slope(\kappa_0)}} = 25.8 \pm 8.2\%$, which is very close to the correct value of $h^2_{all} = 25.4\%$.

It is instructive to compare our approach with two elegant methods recently introduced by Visscher and colleagues, which inspired our own work. Both methods involve regressing phenotypic correlation on genotypic similarity. The first (26) measures genotypic similarity in terms of IBD within sib pairs—essentially measuring $\rho'(1/2)$, in our terminology. It eliminates the effects of shared environment by studying a single type of relative, but is confounded by genetic interactions because it studies close relatives (*SI Appendix, section 10*). The second (27) measures genotypic similarity in terms of identity by state across an SNP catalog for pairs of individuals in a population. As the authors note, the approach is not confounded by genetic interactions, but does not yield a consistent estimator because its sensitivity to causal variants falls with allele frequency. Nonetheless, this method yields a valuable lower bound on h^2_{all} .

Discussion

The main points of this paper are that (i) current estimates of the proportion of heritability explained by known variants ($\pi_{explained}$) implicitly assume that traits involve no genetic interactions; (ii) this assumption is not justified, because many models with interactions are equally consistent with available data; and (iii) under some of these models, the true value of $\pi_{explained}$ may be much larger than current estimates. Accordingly, the widely held belief that missing heritability directly reflects the variance due to as-yet undiscovered variants is unjustified. Rather, missing heritability may be due in significant part to genetic interactions.

We focus here on a simple and biologically natural model, the limiting pathway model; it cannot readily be distinguished from an additive model based on population data or tests of pairwise

epistasis, yet entails substantial phantom heritability. Our focus on the LP model is not meant to imply that real traits necessarily follow this particular model; it simply provides an existence proof that erroneous assumptions may give rise to substantial missing heritability. We discuss more general multiple pathway models (*SI Appendix*, section 4.4), which also show substantial phantom heritability. (Beyond G–G interactions, we note that G–E interactions can produce additional phantom heritability.)

Importantly, we do not mean to propose that missing heritability is entirely, or even primarily, due to genetic interactions. On the contrary, many more causal variants are likely to exist, and to account for a significant part of the missing heritability. Discovery efforts should continue vigorously.

The case of Crohn's disease illustrates these points. The currently known loci can explain ~22%, ~58%, or more of the true heritability, depending on whether the disease follows an *LP*(1), *LP*(3), or other model. The available data cannot distinguish among the models. This spectacular degree of uncertainty undermines "inference by default," for example, the frequent conclusion that rare variants must largely cause a disease, because common variants explain "too little" of the heritability. [Notably, a recent study of Crohn's disease (28) reported that the rare variants explained 10- to 20-fold less of the heritability than the common variants at 56 disease-associated loci.]

Given the dependence of results on genetic architecture, authors reporting proportions of heritability explained or missing should state clearly that the calculations are made under the arbitrary assumption that the trait is additive.

In LP models, phantom heritability increases with the number of pathways. More generally, traits with greater biological complexity may have greater phantom heritability. Current studies are broadly consistent with such a notion: The apparent heritability explained for "simpler" traits such as levels of fetal hemoglobin is greater than for "more complex" traits such as body-mass index or age at menarche (*SI Appendix*, section 6.3). Such differences may reflect both the number of loci and the genetic interactions underlying the traits.

The fraction of the apparent heritability of human traits due to genetic interactions cannot be inferred from available data,

although the pervasiveness of epistasis in experimental organisms suggests that the true heritability h^2 of traits may be much lower than current estimates. (Lower values of h^2 do not mean that traits are "less genetic" in the popular use of the term, which refers to the total contribution of genes, H^2 . It simply means that additive effects comprise a smaller fraction of H^2 .)

We describe a potential solution to overcome the problem of genetic interactions: Theorem 1 provides a top-down method to measure additive heritability that is consistent regardless of the underlying genetic architecture. In principle, the approach can provide an accurate assessment of heritability, as well as allow detection of the presence of genetic interactions by comparing top-down estimates obtained from different methods. To assess its practical utility, it will be necessary to apply it to appropriate data from isolated populations.

Finally, notwithstanding our focus here, we believe that concerns about missing heritability should not distract from the fundamental goals of medical genetics. Human genetic studies to discover variants associated with common traits should primarily be regarded as the analog to mutant hunts in model organisms, with the primary purpose being to identify the underlying pathways and processes. The key focus should be to study the biological role of the variants discovered so far. The proportion of phenotypic variance explained by a variant in the human population is a notoriously poor predictor of the importance of the gene for biology or medicine. [A classic example is the gene encoding HMGCoA reductase, which explains only a tiny fraction of the variance in cholesterol levels but is a powerful target for cholesterol-lowering drugs (1).] Ultimately, the most important goal for biomedical research is not explaining heritability—that is, predicting personalized patient risk—but understanding pathways underlying disease and using that knowledge to develop strategies for therapy and prevention.

ACKNOWLEDGMENTS. We thank David Altshuler, Jeffrey Barrett, Aravinda Chakravarti, Andrew Clark, David Golan, Peter Donnelly, Nick Patterson, Paz Polak, Alkes Price, David Reich, Peter Visscher, John Wakeley, and Noah Zaitlen for valuable discussions and comments. We thank Haley Hunter-Zinck and Andrew Clark for sharing data on inbreeding in Qatar. This work was supported in part by National Institutes of Health Grant HG003067 and by funds from the Broad Institute.

1. Lander ES (2011) Initial impact of the sequencing of the human genome. *Nature* 470(7333):187–197.
2. Manolio TA, Brooks LD, Collins FS (2008) A HapMap harvest of insights into the genetics of common disease. *J Clin Invest* 118:1590–1605.
3. Hirschhorn JN (2009) Genomewide association studies—Illuminating biologic pathways. *N Engl J Med* 360:1699–1701.
4. Eichler EE, et al. (2010) Missing heritability and strategies for finding the underlying causes of complex disease. *Nat Rev Genet* 11:446–450.
5. Manolio TA, et al. (2009) Finding the missing heritability of complex diseases. *Nature* 461:747–753.
6. Goldstein DB (2009) Common genetic variation and human traits. *N Engl J Med* 360: 1696–1698.
7. McClellan J, King MC (2010) Genetic heterogeneity in human disease. *Cell* 141: 210–217.
8. Slatkin M (2009) Epigenetic inheritance and the missing heritability problem. *Genetics* 182:845–850.
9. Maher B (2008) Personal genomes: The case of the missing heritability. *Nature* 456(7218):18–21.
10. Falconer DS, Mackay TF (1996) *Introduction to Quantitative Genetics* (Longman, Essex, UK), 4th Ed.
11. Song YS, Wang F, Slatkin M (2010) General epistatic models of the risk of complex diseases. *Genetics* 186:1467–1473.
12. Culverhouse R, Suarez BK, Lin J, Reich T (2002) A perspective on epistasis: Limits of models displaying no main effect. *Am J Hum Genet* 70:461–471.
13. Franke A, et al. (2010) Genome-wide meta-analysis increases to 71 the number of confirmed Crohn's disease susceptibility loci. *Nat Genet* 42:1118–1125.
14. Lynch M, Walsh B (1998) *Genetics and Analysis of Quantitative Traits* (Sinauer, Sunderland, MA).
15. Risch N (1990) Linkage strategies for genetically complex traits. I. Multilocus models. *Am J Hum Genet* 46:222–228.
16. Berman SM (1964) Limit theorems for the maximum term in stationary sequences. *Ann Math Stat* 35:502–516.
17. Carlborg O, Haley CS (2004) Epistasis: Too often neglected in complex trait studies? *Nat Rev Genet* 5:618–625.
18. Ferguson EL, Horvitz HR (1989) The multivulva phenotype of certain *Caenorhabditis elegans* mutants results from defects in two functionally redundant pathways. *Genetics* 123(1):109–121.
19. Brem RB, Storey JD, Whittle J, Kruglyak L (2005) Genetic interactions between polymorphisms that affect gene expression in yeast. *Nature* 436:701–703.
20. Khan AI, Dinh DM, Schneider D, Lenski RE, Cooper TF (2011) Negative epistasis between beneficial mutations in an evolving bacterial population. *Science* 332: 1193–1196.
21. Chou HH, Chiu HC, Delaney NF, Segre D, Marx CJ (2011) Diminishing returns epistasis among beneficial mutations decelerates adaptation. *Science* 332:1190–1192.
22. Shao H, et al. (2008) Genetic architecture of complex traits: Large phenotypic effects and pervasive epistasis. *Proc Natl Acad Sci USA* 105:19910–19914.
23. Hill WG, Goddard ME, Visscher PM (2008) Data and theory point to mainly additive genetic variance for complex traits. *PLoS Genet* 4:e1000008.
24. Wray NR, Yang J, Goddard ME, Visscher PM (2010) The genetic interpretation of area under the ROC curve in genomic profiling. *PLoS Genet* 6:e1000864.
25. Hunter-Zinck H, et al. (2010) Population genetic structure of the people of Qatar. *Am J Hum Genet* 87(1):17–25.
26. Visscher PM, et al. (2006) Assumption-Free Estimation of Heritability from Genome-Wide Identity-by-Descent Sharing between Full Siblings. *PLoS Genet* 2(3)e41.
27. Yang J, et al. (2010) Common SNPs explain a large proportion of the heritability for human height. *Nat Genet* 42:565–569.
28. Rivas MA, et al.; National Institute of Diabetes and Digestive Kidney Diseases Inflammatory Bowel Disease Genetics Consortium (NIDDK IBDGC); United Kingdom Inflammatory Bowel Disease Genetics Consortium; International Inflammatory Bowel Disease Genetics Consortium (2011) Deep resequencing of GWAS loci identifies independent rare variants associated with inflammatory bowel disease. *Nat Genet* 43: 1066–1073.

The Mystery of Missing Heritability:
Genetic interactions create phantom heritability -
Supplementary Information

Contents

List of Figures	4
List of Tables	5
List of Symbols	6
1 Calculating the top-down heritability h_{pop}^2 from population data	7
1.1 Explained, missing and phantom heritability	7
1.2 Partitioning of phenotypic variance	7
1.3 Genetic interactions confound heritability estimates: The ACE model	8
1.4 Shared environment confounds heritability estimates: The ADE model	9
1.5 Heritability estimation by parent-offspring regression	10
1.6 Summary: Problems of different heritability estimates	10
1.7 Importance of clarity about definitions of heritability	11
1.8 Problems with narrow and broad sense heritability estimates	11
2 The liability-threshold (A_Δ) model	13
2.1 Definition	13
2.2 Risk to relatives	13
2.3 Fitting an A_Δ model from population data	14
2.4 Effect size and heritability explained for a single locus	14
3 The limiting pathway (LP) model for quantitative traits	16
3.1 Definition	16
3.2 Calculating the true heritability, h_{all}^2	16
3.3 Calculating the apparent heritability, h_{pop}^2	17
3.4 Phantom heritability approaches 100% as k increases	19
4 The limiting pathway (LP_Δ) model for disease traits	20
4.1 Definition	20
4.2 Calculating the risk to relatives of affected individuals	20
4.3 Calculating the true heritability, h_{all}^2 , and apparent heritability, h_{pop}^2	21
4.4 Generalized multiple pathways models	21
5 Numerical properties of LP models:	
Traditional formulas mis-estimate heritability	25
5.1 Epidemiological data for quantitative traits	25
5.2 Epidemiological data for disease traits	25
5.3 Data in Fig. 1a: Phantom heritability for quantitative traits	26
5.4 Data in Fig. 1b: Phantom heritability for disease traits	26

5.5 Alternative heritability estimates	26
6 Crohn's disease, schizophrenia and other traits	28
6.1 Crohn's disease	28
6.2 Schizophrenia	29
6.3 Differences among traits	30
7 Detecting epistasis among variants	32
7.1 Experimental evidence for epistasis in humans	32
7.2 Tests for detecting associations and their power	32
7.3 Detecting the marginal effect of each SNP	33
7.4 Detecting interaction between a pair of SNPs	34
7.5 Detecting interaction between two pathways	35
8 Consistent estimator $h_{\text{slope}(\kappa_0)}^2$: Proof of Theorem 1	37
8.1 Heritability on the observed scale	37
8.2 Ascertainment bias in Case-Control studies	41
8.3 Heritability on a hidden liability scale	41
9 Applying the theorem in practice	42
9.1 Heuristic formula for variance of slope	42
9.2 Simulation	43
10 Estimator based on slope of variation in IBD sharing among sibs	44
11 Arguments advanced in support of additivity	45
11.1 Allele frequencies	45
11.2 Breeder's equation	46
11.3 Observed sibling correlations	47
12 Supplementary code	48
References	49
13 Supplementary figures	52
14 Supplementary tables	63

List of Figures

1	Distribution of phenotype for LP traits.	52
2	Phenotypic similarity for relatives for the LP traits.	53
3	Analysis of LP models for quantitative traits.	54
4	Analysis of LP models for disease traits.	55
5	Further analysis of LP model for disease traits.	56
6	Heritability for generalized LP models.	57
7	Additive vs. non-additive models for schizophrenia.	58
8	Sample sizes needed to detect loci and detect interactions.	59
9	Epistatic variance in two-locus model.	60
10	Parent-offspring phenotypic correlation	61
11	Response to selection and parent-offspring phenotypic correlation	62

List of Tables

1	Model parameters for generalized LP model	22
2	Epidemiological parameters for disease traits	25
3	Phantom heritability for Crohn's disease for different epidemiological parameters . .	28
4	Risk for relatives for Crohn's disease for different levels of shared environment . . .	29
5	Epidemiological data and model fit for Schizophrenia	30
6	Epidemiological parameters for quantitative traits	63
7	Model parameters for quantitative traits	66
8	Model parameters for disease traits	71
9	Phantom heritability for Crohn's disease	82

List of Symbols

$\pi_{explained}$	Proportion of heritability explained	7
h_{known}^2	Narrow-sense heritability explained by known variants	7
$\pi_{phantom}$	Phantom heritability	7
h_{all}^2	True (narrow-sense) heritability	7
h_{pop}^2	Apparent heritability, inferred from population data	7
β_i	Additive effect size of the i-th locus	7
r_R	Phenotypic correlation for relatives of degree R	7
Ψ	A genetic architecture	7
H^2	Broad-sense heritability	11
A_Δ	The liability-threshold model	13
c_R	Fraction of environmental variance shared by relatives of degree R	13
μ	Disease prevalence	13
λ_R	Relative risk for diseases for relatives of degree R	13
IBD	Identity-By-Descent	13
κ_R	Kinship coefficient for relatives of degree R	13
f_i	Minor allele frequency of the i-th locus	14
η_i	Genetic relative risk of the i-th locus	14
LP	The limiting pathway model for quantitative traits	16
$h_{pathway}^2$	Heritability in a given pathway	16
V_c	Proportion of variance due to common environment	16
LP_Δ	The limiting pathway model for disease	20
NCP	Non-Centrality-Parameter	33
$h_{slope(\kappa_0)}^2$	Heritability estimator from IBD sharing	37

1 Calculating the top-down heritability h_{pop}^2 from population data

1.1 Explained, missing and phantom heritability

The proportion of heritability explained by a set of loci is $\pi_{explained} = \frac{h_{known}^2}{h_{pop}^2}$. The missing heritability is $\pi_{missing} = 1 - \pi_{explained} = 1 - \frac{h_{known}^2}{h_{pop}^2}$. The phantom heritability is the missing heritability remaining after all causal loci were discovered, $\pi_{phantom} = 1 - \frac{h_{all}^2}{h_{pop}^2}$.

The values h_{all}^2 and h_{known}^2 are typically obtained by summing the individual variances explained over all causal loci, and all known loci, respectively (see main text). The value h_{pop}^2 is typically obtained by measuring phenotypic similarity among family members, as described next in Sections 1.2 - 1.5.

Throughout the paper, we are interested in the issue of *consistency*, that is, whether or not the population estimates h_{pop}^2 converge asymptotically to the heritability h_{all}^2 as the sample size grows. We therefore focus on the actual values of the quantities h_{pop}^2 , h_{known}^2 and h_{all}^2 . We are not interested here in issues of precision - that is, sampling variation in estimates due to sample size. In focusing on consistency, we can assume that we know the true population values of the various parameters such as genetic effect size (for example, β_i , defined as the additive effect of the i -th variant to the trait) or phenotypic similarity (for example, r_R , defined as the phenotypic correlation coefficient between two individuals of familial relationship R).

1.2 Partitioning of phenotypic variance

For a general genetic architecture $\Psi(G, E)$, and assuming no GxE interactions, the genetic architecture is written as,

$$Z = \Psi(G, E) = \Psi'(g_1, \dots, g_n) + \epsilon \quad (1.1)$$

where Ψ' is a function only of genotypes, giving the genotypic value $\Psi'(g_1, \dots, g_n)$, i.e. the average level of the phenotype for individuals with genotype vector (g_1, \dots, g_n) . Here Z is the value of the trait. It is a random variable, with a distribution depending both on the distribution of noise ϵ , and a distribution of the genotypes (g_1, \dots, g_n) in the population. Here and throughout, we will use upper-case (e.g. Z) to denote random variables, and lower-case (e.g. z) to denote their realized values. The quantity g_i typically denotes the diploid genotype at the i -th variant site, which is 0, 1 or 2 according to the number of variant alleles. (Alternatively we can choose to distinguish between the maternally- and paternally-inherited sites, in which case the g_i are binary variables.) ϵ is an (unobserved) environmental variable contributing to the trait's value. Here and throughout, we assume that the trait is normalized to have mean zero and variance one, and that the environmental component ϵ has a Gaussian distribution, $\epsilon \sim N(0, V_e)$. The variance in the trait can be partitioned as (see e.g. ref.,¹ pages 85-87),

$$V_P = V_G + V_e = \sum_{i,j=0}^n V_{A^i D^j} + V_e \quad (1.2)$$

Here $V_{A^i D^j}$ represents the interaction of additive variance of order i and dominance variance of order j , and we use the convention $V_{A^0 D^0} = V_{A^n D^n} = 0$.

V_e is the environmental variance. When considering the variance decomposition for *two* individuals, the environmental variable ϵ is further partitioned into a shared part, ϵ_c , with variance V_c , and a unique part, ϵ_u , with variance V_u (such that $V_c + V_u = V_e$). This partitioning varies based on the degree of shared environment between the two individuals, which we assume is determined by the familial relationship. We therefore write, for example, $V_{c,sib}$, $V_{c,cousin}$ to represent the level of shared environment for siblings, cousins etc.

1.3 Genetic interactions confound heritability estimates: The ACE model

This section and the following two sections describe three common approaches for estimating the narrow-sense heritability h_{all}^2 from population data. All three estimators are based on the notion of comparing phenotypic similarity of close family members.

The similarity is measured by phenotypic correlation, $r_R = \text{corr}(Z, Z_R)$, where Z is the value of the trait for an individual and Z_R is the value for a relative with familial relationship R . According to eq. (1.2), the phenotypic variance depends on genetic interactions of different levels and different environmental variance components.

Ideally, an estimator of the heritability from population data will consider all the different variance components, and will converge, as sample size increases, to the true heritability. However, the problem is that such estimators are typically based on only two or a few more familial relations (for example, twins, siblings, parent-offspring) and there is no way to estimate the different variance components from so few observations. The “solution” has been to introduce simplifying assumptions. We next examine the effect of such simplifying assumptions on heritability estimates.

In twin studies, one observes two variables, the monozygotic twin correlation r_{MZ} , and the dizygotic twin correlation r_{DZ} . The ACED model is often used for twin studies. It partitions the variance of a trait to four components: Additive, Common environment, unique Environment and Dominance (see e.g.²). Since all variance components should sum to one, the model has 3 free parameters - Additive, Dominance and Common environmental variances. Based on the two observed values r_{MZ}, r_{DZ} , there is no way to estimate these 3 parameters of the ACED model from the data. One must therefore give up one component of the model. The most widely used choice is the ACE model described in the main text, where one completely neglects interactions (both Dominance and epistasis). To illustrate the effect of interactions on the ACE model, we give the formulas for monozygotic and dizygotic twin correlations obtained from eq. (1.2),

$$r_{MZ} = V_{c,MZ} + \sum_{i,j=0}^n V_{A^i D^j} \quad (1.3)$$

$$r_{DZ} = V_{c,DZ} + \sum_{i,j=0}^n 2^{-(i+2j)} V_{A^i D^j} \quad (1.4)$$

The formula for calculating h_{pop}^2 in the ACE model is,

$$h_{pop}^2(ACE) = 2(r_{MZ} - r_{DZ}) \quad (1.5)$$

The estimator attempts to eliminate the effect of shared environment by subtracting r_{DZ} from r_{MZ} . (N.B. the estimator makes the implicit assumption that shared environment is identical for MZ and DZ twins ($V_{c,MZ} = V_{c,DZ}$). If there are differences in the shared environment due to in-utero or subsequent effects ($V_{c,MZ} > V_{c,DZ}$), then the ACE model will not fully eliminate the effect of shared environment.)

The estimator (obtained from eqs. (1.3, 1.4)) can be partitioned as,

$$h_{pop}^2(ACE) = \sum_{i,j=0}^n (1 - 2^{-(i+2j)})V_{A^i D^j} = h_{all}^2 + \sum_{(i,j) \neq (1,0)} (1 - 2^{-(i+2j)})V_{A^i D^j} = h_{all}^2 + W(ACE) \quad (1.6)$$

where we have used $h_{all}^2 = V_A$ since we assume that the overall phenotypic variance is $V_p = 1$. The term $W = \sum_{(i,j) \neq (0,1)} (1 - 2^{-(i+2j)})V_{A^i D^j}$ is the error in estimating h_{all}^2 . It is always non-negative, and is zero only when the trait follows a strictly additive model. Otherwise, we have $W > 0$ and the heritability estimate is biased upwards, $h_{pop}^2 > h_{all}^2$.

1.4 Shared environment confounds heritability estimates: The ADE model

Alternatively, the ADE model assumes a dominance term (which allows a partial correction for genetic interactions) but completely ignores shared environment among relatives. In the ADE model, the formula for h_{pop}^2 is

$$h_{pop}^2(ADE) = 4r_{DZ} - r_{MZ} \quad (1.7)$$

This gives,

$$\begin{aligned} h_{pop}^2(ADE) &= \sum_{i,j=0}^n (4 \times 2^{-(i+2j)} - 1)V_{A^i D^j} + 3V_{c,sib} = \\ h_{all}^2 + \left[\sum_{(i,j) \neq \{(1,0), (0,1), (2,0)\}} -(1 - 2^{2-(i+2j)})V_{A^i D^j} + 3V_{c,sib} \right] &\equiv \\ h_{all}^2 + W(ADE) \end{aligned} \quad (1.8)$$

The term $W(ADE)$ represents our error in estimating the heritability. It is composed of two parts. The first (summation) term is composed of genetic interactions, and is always non-positive. The ADE estimator eliminates V_D and V_{AA} , but higher order interactions are still present and will lead to an under-estimate (as opposed to over-estimate) of the heritability when genetic interactions exist. More disturbingly, the ADE estimator completely ignores shared environment and thus gives rise to the second part, $3V_{c,sib}$; it is always non-negative and will inflate the heritability estimation when shared environment is present. This can yield substantial phantom heritability.

1.5 Heritability estimation by parent-offspring regression

Another estimator for the heritability is obtained by regression of offspring phenotype on the mid-parents phenotype,

$$h_{pop}^2(PO) = \sqrt{2}r_{PO} \quad (1.9)$$

that is, one regresses the phenotype of the offspring Z_{off} on the average phenotype of the two parents, $\frac{Z_p+Z_m}{2}$ to get $r_{PO} = \text{corr}(Z_{off}, \frac{Z_p+Z_m}{2})$. This estimate goes back to Galton,³ who coined the expression “regression toward the mean”, which simply means that the offspring value, Z_{off} , is on average closer to the population mean than the mid-parent value $\frac{Z_p+Z_m}{2}$ - which is mathematically equivalent to having $r_{PO} < 1$. The correlation coefficient r_{PO} measures the strength of the regression to the mean, which in turn is a measure of the role of genetics in the trait, i.e. heritability. The variance partitioning for this estimator is as follows,

$$h_{pop}^2(PO) = V_{c,p0} + \sum_{i=0}^n 2^{1-i}V_{A^i} = h_{all}^2 + V_{c,p0} + \sum_{i=1}^n 2^{1-i}V_{A^i} = h_{all}^2 + W(PO) \quad (1.10)$$

where $V_{c,p0}$ is the expected shared environment between offspring and their parents (which may be different than $V_{c,sib}$ used previously). The term $W(PO) = V_{c,p0} + \sum_{i=1}^n 2^{1-i}V_{A^i}$ represents our error for this estimator. An advantage of using parent-offspring regression is that dominance effects and their interactions completely vanish. However, the estimator may be still greatly inflated by both shared environment components between parents and their offspring $V_{c,p0}$, and genetic interactions between different loci (additive-by-additive interactions), V_{A^i} for $i > 1$.

Again, under an additive model with no shared environment, this is a consistent estimator for the true heritability h_{all}^2 . Under a general model, we get an over-estimation due to genetic interactions (albeit a different over-estimation than the one obtained by the ACE model), and also an over-estimation due to shared environment between parents and their offspring.

1.6 Summary: Problems of different heritability estimates

The estimator $h_{pop}^2(ACE)$ yields an overestimate, by failing to account for genetic interactions. The estimator $h_{pop}^2(ADE)$ may yield an underestimate (by failing to account for genetic interactions) or an overestimate (by failing to account for shared environment). The estimator $h_{pop}^2(PO)$ yields an overestimate (by failing to account for additive x additive interactions and by failing to account for shared environment).

None of the widely used estimators are immune to overestimation for a general architecture Ψ . Each estimator may inflate the apparent heritability in different circumstances. In Sections 3 and 4, we compute the values of the three heritability estimators under various (non-additive) genetic architectures.

1.7 Importance of clarity about definitions of heritability

Authors often use the term “heritability” and the symbol h^2 to refer to both the true heritability h_{all}^2 and the apparent heritability h_{pop}^2 , despite the fact that these quantities need not be equal. For example, Falconer and MacKay² (page 154) state that

“There are similarly two definitions of additive variance, which is the variance of breeding values. The theoretical one, described in the previous chapter, is derived by summation over loci considered separately, and it excludes interaction variances. The practical one is that which determines, and is estimated from, covariances of relatives, and it contains fractions of the additive x additive interaction variance; for example, twice the offspring-parent covariance estimates $V_A + 0.5V_{AxA}$ + smaller fractions of the higher order interactions, where V_A is the theoretically defined additive variance. The only way of estimating the additive variance is from covariances of relatives, and it is this that is needed for predictions, such as responses to selection. So when we speak of “additive variance” and write “ V_A ” it is best to regard these as referring to the practical definition with its included fractions of interaction variances. In reality, however, the difference between the two definitions is probably seldom more than trivial compared with the errors of estimation.”

The text illustrates two important issues:

- i. The notion that a single term “additive variance” has two definitions that are not equivalent is unacceptable. It gives rise to considerable potential for confusion, including conflating estimators for the two quantities.
- ii. The authors also suggest that the differences between h_{all}^2 and h_{pop}^2 are likely to be small. In fact, the results here show that the difference may be large. In contrast to errors in estimation, which can be overcome by simply increasing sample size, there is no practical way to overcome the difference between the two quantities when considering close relatives.

Throughout the paper, we introduce distinct terminology and nomenclature to distinguish between quantities with distinct definitions.

1.8 Problems with narrow and broad sense heritability estimates

Calculating missing heritability is problematic for both the additive (narrow-sense) heritability h^2 and the overall (broad-sense) heritability H^2 . Consider a trait function $P = \Psi(G, E)$ that depends on genotype $G = (g_1, g_2, \dots, g_n)$ and environment $E = (\epsilon_R, \epsilon_u)$.

The situation for the narrow-sense heritability h^2 is discussed at length in the main text. The fundamental issue is this: it is straightforward to calculate h^2 based on a bottom-up calculation given the loci, but there is no way to obtain a top-down measure based on epidemiological data for an arbitrary (non-additive) function Ψ .

For H^2 , the situation is roughly reversed. If we assume that the phenotype has no shared environmental component ($V_C = 0$), then we can obtain a straightforward top-down estimate of H^2 :

$$H_{all}^2 = r_{MZ}. \quad (1.11)$$

However, there is no practical way to obtain a bottom-up estimate of the overall heritability explained by a set of variants, for an arbitrary (non-additive) function Ψ . The variance explained by a subset of the variants $S = \{g_1, g_2, \dots, g_m\}$ is

$$H_S^2 = 1 - \sum_{(g_1, \dots, g_m) \in \{0,1,2\}^m} Pr(g_1, \dots, g_m) Var(Z|g_1, \dots, g_m) \quad (1.12)$$

(Recall that the trait is normalized, $V_P = 1$). To calculate H_S^2 , we need to estimate the value of the 3^m terms in the sum. For an arbitrary function Ψ , this would require enough observations of each of the 3^m genotypes at the variant loci. Except when m is very small, the required sample size would be too large to be practical.

2 The liability-threshold (A_Δ) model

2.1 Definition

We adopt the classical liability threshold (A_Δ) model.^{4,5} In the main text we describe a minor variation where disease occurs if the liability is *below* (rather than above) a pre-specified threshold. This changes the biological interpretation of the model, but by symmetry, all quantities of interest remain unchanged. We describe the computations in terms of the classic model but they hold also for the model described in the main text.

Briefly, the $A_\Delta(h^2, \tau)$ model defines an (observed) disease Z in terms of an (unobserved) quantitative trait P , called a liability. The trait P follows an additive model $P = \sum_{i=1}^n \beta_i g'_i + \epsilon$ (as in eq. (3) in the main text), with additive heritability h^2 , and the disease occurs ($Z=1$) if and only if $P \geq \tau$, for the specified threshold τ . The model is largely insensitive to the number of loci, their effect sizes and allele frequencies - as long as n is sufficiently large we can assume that P is approximately normally distributed. We will normalize P so that it follows a standard normal distribution $N(0, 1)$, with mean 0 and variance 1. We assume that the genetic component $\sum_i \beta_i g'_i \sim N(0, h^2)$ and the environmental component $\epsilon \sim N(0, 1 - h^2)$ are also normally distributed (with smaller variances). We can further partition the environmental component into shared and unique environmental variance, $\epsilon = \epsilon_{c,R} + \epsilon_{u,R}$, as discussed in the main text, where $\epsilon_{c,R}$ is the shared environmental component between two individuals with familial relationship R . In this case, we can parameterize the model as $A_\Delta(h^2, \tau, c_R)$, where c_R denotes the fraction of environmental variance which is shared, $c_R = \text{Var}(\epsilon_{c,R})/(1 - h^2)$.

2.2 Risk to relatives

The two parameters (h^2, τ) completely specify the genetic architecture and all observable parameters - including the prevalence μ and risk λ_R to relatives of each type R of an affected individual. The prevalence is simply $\mu = \Phi(\tau)$, where Φ is the standard Gaussian cumulative distribution function.

To compute risk to relatives, we first write the joint distribution of liabilities of two family members, denoted P and P_R . Each of the two values is a standard Gaussian random variable, but they are correlated due to Identity-By-Descent (*IBD*) sharing. The average level of IBD sharing for relatives of degree R is $2\kappa_R$, where κ_R is the kinship coefficient ($\kappa_R = \frac{1}{2}, \frac{1}{4}, \frac{1}{8}, \frac{1}{16}, \dots$ for monozygotic twins, dizygotic twins, grandchildren-grandparents, cousins .. respectively). We do not consider here variations around these average values which arise in practice (see Sections 8-10). The average IBD sharing level determines the average correlation between P and P_R , and the vector (P, P_R) is a bivariate Gaussian random variable, with the mean (zero) vector and covariance matrix given by

$$\begin{pmatrix} P \\ P_R \end{pmatrix} \sim N\left(\begin{pmatrix} 0 \\ 0 \end{pmatrix}, \begin{pmatrix} 1 & 2\kappa_R h^2 \\ 2\kappa_R h^2 & 1 \end{pmatrix}\right) \quad (2.1)$$

Using standard properties of the bivariate Gaussian distribution, we can derive the *conditional* distribution of the liability of one family member, P_R , given that we know the value of the liability for another family member, P ,

$$P_R|P \sim N(2\kappa_R h^2 P, 1 - 4\kappa_R^2 h^4) \quad (2.2)$$

We compute the relative risk λ_R by integrating the bivariate Gaussian in the quarter of the (P, P_R) plane which lies above the liability threshold τ , that is $(P \geq \tau, P_R \geq \tau)$,

$$\lambda_R = \frac{1}{\mu^2} Pr(P, P_R \geq \tau) = \frac{1}{\mu^2} \int_{x=\tau}^{\infty} \varphi(x) Pr(P_R \geq \tau | P = x) dx \quad (2.3)$$

where $\varphi (= \Phi')$ is the standard Gaussian probability density function. We get the following expression for the relative risk,

$$\lambda_R = \frac{1}{\mu^2} \int_{x=\tau}^{\infty} \varphi(x) \left[1 - \Phi \left(\frac{\tau - \kappa_R h^2 x}{\sqrt{1 - \kappa_R^2 h^4}} \right) \right] dx \quad (2.4)$$

2.3 Fitting an A_Δ model from population data

To apply the A_Δ model to a disease, one takes epidemiological observable parameters and fits the unseen parameters τ, h^2 and c_R . When only two epidemiological parameters are observable (say, μ and λ_{MZ}), we cannot fit 3 parameters. We therefore neglect the shared environment component c_R and fit only τ, h^2 (this will bias the estimation of h^2 upwards when shared environment is significant). First, for a given prevalence μ , we can compute the corresponding threshold $\tau = \tau(\mu)$ directly from the Gaussian distribution function, $\tau = \Phi^{-1}(\mu)$. Given the risk to a particular type of relative (for example, the risk λ_{MZ} to a monozygotic twin of an affected individual), we can solve for h^2 numerically in eq. (2.4) above to get the heritability.

If we observe three population parameters, μ , λ_{MZ} and λ_s , we can fit all three parameters, τ, h^2 and c_R . This allows us to separate the phenotypic similarity among relatives to genetic (h^2) and shared environmental (c_R) parts. We solve again eq. (2.4), this time twice, for λ_{MZ} and λ_s separately, to get two different estimators h_s^2 and h_{MZ}^2 . Then the heritability h^2 and the shared environment coefficient c_R are determined by solving the linear system of two equations,

$$h_{MZ}^2 = h^2 + c_R(1 - h^2); \quad h_s^2 = h^2 + 2c_R(1 - h^2) \quad (2.5)$$

2.4 Effect size and heritability explained for a single locus

In practice, the variants discovered in a GWAS (with genotypes g_i) are described in terms of risk allele frequency, f_i , and genetic relative risk η_i . The genetic relative risk can be defined as the relative increase in likelihood of disease given a homozygous risk *genotype*, compared to a heterozygous state, $\eta_i = \frac{Pr(Z=1|g_i=2)}{Pr(Z=1|g_i=1)}$. We can write the two alleles as $g_{i,(M)}, g_{i,(F)}$, with $g_i = g_{i,(M)} + g_{i,(F)}$, and can

also define the genetic relative risk in terms of *alleles*, for example $\eta_i = \frac{Pr(Z=1|g_{i,(M)}=1)}{Pr(Z=1|g_{i,(M)}=0)}$. That is, η_i is the increased risk to a carrier of a risk allele compared to a non-carrier (we can write a similar equation for the paternal allele). We assume that the risk due to the paternal allele is identical, and that there is no dominance interaction between the two alleles - in this case the two definitions for η_i are equivalent.⁶ For a genotype g_i , we need to convert between η_i , the genetic relative risk on the observed disease scale, and β_i , the effect size; or equivalently h_i^2 , the heritability explained by the locus on the liability scale. For a genotype g_i with risk allele frequency f_i and additive effect β_i , the heritability explained is $h_i^2 = 2\beta_i^2 f_i(1 - f_i)$. The risk for disease for a given value of each allele (0 or 1) is,

$$Pr(Z = 1|g_{i,(M)} = j) = 1 - \Phi\left(\frac{\tau + \beta_i f_i^j (f_i - 1)^{1-j}}{\sqrt{1 - \beta_i^2 f_i (1 - f_i)}}\right), \quad j = 0, 1 \quad (2.6)$$

and the genetic relative risk η_i is,

$$\boxed{\eta_i = \eta(\beta_i, f_i) = \frac{1 - \Phi\left(\frac{\tau - \beta_i(1 - f_i)}{\sqrt{1 - \beta_i^2 f_i (1 - f_i)}}\right)}{1 - \Phi\left(\frac{\tau + \beta_i f_i}{\sqrt{1 - \beta_i^2 f_i (1 - f_i)}}\right)}} \quad (2.7)}$$

Assuming that there is no dominance interaction between the maternal and paternal alleles, the increased risk for a homozygous risk-allele carrier ($g_i = 2$), compared to a homozygous alternative allele carrier ($g_i = 0$), will be simply η_i^2 .

3 The limiting pathway (LP) model for quantitative traits

3.1 Definition

The Limiting Pathways model for quantitative trait $LP(k, h_{pathway}^2, c_R)$ is defined as the minimum of k standard Gaussian i.i.d. random variables, Z_i , with each being the sum of genetic, common environmental and unique environmental components, with respective variances $h_{pathway}^2$, $c_R(1 - h_{pathway}^2)$ and $(1 - c_R)(1 - h_{pathway}^2)$ (see main text). For a single pathway ($k = 1$), this definition reduces to the simple additive model (see eq. (3) in the main text). From this definition, we can compute all parameters of interest - including the phenotypic correlation between relatives, the true (additive) heritability h_{all}^2 and the apparent heritability h_{pop}^2 that one would calculate from epidemiologically observable parameters.

The overall shared environment for the trait, V_c , is defined as the difference between the MZ twin phenotypic correlation, and the correlation of MZ twins reared apart, $V_c = r_{MZ} - r_{MZ\{c_R=0\}}$. The latter correlation, $r_{MZ\{c_R=0\}}$ is simply computed as the MZ twin correlation for the model $LP(k, h_{pathway}^2, 0)$.

3.2 Calculating the true heritability, h_{all}^2

This section provides a detailed calculation of the heritability in the LP model $LP(k, h_{pathway}^2, c_R)$. The observed trait can be written as the maximum of k i.i.d. standard Gaussian random variables, $Z = \max(Z_1, \dots, Z_k)$. The probability distribution function G_k and probability density function g_k of Z are,

$$G_k(z) = Pr(Z \leq z) = \Phi(z)^k; \quad g_k(z) = k\Phi(z)^{k-1}\varphi(z) \quad (3.1)$$

The mean and variance of z are,

$$\mu_Z = E[Z] = \int_{z=-\infty}^{\infty} g_k(z)zdz = k \int_{z=-\infty}^{\infty} \Phi(z)^{k-1}\varphi(z)zdz \quad (3.2)$$

$$\begin{aligned} \sigma_Z^2 &= E[Z^2] - (E[Z])^2 = \int_{z=-\infty}^{\infty} g_k(z)z^2dz - \left[\int_{z=-\infty}^{\infty} g_k(z)zdz \right]^2 = \\ &k \int_{z=-\infty}^{\infty} \Phi(z)^{k-1}\varphi(z)z^2dz - \left[k \int_{z=-\infty}^{\infty} \Phi(z)^{k-1}\varphi(z)zdz \right]^2 \end{aligned} \quad (3.3)$$

The true (bottom-up) heritability h_{all}^2 is defined as the sum of the additive contributions over all loci $h_{all}^2 = \sum_j h_j^2 = \sum_j \beta_j^2 f_j(1 - f_j)$. Since the genetic contribution within each pathway is additive (in similar to eq. (3) in the main text), we can compute the heritability directly by calculating the variance explained by the entire pathway variable Z_i . By symmetry, each pathway contributes the same amount to the true heritability h_{all}^2 . We can therefore express h_{all}^2 as

$$h_{all}^2 = k \cdot corr(Z_1, Z)^2 h_{pathway}^2 = kh_{pathway}^2 \left[\frac{E[Z_1 \cdot Z] - E[Z_1]E[Z]}{\sigma_{Z_1}\sigma_Z} \right]^2 = kh_{pathway}^2 \frac{(E[Z_1 \cdot Z])^2}{\sigma_Z^2} \quad (3.4)$$

We compute the expectation $E[Z_1 \cdot Z]$ by introducing a new variable $Z^{(\sim 1)} \equiv \max(Z_2, \dots, Z_k)$, which is the maximum over all liabilities *except* Z_1 . We can represent the trait Z as $Z = \max(Z_1, Z^{(\sim 1)})$. The variables $Z_1, Z^{(\sim 1)}$ are independent, and we compute the expectation by summing over two disjoint events - either the maximum is attained for Z_1 (i.e., $Z_1 \geq Z^{(\sim 1)}$), or it is attained for some other Z_i (i.e. $Z_1 < Z^{(\sim 1)}$),

$$\begin{aligned} E[Z_1 \cdot Z] &= \int_{-\infty}^{\infty} \int_{-\infty}^{\infty} \varphi(z_1) g_{k-1}(z^{(\sim 1)}) z_1 \max(z_1, z^{(\sim 1)}) dz_1 dz^{(\sim 1)} = \\ &\int_{-\infty}^{\infty} \varphi(z_1) z_1^2 \left[\int_{-\infty}^{z_1} g_{k-1}(z^{(\sim 1)}) dz^{(\sim 1)} \right] dz_1 + \int_{-\infty}^{\infty} g_{k-1}(z^{(\sim 1)}) z^{(\sim 1)} \left[\int_{-\infty}^{z^{(\sim 1)}} \varphi(z_1) z_1 dz_1 \right] dz^{(\sim 1)} = \\ &\int_{-\infty}^{\infty} \varphi(z_1) z_1^2 \Phi(z_1)^{k-1} dz_1 + (k-1) \int_{-\infty}^{\infty} -\varphi(z^{(\sim 1)})^2 z^{(\sim 1)} \Phi(z^{(\sim 1)})^{k-2} dz^{(\sim 1)} = \\ &\int_{-\infty}^{\infty} \Phi(z_1)^{k-2} \varphi(z_1) z_1 [z_1 \Phi(z_1) - (k-1) \varphi(z_1)] dz_1 \end{aligned} \tag{3.5}$$

Substituting eqs. (3.3,3.5) in eq. (3.4), the bottom-up heritability explained by all loci is,

$$h_{all}^2 = \frac{h_{pathway}^2 \left[\int_{-\infty}^{\infty} \Phi(z)^{k-2} \varphi(z) z [z \Phi(z) - (k-1) \varphi(z)] dz \right]^2}{\int_{z=-\infty}^{\infty} \Phi(z)^{k-1} \varphi(z) z^2 dz - k [\int_{z=-\infty}^{\infty} \Phi(z)^{k-1} \varphi(z) z dz]^2} \tag{3.6}$$

3.3 Calculating the apparent heritability, h_{pop}^2

Our goal is to calculate the value of h_{pop}^2 if the trait follows the *LP* model. We use the traditional estimate from eq. (1.5), which requires the calculation of r_{MZ} and r_{DZ} . We calculate below $r_R = \text{corr}(Z, Z_R)$ for general degree of relationship R , which includes as special cases r_{MZ} and r_{DZ} . If z and z_R are the trait's values for two family members of degree R , then

$$r_R = \frac{E[Z \cdot Z_R] - E[Z]E[Z_R]}{\sigma_Z \sigma_{Z_R}} = \frac{E[Z \cdot Z_R] - \mu_Z^2}{\sigma_Z^2} \tag{3.7}$$

with μ_Z, σ_Z^2 given in eqs. (3.2, 3.3), respectively. To compute $E[Z \cdot Z_R]$, recall that $Z = \max(Z_1, \dots, Z_k)$ and $Z_R = \max(Z_{1,R}, \dots, Z_{k,R})$, with Z_i 's i.i.d., $Z_{i,R}$ i.i.d., and for each i the pair $(Z_i, Z_{i,R})$ has the joint bivariate Gaussian distribution given in eq. (2.1), with correlation coefficient

$$\rho_R \equiv \text{corr}(Z_i, Z_{i,R}) = 2\kappa_R h_{pathway}^2 + c_R(1 - h_{pathway}^2) \tag{3.8}$$

(we assume that shared environment is similar for any familial relationship.) We define $g_{k,R}(z_R|z)$ as the *conditional* density function of Z_R , the trait's value for a relative of degree R , given that the

value of Z , the trait's value for a given individual, is known. The conditional cumulative distribution function is,

$$G_{k,R}(z_R|z) = Pr(Z_R \leq z_R | Z = z) = Pr(Z_R \leq z_R | Z_1 = z; Z_2, \dots, Z_k \leq z) =$$

$$Pr(Z_{1,R} \leq z_R | Z_1 = z) \prod_{i=2}^k Pr(Z_{i,R} \leq z_R | Z_i \leq z) = \Phi\left(\frac{z_R - \rho_R z}{\sqrt{1 - \rho_R^2}}\right) \left[\frac{1}{\Phi(z)} \int_{t=-\infty}^z \varphi(t) \Phi\left(\frac{z_R - \rho_R t}{\sqrt{1 - \rho_R^2}}\right) dt \right]^{k-1} \quad (3.9)$$

where in the calculation we assume without loss of generality that the maximum for Z was obtained by the first Gaussian Z_1 , and use the conditional Gaussian distribution as in eq. (2.2) for each pair of liability $(Z_i, Z_{i,R})$. Differentiating with respect to Z_R gives the conditional density function $g_{k,R}$,

$$g_{k,R}(z_R|z) = \frac{1}{\Phi(z)^{k-1} \sqrt{1 - \rho_R^2}} \left[\int_{t=-\infty}^z \varphi(t) \Phi\left(\frac{z_R - \rho_R t}{\sqrt{1 - \rho_R^2}}\right) dt \right]^{k-2} \\ \left[\varphi\left(\frac{z_R - z\rho_R}{\sqrt{1 - \rho_R^2}}\right) \int_{t=-\infty}^z \varphi(t) \Phi\left(\frac{z_R - t\rho_R}{\sqrt{1 - \rho_R^2}}\right) dt + (k-1)\Phi\left(\frac{z_R - z\rho_R}{\sqrt{1 - \rho_R^2}}\right) \int_{t=-\infty}^z \varphi(t) \varphi\left(\frac{z_R - t\rho_R}{\sqrt{1 - \rho_R^2}}\right) dt \right] \quad (3.10)$$

We use g_k and $g_{k,R}$ to express the expectation $E[Z \cdot Z_R]$,

$$E[Z \cdot Z_R] = \int_{z=-\infty}^{\infty} g_k(z) z \left[\int_{z_R=-\infty}^{\infty} g_{k,R}(z_R|z) z_R dz_R \right] dz = \\ \int_{z=-\infty}^{\infty} g_k(z) z \int_{z_R=-\infty}^{\infty} \left\{ \frac{1}{\Phi(z)^{k-1} \sqrt{1 - \rho_R^2}} \left[\int_{t=-\infty}^z \varphi(t) \Phi\left(\frac{z_R - t\rho_R}{\sqrt{1 - \rho_R^2}}\right) \times dt \right]^{k-2} \right. \\ \left. \left[\varphi\left(\frac{z_R - z\rho_R}{\sqrt{1 - \rho_R^2}}\right) \int_{t=-\infty}^z \varphi(t) \Phi\left(\frac{z_R - t\rho_R}{\sqrt{1 - \rho_R^2}}\right) dt + (k-1)\Phi\left(\frac{z_R - z\rho_R}{\sqrt{1 - \rho_R^2}}\right) \int_{t=-\infty}^z \varphi(t) \varphi\left(\frac{z_R - t\rho_R}{\sqrt{1 - \rho_R^2}}\right) dt \right] \right\} z_R dz_R dz \quad (3.11)$$

Substituting eqs. (3.2, 3.3, 3.11) in eq. (3.7) gives the familial correlation,

$$r_R = \frac{1}{k \int_{z=-\infty}^{\infty} \Phi(z)^{k-1} \varphi(z) z^2 dz - \left[k \int_{z=-\infty}^{\infty} \Phi(z)^{k-1} \varphi(z) z dz \right]^2} \times \\ \left\{ \int_{z=-\infty}^{\infty} g_k(z) z \int_{z_R=-\infty}^{\infty} \left\{ \frac{1}{\Phi(z)^{k-1} \sqrt{1 - \rho_R^2}} \left[\int_{t=-\infty}^z \varphi(t) \Phi\left(\frac{z_R - t\rho_R}{\sqrt{1 - \rho_R^2}}\right) dt \right]^{k-2} \times \right. \right.$$

$$\begin{aligned}
& \left[\varphi\left(\frac{z_R - z\rho_R}{\sqrt{1 - \rho_R^2}}\right) \int_{t=-\infty}^z \varphi(t)\Phi\left(\frac{z_R - t\rho_R}{\sqrt{1 - \rho_R^2}}\right) dt + \right. \\
& \left. (k-1)\Phi\left(\frac{z_R - z\rho_R}{\sqrt{1 - \rho_R^2}}\right)e^{-z_R^2/2} \sqrt{\frac{1 - \rho_R^2}{2\pi}} \Phi\left(\frac{z - z_R\rho_R}{\sqrt{1 - \rho_R^2}}\right) \right] \Big\} z_R dz_R dz - \left[k \int_{z=-\infty}^{\infty} \Phi(z)^{k-1} \varphi(z) z dz \right]^2 \Big\} \tag{3.12}
\end{aligned}$$

The apparent (top-down) heritability h_{pop}^2 is then computed according to the ACE model by substituting eq. (3.12) in eq. (1.5).

3.4 Phantom heritability approaches 100% as k increases

According to the $LP(k, h_{pathway}^2, c_R)$ model, the trait distribution is the (normalized) minimum of k independent standard Gaussian random variables. Each locus contributes additively to one of these Gaussians. Therefore, (see eq.(3.4)), the true heritability h_{all}^2 is proportional to the correlations between each liability, Ψ_i , and the trait $P = \min(\Psi_i)$. We show that as k goes to ∞ , the phantom heritability $\pi_{phantom}$ goes to zero. Berman⁷ showed that $\sum_i \Psi_i$ and $P = \min(\Psi_i)$ are asymptotically independent as $k \rightarrow \infty$. Hence, $h_{all}^2 \rightarrow 0$, that is, the true heritability, measuring the additive contribution of all loci to the trait, goes to zero. On the other hand, the apparent heritability may not approach zero, or approach zero at a slower rate. Therefore, the ratio $\frac{h_{all}^2}{h_{pop}^2}$ approaches zero as k increases, and therefore,

$$\pi_{phantom} = 1 - \frac{h_{all}^2}{h_{pop}^2} \rightarrow 1, \quad \text{as } k \rightarrow \infty \tag{3.13}$$

This is easiest to see first for the special case where we set the parameter $h_{pathway}^2 = 100\%$. In this case, the additive contribution of all loci to each liability is 100% and the trait is entirely determined by genetics (albeit in a non-linear way). Therefore $r_{MZ} = 1$ irrespective of k . Since $r_{DZ} \leq 1/2$ (again, for any k) we have $h_{pop}^2 = 1$ and $\pi_{phantom} \rightarrow 100\%$ as $k \rightarrow \infty$. Although h_{all}^2 goes to zero, the total variance in the trait remains constant, since by definition the trait is normalized.

More generally, for a given observable population parameters r_{MZ}, r_{DZ} , and for each k , we can fit $h_{pathway}^2(k)$ and $c_R(k)$ to match r_{MZ}, r_{DZ} precisely, and therefore h_{pop}^2 . Thus, the heritability estimated from population data remains constant (the fitted parameter $h_{pathway}^2(k)$ goes to 1 as k increases in order to achieve a constant non-zero h_{pop}^2). However, as before, $h_{all}^2 \rightarrow 0$, giving $\pi_{phantom} \rightarrow 1$.

4 The limiting pathway (LP_Δ) model for disease traits

4.1 Definition

Using the Limiting Pathway model $LP(k, h_{pathway}^2, c_R)$ above, we define a disease trait whereby disease occurs if and only if $LP(k, h_{pathway}^2, c_R) \leq \tau$. We denote this trait by $Z = LP_\Delta(k, h_{pathway}^2, c_R, \mu)$ where μ is the disease prevalence, $\mu = 1 - \Phi(\tau)^k$. ($Z=1$ corresponds to disease, $Z=0$ to non-disease.) For a single pathway ($k = 1$), this definition reduces to the A_Δ model above. From this definition, we can compute all parameters - including the risks to relatives of affected individuals, the true (additive) heritability h_{all}^2 and the apparent heritability h_{pop}^2 that would be calculated from epidemiologically observable parameters.

4.2 Calculating the risk to relatives of affected individuals

We can compute the risk for a family member of degree R as follows. First, we compute the joint 2×2 matrix p_R of probabilities that a given liability exceeds the threshold in each of the two relatives:

$$p_R = \begin{pmatrix} p_R(00) & p_R(01) \\ p_R(01) & p_R(11) \end{pmatrix} \quad (4.1)$$

That is, $p_R(ij)$ is the probability that one liability (say Ψ_1) is at state i in a given individual, and at a state j in a relative of degree R of this individual, where $i, j = 1$ means that the threshold τ is exceeded and $i, j = 0$ means that the threshold is not exceeded. We mark the (zero/one) state of the i th liability in a given individual by Z_i - that is, $Z_i = 1$ if and only if $\Psi_i \geq \tau$. Similarly, Z_{iR} denotes the state of the i th liability for a relative of degree R . We can compute the matrix p_R as in eq. (2.4):

$$p_R(11) \equiv Pr(Z_i = 1, Z_{iR} = 1) = \int_{x=\tau}^{\infty} \varphi(x) \left[1 - \Phi\left(\frac{\tau - 2\kappa_R h_{pathway}^2 x}{\sqrt{1 - 4\kappa_R^2 h_{pathway}^4}}\right) \right] dx \quad (4.2)$$

where we denote $h_{pathway}^4 = (h_{pathway}^2)^2$. Similarly,

$$p_R(01) = p_R(10) \equiv Pr(Z_i = 0, Z_{iR} = 1) = \mu - \int_{x=\tau}^{\infty} \varphi(x) \left[1 - \Phi\left(\frac{\tau - 2\kappa_R h_{pathway}^2 x}{\sqrt{1 - 4\kappa_R^2 h_{pathway}^4}}\right) \right] dx \quad (4.3)$$

$$p_R(00) \equiv Pr(Z_i = 0, Z_{iR} = 0) = 1 - 2\mu + \int_{x=\tau}^{\infty} \varphi(x) \left[1 - \Phi\left(\frac{\tau - 2\kappa_R h_{pathway}^2 x}{\sqrt{1 - 4\kappa_R^2 h_{pathway}^4}}\right) \right] dx \quad (4.4)$$

We express the probability of both relatives being affected in terms of the $p_R(ij)$ as follows,

$$Pr(Z = 1, Z_R = 1) = \sum_{j=1}^k \sum_{j'=1}^k Pr\left(\sum_{i=1}^k Z_i = j, \sum_{i=1}^k Z_{iR} = j'\right) =$$

$$\sum_{j=1}^k \sum_{j'=1}^k \sum_{l=\max(0,j+j'-k)}^{\min(j,j')} \binom{k}{l, j-l, j'-l, k-j-j'+l} p_R(11)^l p_R(01)^{j+j'-2l} p_R(00)^{k-j-j'+l} \quad (4.5)$$

Here l denotes how many liabilities are common to the two relatives. The multinomial coefficient determines the number of liabilities exceeding the threshold τ for both (l), each one ($j-l$ and $j'-l$) or none ($k-j-j'+l$) of the individuals. We obtain the relative risk λ_R by normalizing by $\mu^{(D)2}$,

$$\lambda_R = \frac{1}{\mu^{(D)2}} \sum_{j,j'=1}^k \sum_{l=\max(0,j+j'-k)}^{\min(j,j')} \left[\binom{k}{l, j-l, j'-l, k-j-j'+l} p_R(11)^l p_R(01)^{j+j'-2l} p_R(00)^{k-j-j'+l} \right] \quad (4.6)$$

4.3 Calculating the true heritability, h_{all}^2 , and apparent heritability, h_{pop}^2

Since we measure heritability on the liability scale, the true additive heritability h_{all}^2 explained by all loci is the heritability under the model $LP(k, h_{pathway}^2, c_R)$ for quantitative traits, and is given in eq. (3.6). To calculate the apparent heritability h_{pop}^2 we first compute the familial risks λ_{MZ}, λ_s using eq. (4.6). Then, we convert the risks to correlations on the (single) liability scale by assuming that in fact the A_Δ model is the true disease model and solving for r_{MZ} or r_{DZ} in eq. (2.4). Finally, we compute the heritability according to the ACE model as in eq. (1.5).

We also describe below how to compute the heritability on the observed disease scale, $h_{all,\Delta}^2$. Similarly to eq. (3.4), we have

$$h_{all,\Delta}^2 = kh_{pathway}^2 \frac{(E[Z_1 \cdot Z])^2}{\sigma_Z^2} = kh_{pathway}^2 \frac{(E[Z_1 \cdot Z])^2}{\mu(1-\mu)} \quad (4.7)$$

We get,

$$E[Z_1 \cdot Z] = \int_{-\infty}^{\infty} \varphi(z_1) z_1 E[Z|z_1] dz_1 = \\ \int_{-\infty}^{\tau} \varphi(z_1) z_1 [1 - (1-\mu)^{(k-1)/k}] dz_1 + \int_{\tau}^{\infty} \varphi(z_1) z_1 dz_1 = (1-\mu)^{(k-1)/k} \varphi(\tau) \quad (4.8)$$

where we have used the relation $\Phi(\tau)^k = 1 - \mu$. Substituting in eq. (4.7) gives,

$$h_{all,\Delta}^2 = \frac{k\varphi(\tau)^2}{\mu(1-\mu)^{(2-k)/k}} h_{pathway}^2 \quad (4.9)$$

Eq. (4.9) is a generalization of the transformation from Dempster and Lerner⁴, proven for $k = 1$ (the additive A_Δ model), where $h_{pathway}^2 = h_{all}^2$ (see Section 8.3).

4.4 Generalized multiple pathways models

Substantial phantom heritability is not a unique property of the LP models. We can generalize the LP model to a multiple pathway (MP) model, which we define as any trait T determined by the output of multiple pathways:

$$T = u(\Psi_1, \Psi_2, \dots, \Psi_k), \quad (4.10)$$

with the Ψ_i 's as above. We discuss some specific examples:

- i. **Several pathways below threshold.** A trait might occur if j of the k pathways fall below a threshold τ . The LP models represent the case where $j = 1$.
- ii. **Synthetic traits: All pathways below threshold.** The special case where $j = k$ is known in genetics as a synthetic trait - that is, a trait that occurs when several components are all disrupted (corresponding to $\max(\Psi_i) \leq \tau$). Synthetic traits, are well known in genetics (see e.g.⁸).
- iii. **Non-linear combinations.** Various other non-linear function u can be used. For example, we could choose $u(\Psi_1, \Psi_2, \dots, \Psi_k) = \log[\sum_i e^{\alpha\Psi_i}]$. For $\alpha \rightarrow 0$, this reduces to additive traits. When $\alpha \rightarrow \infty$, this reduces to the LP model (with $\max(\Psi_i)$ instead of $\min(\Psi_i)$). In Supp. Fig. 6 we display the heritability calculated for a model with $k = 3$ pathways as a function of α . The phantom heritability increases with α : it is already at $\sim 33\%$ for $\alpha = 2$ and rapidly approaches the levels for the LP model for $\alpha > 5$.
- iv. **Linear combinations.** Another interesting case is obtained by considering a linear combination of different LP models. Consider for example, two different LP models:

$$\begin{aligned} P^{(1)} &\equiv LP(k = 2, h_{pathway}^2 = 70\%, c_R = 50\%) \text{ and} \\ P^{(2)} &\equiv LP(k = 3, h_{pathway}^2 = 50\%, c_R = 50\%) \end{aligned} \quad (4.11)$$

Also, consider the average of these two models (normalized to have variance 1):

$$P^{(1+2)} = \frac{1}{\sqrt{2}}P^{(1)} + \frac{1}{\sqrt{2}}P^{(2)} \quad (4.12)$$

The true, apparent and phantom heritabilities for these models are listed below in Supp. Table 1.

Heritability	Model $P^{(1)}$	Model $P^{(2)}$	Model $P^{(1+2)}$
h_{all}^2	51.3%	29.8%	40.6%
h_{pop}^2	75.9%	53.5%	64.7%
$\pi_{phantom}$	32.3%	44.3%	37.3%

Table 1: True, apparent and phantom heritabilities for the two LP models $P^{(1)}, P^{(2)}$ and their linear combination $P^{(1+2)}$.

For $P^{(1+2)}$, the quantities of interest, including the phantom heritability, are all intermediate between the levels for $P^{(1)}$ and $P^{(2)}$.

More generally, we have the following result:

Proposition 1 Let $\Psi^{(1)}, \dots, \Psi^{(m)}$ be different genetic architectures, where each architecture is comprised of distinct causal loci, with the causal loci for different architectures being in linkage equilibrium. Assume the architectures are normalized to have mean zero and variance one. Let $h_{all}^2(i)$ be the individual bottom-up heritabilities (and similarly for $h_{pop}^2(i)$ and $\pi_{phantom}(i)$). Let $\Psi = \sum_i \alpha_i \Psi^{(i)}$ with the α_i 's satisfying $0 \leq \alpha_i \leq 1$, $\sum_i \alpha_i^2 = 1$. Let $h_{all}^2(\Psi)$ be the bottom-up heritability of Ψ (and similarly for $h_{pop}^2(\Psi)$ and $\pi_{phantom}(\Psi)$). Then, we have,

- (a) $h_{all}^2(\Psi) = \sum_i \alpha_i^2 h_{all}^2(i)$
- (b) $h_{pop}^2(\Psi) = \sum_i \alpha_i^2 h_{pop}^2(i)$
- (c) $\pi_{phantom}(\Psi) = 1 - \frac{h_{all}^2(\Psi)}{h_{pop}^2(\Psi)}$ is an intermediate value between the highest and lowest individual phantom heritabilities.

Proof:

- (a) Consider one causal locus x_{ij} with effect size β_{ij} on the i -th architecture $\Psi^{(i)}$, and variance explained $V_{ij} = \beta_{ij}^2 \text{Var}(x_{ij})$. Denote $\beta_{ij}(\Psi)$ the effect size of the same locus on the combined trait Ψ . Then,

$$\beta_{ij}(\Psi) = \text{Corr}(x_{ij}, \Psi) = \frac{E[x_{ij}\Psi]}{\sigma(x_{ij})} = \frac{1}{\sigma(x_{ij})} \sum_l \alpha_l E[x_{ij}\Psi^{(l)}] = \alpha_i \frac{1}{\sigma(x_{ij})} E[x_{ij}\Psi^{(i)}] = \alpha_i \beta_{ij} \quad (4.13)$$

Therefore, $V_{ij}(\Psi)$, the variance explained by x_{ij} of the trait Ψ is

$$V_{ij}(\Psi) = \beta_{ij}(\Psi)^2 \text{Var}(x_{ij}) = \alpha_i^2 V_{ij} \quad (4.14)$$

Summing over all loci within the i -th architecture gives $\sum_j V_{ij}(\Psi) = \alpha_i^2 h_{all}^2(i)$. Summing over all the individual architectures gives the desired result.

- (b) In all three models we have considered, h_{pop}^2 is obtained by a linear combination of the phenotypic correlation r_R , for different family relationship R (see eqs. (1.5, 1.7, 1.9)). It therefore suffices to show that $r_R(\Psi) = \sum_i \alpha_i^2 r_R(i)$. This follows from linearity of expectation,

$$\begin{aligned} r_R(\Psi) &= \text{Corr}(Z, Z^{(R)}) = E[ZZ^{(R)}] = E[(\sum_i \alpha_i \Psi^{(i)})(\sum_i \alpha_i \Psi^{(i),R})] = \\ &\sum_{i,j} \alpha_i \alpha_j E[\Psi^{(i)} \Psi^{(j),R}] = \sum_i \alpha_i^2 E[\Psi^{(i)} \Psi^{(i),R}] = \sum_i \alpha_i^2 r_R(i) \end{aligned} \quad (4.15)$$

- (c) Plugging in the formulas for h_{all}^2 and h_{pop}^2 gives the formula for $\pi_{phantom}$ for the combined model. The resulting h_{all}^2 and h_{pop}^2 are a weighted average of the individual $h_{all}^2(i)$'s and $h_{pop}^2(i)$'s. It easily follows by simple induction that $\pi_{phantom}$ lies within the range $[\min_i \pi_{phantom}(i), \max_i \pi_{phantom}(i)]$.

We conclude that a linear combination of different non-linear (e.g. LP) models yields an intermediate value of the phantom heritability. Thus, if several biological processes each have substantial phantom heritability, then an additive combination of the processes will also have substantial phantom heritability.

If the architecture involves a non-linear combination of different non-linear (e.g. LP) models, the phantom heritability is likely to increase further. An obvious example is an $LP(m)$ model of m different $LP(n)$ model, which is in fact an $LP(mn)$ model, with phantom heritability greater than the individual $LP(n)$ models.

5 Numerical properties of LP models: Traditional formulas mis-estimate heritability

In this section we describe the details of comparing the predictions provided by the different LP models, to actual epidemiological data collected for various quantitative traits and diseases in human. We describe the data and models used to produce Fig. 1 in the main text and Supp. Figs. 2 – 5 (for both quantitative and disease traits).

5.1 Epidemiological data for quantitative traits

Data for 86 different traits from Hill et al.⁹ are shown in Supp. Fig. 2a. The data were kindly provided by P. Visscher. They are given in Supp. Table 6.

5.2 Epidemiological data for disease traits

Data for 15 different diseases from Wray et al.¹⁰ are shown in Supp. Fig. 2b. They are given below in Supp. Table 2.

Disease	λ_{MZ}	λ_s	$\mu(\%)$	λ_s (exp.)	$Dev.(\lambda)$ (%)	$h_{pop}^2(\%)$
Depression	2.0	1.3	24.0	1.5	12.4	68.5
AMD	4.7	2.1	12.0	2.4	14.1	92.0
Myocardial infarction	4.6	3.2	5.6	2.4	-25.8	29.0
Breast cancer	4.1	2.2	3.6	2.2	-0.2	37.1
Type 2 diabetes	10.4	3.5	2.8	3.9	11.6	70.6
Asthma	6.6	3.4	19.0	2.2	-34.0	100.0
Rheumatoid Arthritis	12.2	3.5	1.0	4.2	20.4	55.7
Bipolar Disorder	60.0	7.0	1.0	11.2	59.7	100.0
Schizophrenia	52.1	8.6	0.9	10.5	22.5	94.5
Type 1 diabetes	79.0	14.0	0.5	13.7	-1.9	83.1
Multiple sclerosis	190.0	20.0	0.1	23.8	18.8	78.6
Crohn's disease	600.0	64.0	0.1	47.2	-26.3	90.5
Ankylosis spondylitis	630.0	82.0	0.1	48.2	-41.2	92.0
Lupus ⁽¹⁾	841.0	29.0	0.1	53.2	83.3	100.0
Lupus ⁽²⁾	774.0	65.0	0.0	58.3	-10.3	78.0

Table 2: Reported values of the relative risk for monozygotic twins (λ_{MZ}), relative risk for siblings (λ_s), and prevalence μ for each disease. λ_s (exp.) is the value of λ_s which would be expected for a disease that follows an additive A_Δ model with no shared environment and the reported prevalence μ and monozygotic twin risk λ_{MZ} . $Dev.(\lambda) = \frac{\lambda_s - \lambda_s(\text{exp.})}{\lambda_s(\text{exp.})}$ is the relative deviation in sibling relative risk compared to the expected value $\lambda_s(\text{exp.})$. h_{pop}^2 is the heritability obtained from μ , λ_s and λ_{MZ} assuming an additive A_Δ model and using the ACE estimator.

5.3 Data in Fig. 1a: Phantom heritability for quantitative traits

In Fig. 1a in the main text, we studied various quantitative traits defined by LP models. The data in Fig. 1a were calculated using the formulas in Section 3. For each model, the relevant parameters ($r_{MZ}, r_{DZ}, h_{all}^2, h_{pop}^2, \pi_{phantom}$) are listed in Supp. Table 7.

We varied $k = 1, \dots, 10$, the number of pathways, $h_{pathway}^2 = 0.1, 0.3, 0.5, 0.7, 0.9$, the heritability in each pathway, and $C_R = 0, 0.25, 0.5, 0.75$, the fraction of environmental variance shared among siblings or parent-offspring. $h_{c,env}^2$ denotes the shared environmental component in each pathway (which is equal to $c_R(1 - h_{pathway}^2)$). We display also the monozygotic and dizygotic twin correlations, r_{MZ} and r_{DZ} , respectively. For each LP model, we have computed the true (bottom-up) heritability h_{all}^2 . The h_{all}^2 values should be contrasted with the top-down heritability h_{pop}^2 , computed using the ACE model, with $\pi_{phantom}$ showing the lack of agreement between these two measures. In addition, we display in Supp. Table 7 the values of h_{pop}^2 and $\pi_{phantom}$ for two other population estimates, using the ADE and PO models (see Section 5.5 for more details on the alternative estimates).

5.4 Data in Fig. 1b: Phantom heritability for disease traits

In Fig. 1b in the main text, we studied various quantitative traits defined by LP models. The data in Fig. 1b were calculated using the formulas in Section 4. For each model, the relevant parameters ($\lambda_{MZ}, \lambda_{sib}, h_{all}^2, h_{pop}^2, \pi_{phantom}$) are listed in Supp. Table 8.

5.5 Alternative heritability estimates

Fig. 1a (for quantitative traits) and Fig. 1b (for diseases) in the main text show the values of h_{pop}^2 that would be calculated under the ACE estimate for the LP models, using eq. (1.5). We also calculated the values of h_{pop}^2 for these same LP models using the two other estimates, $h_{pop}^2(ADE)$ (see eq. (1.7)) and $h_{pop}^2(PO)$ (see eq. (1.9)). The data these all estimators is also displayed in Supp. Table 8 (for quantitative traits) and Supp. Table 8 (for diseases).

Consider, for example, the P^* model $LP(k = 4, h_{pathway}^2 = 50\%, c_R = 50\%)$, where 50% of the environmental variance (and thus 25% of the overall variance) in each pathway is shared. The true heritability is $h^2 = h_{all}^2 = 25.4\%$. The apparent heritabilities are $h_{pop}^2(ACE) = 54.0\%$, $h_{pop}^2(ADE) = 79.2\%$ and $h_{pop}^2(PO) = 70.8\%$, yielding phantom heritabilities of 52.9%, 67.9% and 64.1%, respectively.

Some observations:

- The true heritability h_{all}^2 does not depend on c_R , the proportion of the environmental variance that is shared. However, the apparent heritability h_{pop}^2 for all three estimators is inflated by shared environment (with the exception of the ACE estimator in the case of additive models, LP(1)).
- Genetic interactions cause large inflation of the ACE estimator.
- Genetic interactions also inflate the PO estimator, although somewhat less so.

- As noted in Section 1, genetic interactions lead to underestimates for the ADE estimator. However, shared environment causes substantial overestimation, due to the term $3V_{c,env}$ appearing in the error term (see eq.(1.8)). As a result, the ADE model actually gives the highest phantom heritability for the P^* model.
- For disease traits, the picture is largely similar. An important major difference is that the ADE estimator for diseases can give substantial phantom heritability even when there is no shared environment. For example, for the model $LP(k = 3, h_{pathway}^2 = 70\%, c_R = 0\%)$, the ADE estimator gives 25.9% phantom heritability. This is lower than values given by the ACE estimator (60.6%) and the PO estimator (42.7%), but still considerable.

6 Crohn's disease, schizophrenia and other traits

6.1 Crohn's disease

A recent meta-analysis with $\sim 15,000$ cases and $\sim 6,000$ controls reported 71 loci associated with Crohn's disease.¹¹ We analyzed these loci, together with three previously known independent variants at the *NOD2* locus, in terms of their contribution to heritability [M. Daly, personal communication]; hence we refer hereafter to this set as 'the 74 loci'. For our analysis, we used values for the heritability $h_{pop}^2 = 50\%$ and the prevalence $\mu = 0.1\%$ reported in the literature.^{11,12} If we assume that the disease follows an additive model A_Δ with these parameters, then the current set of 74 variants explain 10.8% of the phenotypic variance and 21.5% of the heritability. Under this model, the relative risks are $\lambda_{MZ} = 54.3$ and $\lambda_s = 10.3$.

We then fit an $LP_\Delta(3)$ model with the same prevalence μ , and relative risks, λ_{MZ} and λ_s . The model is $LP_\Delta(k = 3, h_{pathway}^2 = 47.6\%, c_R = 16\%, \mu = 0.1\%)$. We assigned the 74 loci randomly to the 3 different pathways. Because the LP(3) model was chosen to fit the population parameters precisely, it obviously cannot be distinguished from the additive model based on the population parameters. Yet, the true heritability for the LP(3) model is only $h_{all}^2 = 18.7\%$ (vs 50% for the additive model) and thus the phantom heritability is $\pi_{phantom} = 62.6\%$. Under this model, the known variants explain 57.5% ($= 10.8/18.7$) of the heritability. The contribution of all loci to heritability under both models is displayed in Supp. Table 9.

Above, we chose one specific set of epidemiological parameters to illustrate the problem. Different epidemiological estimates available in the literature (for prevalence, relative risk and heritability) yield different values for the total heritability and therefore for the heritability explained, as shown below in Supp. Table 3.

$\mu(\%)$	λ_{MZ}	λ_s	Model	$h_{pathway}^2(\%)$	$c_R(\%)$	$h_s^2(\%)$	$h_{all}^2(\%)$	$V_c(\%)$	$\pi_{phantom}(\%)$	$\pi_{explained}(\%)$
0.1 ⁽¹¹⁾	54.3	10.3	A_Δ	50 ⁽¹¹⁾	0	10.8	50	0	0	21.5
0.1 ⁽¹¹⁾	230	27 ⁽¹²⁾	$LP_\Delta(3)$	47.6	16	10.8	18.7	18.2	62.6	57.5
0.1 ⁽¹¹⁾	230	27 ⁽¹²⁾	A_Δ	77.3	0	10.8	77.3	0	0	13.9
0.2 ⁽¹³⁾	35.1	7.92	$LP_\Delta(3)$	70.1	34.7	10.8	27.6	23.7	64.3	39
0.2 ⁽¹³⁾	35.1	7.92	A_Δ	50 ⁽¹¹⁾	0	12.1	50	0	0	24.3
0.2 ⁽¹³⁾	250	35 ⁽¹⁴⁾	$LP_\Delta(3)$	47.6	17	12.1	19.1	19.4	61.9	63.7
0.2 ⁽¹³⁾	250	35 ⁽¹⁴⁾	A_Δ	82.8	10.3	12.1	82.8	1.8	0	14.7
			$LP_\Delta(3)$	72.5	73.5	12.1	29	32.2	64.9	41.8

Table 3: Cumulative assumed and actual variance explained by associated SNPs for Crohn's disease. (Source: Franke et al.¹¹). The table shows various estimates for prevalence (μ), monozygotic twin (λ_{MZ}) and sibling (λ_s) relative risks obtained from different sources. The cited sources are shown in parenthesis next to numbers in the table. h_s^2 is the total variance explained under an A_Δ model for the 74 known loci. For each set of parameters we fitted an additive A_Δ model and a non-additive LP model $LP_\Delta(3)$. $h_{pathway}^2$, the heritability in each pathway and c_R , the fraction of shared environment in each pathway, are the fitted model parameters. We then computed h_{all}^2 , the heritability explained by all loci, and the resulting $\pi_{explained}$ and $\pi_{phantom}$ under either the A_Δ or the LP_Δ model.

While both models fit the data, the additive model has no phantom heritability and the $LP_\Delta(3)$ model has 60–65% phantom heritability.

However, our results are robust to the choice of epidemiological parameters in that the phantom heritability under the $LP_{\Delta}(3)$ model is broadly similar: > 60% in all cases examined.

The additive and non-additive models thus cannot be distinguished based on the relative risks to *MZ* twins and sibs (λ_{MZ} and λ_{sib}). We further explored whether the models can be readily distinguished based on risks to more distant relatives, such as grandchildren and first cousins (λ_g and λ_{cousin}). This turns out to be difficult due to two challenges:

- i. The first challenge is that one must specify the extent of shared environment for each type of relative pair. Many diseases have significant shared environment that extends beyond family households. (In particular, the risk for Crohn’s disease is believed to be decrease by some environmental exposures, and may be increased by others. Another example is multiple sclerosis, which is influenced by the latitude of residence during one’s first two decades of life.) We examined models where the shared environment for grandchildren and cousins is $x = c_R/c_{sib} = 25\%, 50\%$, or 75% of the level for sibs. (see Table 4).

Model	$V_{c,sib}(\%)$	λ_{MZ}	λ_{sib}	λ_g	λ_{cousin}
A_{Δ}	0	54.3	10.3	3.58	1.96
$LP_{\Delta}(3)(x = 25\%)$	18.2	54.3	10.3	2.43	1.58
$LP_{\Delta}(3)(x = 50\%)$	18.2	54.3	10.3	2.86	1.82
$LP_{\Delta}(3)(x = 75\%)$	18.2	54.3	10.3	3.38	2.12

Table 4: The table shows the relative risk to *MZ* twins, sibs, grand-children and cousins of individuals affected by Crohn’s disease, according to the additive A_{Δ} and $LP_{\Delta}(3)$ models, for different levels of shared environment x for distant relatives. The shared environment variance for sibs is $c_{sib} = 16\%$ (corresponding to $V_{c,sib} = 18.2\%$). x is the ratio $c_g/c_{sib} (= c_{cousin}/c_{sib})$, quantifying the level of shared environment for grand-children and cousins, compared to the level of shared environment for siblings.

The results show that the relative recurrence risks depend on the extent of shared environment among grandchildren and cousins. In practice, it may be difficult to achieve sufficient precision to distinguish among these models (let alone other models).

- ii. The second challenge is that good data are lacking concerning risks to grandchildren and cousins for Crohn’s disease (and for most diseases). It is difficult to obtain data with accurate diagnosis and without ascertainment biases from sufficiently large samples to provide adequate precision. In addition, comparisons of grandparents and grandchildren may be confounded by secular trends affecting disease prevalence and environmental exposure.

In summary, it is not simple to distinguish among models involving even a modest number of parameters based on a small number of observables (e.g., μ , λ_{MZ} , λ_{sib} , λ_g and λ_{cousin}).

6.2 Schizophrenia

Using epidemiological data for schizophrenia from refs^{15, 16, 17} we fit both an $LP_{\Delta}(1)$ (that is, additive) and an $LP_{\Delta}(2)$ model. Since *MZ* risk is available for only one data set and is less reliable, we

fitted the models using the sibling risk λ_s and the grand-child risk λ_g . We then examined the risk to other relatives (Supp. Table 5).

Both models fit the data reasonably well (see Supp. Fig. 7 and Supp. Table 5), with the $LP_\Delta(2)$ model arguably showing a somewhat better fit. A striking observation from Supp. Fig. 7 is that the two models produce very small differences in the population correlations but yield a large difference in phantom heritability. The correlation among relatives follows a straight line for the A_Δ (additive) model and a curve that is just slightly concave up for the $LP_\Delta(2)$ model. Yet, the phantom heritability is 0% for the A_Δ (additive model) and 46% for the $LP_\Delta(2)$ model. This observation underscores how challenging it is to detect the presence of genetic interactions based on phenotypic correlations.

	Risch et al. ¹⁶	A_Δ	$LP_\Delta(2)$	Lichtenstein et al. ¹⁷	A_Δ	$LP_\Delta(2)$
Prevalence (%)	0.85	0.85	0.85	0.41	0.41	0.41
λ_{MZ}	52.1	37.2	44.1	-	37.8	50.3
λ_s	8.6	8.6	8.6	8.55	8.55	8.55
λ_g	3.3	3.36	3.3	2.95	3.29	2.95
λ_{cousin}	1.8	1.91	1.98	2.29	1.88	1.7
$h_{all}^2(\%)$	-	75.8	45.9	-	61.7	40.8
$h_{pop}^2(\%)$	-	75.8	85.3	-	61.7	75.3
$h_{pathway}^2(\%)$	-	75.8	78.8	-	61.7	71.3
$c_R(\%)$	-	0	20.0	-	0	2.0
$V_c(\%)$	-	0	4.8	-	0	0.6
$\pi_{phantom}(\%)$	-	0	46.2	-	0	45.9

Table 5: Epidemiological data and model fit for Schizophrenia. Shown are data obtained for disease prevalence (μ) and relative risk to monozygotic twins, siblings, grand-children and cousins ($\lambda_{MZ}, \lambda_s, \lambda_g, \lambda_{cousin}$ respectively) obtained from two different sources. Given the values of μ, λ_s and λ_g (shown in bold-face) from each of the two sources, we then fit two models (A_Δ and $LP_\Delta(2)$) and show the values of $h_{pathway}^2, c_R, h_{all}^2, h_{pop}^2$ and $\pi_{phantom}$ associated with each model.

6.3 Differences among traits

Under the LP model, phantom heritability increases with the number of pathways. This observation suggests that, in general, traits with greater biological complexity may have greater phantom heritability. In this context, it is interesting to observe that genetic studies tend to explain more of the apparent heritability for “simpler” traits than for more “complex” traits. For example, GWAS has explained $\sim 50\%$ of the apparent heritability for the regulation of the levels of fetal hemoglobin.¹⁸ By contrast, GWAS have explained much less of the apparent heritability for arguably more “complex” traits - such as 2% for body-mass index¹⁹ or $< 5\%$ for age of onset of menarche.²⁰ These differences may reflect both the number of loci involved in the traits (indicating that many are still to be discovered) and the physiological interactions underlying the traits (resulting in higher levels

of phantom heritability).

7 Detecting epistasis among variants

7.1 Experimental evidence for epistasis in humans

Despite considerable efforts, few well-replicated instances of epistasis in common human disease and trait genetics have been discovered thus far. The only examples to date involve interactions featuring at least one locus with a large marginal effect, such as HLA. We describe four examples below.

Two recent GWAS, in ankylosing spondylitis²¹ and psoriasis,²² discovered interactions between two different HLA alleles and *ERAP1*. (In ankylosing spondylitis, the HLA-B27 allele has an odds ratio of 40.8, and in psoriasis the HLA-C allele has an odds ratio of 4.66.) HLA also plays a role in an interaction effect described in a GWAS of Type 1 diabetes. (In Type 1 diabetes, HLA has a main effect of 5.5, but acts non-additively with the risk of all other alleles considered cumulatively.²³)

Finally, interaction between *RET* and *EDNRB* in Hirschsprung's disease was discovered in a genome-wide linkage study,²⁴ in which *RET* was strongly associated with disease (log-odds score of 5.6).

If the magnitude of interaction effects scales with marginal effects, then current studies will only be powered to see interactions in which the main effect is large. Thus, many more epistatic interactions between loci with more modest marginal effect size (e.g. 1.1-1.5 as is typical in recent GWAS) might well exist but go undetected due to lack of power.

7.2 Tests for detecting associations and their power

The main problem in detecting these interactions is lack of statistical power. In this section we present three tests for identifying associations between variants or their interactions and a phenotype. We then describe how to compute detection power for the three tests in a GWAS with n individuals, where we consider for simplicity that $n/2$ individuals are cases and $n/2$ are controls.

We assume that the genetic architecture used to generate the data follows the LP model $LP_{\Delta}(k, h_{pathway}^2, c_R, \mu)$ for disease from before. When testing the power of specific loci (or their interactions), we need to fully specify the effect of a single locus (this is not determined by the definition of the LP_{Δ} model). For simplicity, we assume that each pathway consists of m identical loci, where each locus has a single risk allele with frequency f . For a given LP model, the frequency f and the number of loci m determine uniquely the effect of each locus on the trait (represented as genetic relative risk η), and the interactions between different loci (discussed later). We thus compute power as a function of the parameters k , $h_{pathway}^2$, c_R , μ , m and f . The three tests we consider are

- i. a test for detection of association of a single locus with disease.
- ii. a test for detection of a pairwise interaction between two *individual loci*.
- iii. a test for detection of a pairwise interaction between two *pathways*.

In all cases, we compute power efficiently using analytical approximations, which enables us to explore a wide parameters space, including very large sample sizes (on the order of millions). We plot in Supp. Fig. 8 the detection power as function of sample size for the three tests.

7.3 Detecting the marginal effect of each SNP

We first focused on detecting the individual variants. We used the Cochran-Armitage trend test, which detects an association between a (diploid) SNP and the value of a binary trait (e.g. disease).^{25,26} We computed power for this test using an analytic approximation. The test statistic has an approximate chi-square distribution $\chi^2(1)$ under the null hypothesis, and a non-central chi-square distribution $\chi^2(1, NCP)$ under an alternative model. The non-centrality-parameter NCP is a function of the effect size, determined by μ, f and the genetic relative risk η , and the sample size n . To calculate NCP for a locus with risk allele frequency f and effect size η , we first need to compute the observed 2x3 joint probability table $p = \{p_{ij}\}$ for genotype and disease status,

$$p_{ij} \equiv Pr(Z = i, g_{(F)} + g_{(M)} = j), \quad \forall i = 0, 1, j = 0, 1, 2 \quad (7.1)$$

where $g_{(F)}$ and $g_{(M)}$ are the paternal and maternal alleles at a given locus, respectively. The table p is a function of the parameters μ, f and η . We compute $p = \{p_{ij}\}$ in a few steps,

- i. We denote the joint 2x2 table of one allele and disease status in a random sample drawn from the population by p_μ . It is given by,

$$p_{\mu,ij} = f^j(1-f)^{1-j} \left[1 - \frac{\mu\eta^j}{1-f+f\eta}\right]^i \left[\frac{\mu\eta^j}{1-f+f\eta}\right]^{1-i}, \quad \forall i, j = 0, 1 \quad (7.2)$$

- ii. In a balanced study design, with an equal number of cases and controls, the observed joint frequencies frequencies of the allele and disease status change to

$$p_{\frac{1}{2},ij} = \frac{p_{\mu,ij}}{2\mu^i(1-\mu)^{1-i}}, \quad \forall i, j = 0, 1 \quad (7.3)$$

- iii. We compute the genotype 2x3 table from the allele 2x2 table as,

$$p_{ij} = 2^{2-|j-1|} p_{\frac{1}{2},i0}^{2-j} p_{\frac{1}{2},i1}^j, \quad \forall i = 0, 1, j = 0, 1, 2 \quad (7.4)$$

- iv. Let q_{ij} denote the *conditional* probability of genotype j given disease status i . We compute q from p as

$$q_{ij} \equiv Pr(x = j | z = i) = \frac{p_{ij}}{\sum_{j'=0}^2 p_{ij'}} \quad (7.5)$$

- v. We express the non-centrality parameter NCP in terms of the q_{ij} 's (see e.g.^{27,28}). When the number of cases and controls are equal ($n/2$), the formula for NCP is,

$$NCP(n, f, \eta) = \frac{n \left[\sum_{i=0}^2 i(q_{1i} - q_{0i}) \right]^2}{2 \sum_{i=0}^2 i^2(q_{0i} + q_{1i}) - \left[\sum_{i=0}^2 i(q_{0i} + q_{1i}) \right]^2} \quad (7.6)$$

We next write an explicit expression for the power in terms of the non-centrality parameter using the χ^2 distribution. We denote by $F_{\chi^2}(x; d, NCP)$ the cumulative non-central χ^2 distribution function with d degrees of freedom and non-centrality parameter NCP at the value x (that is, the probability that a $\chi^2(d, NCP)$ random variable is smaller than x). When NCP is omitted, $F_{\chi^2}(x; d)$ denotes the central χ^2 distribution. $F_{\chi^2}^{-1}$ is simply the inverse χ^2 cumulative distribution function. With this notation, the power is,

$$Power(n, f, \eta, \alpha) = 1 - F_{\chi^2} \left(F_{\chi^2}^{-1}(1 - \alpha; 1); 1, NCP(n, f, \eta) \right) \quad (7.7)$$

that is, the power is the area under the (true) alternative non-central χ^2 distribution to the right of the value $F_{\chi^2}^{-1}(1 - \alpha; 1)$, which is the expected $1 - \alpha$ quantile under the (null) central χ^2 distribution. We used significance level $\alpha = 5 \times 10^{-8}$, a figure often used in GWAS for genome-wide significance.

7.4 Detecting interaction between a pair of SNPs

We next focused on detecting pairwise interactions between individual variants. We tested for deviations from the A_Δ model for a pair of identified loci. Specifically, for two loci g_1 and g_2 , and a trait z (all three are binary 0/1 variables) we compute the expected and observed joint 2x2x2 tables $p_{ij_1j_2}^{(A_\Delta)}$, $p_{ij_1j_2}^{(LP)}$, obtained under the (false) null model A_Δ and the (true) alternative model LP, respectively.

In a sample drawn at random from the population, the *expected* joint 2x2x2 table $p_{\mu,ij_1j_2}^{(A_\Delta)}$ under the A_Δ model is,

$$\begin{aligned} p_{\mu,ij_1j_2}^{(A_\Delta)} &= Pr(Z = i, g_1 = j_1, g_2 = j_2) = \\ &f^{j_1+j_2} (1-f)^{2-j_1-j_2} \left[1 - \Phi(\tau - \frac{\beta g'_1 + \beta g'_2}{\sqrt{1-2h^2}}) \right]^i \Phi(\tau - \frac{\beta g'_1 + \beta g'_2}{\sqrt{1-2h^2}})^{1-i} \end{aligned} \quad (7.8)$$

where β is the effect size of each of the genotypes under the A_Δ model, computed from f, η and μ by solving eq. (2.7) for β (with $\tau(\mu) = \Phi^{-1}(\mu)$), and $g'_i = h_i - f$ are the normalized genotypes. The observed 2x2x2 table $p_{\mu,ij_1j_2}^{(LP)}$ under the (true) LP model is,

$$\begin{aligned} p_{\mu,ij_1j_2}^{(LP)} &= Pr(Z = i, g_1 = j_1, g_2 = j_2) = \\ &f^{j_1+j_2} (1-f)^{2-j_1-j_2} \left[1 - \Phi(\tau)^{k-2} \Phi(\tau - \frac{\beta g_1}{\sqrt{1-h^2}}) \Phi(\tau - \frac{\beta g_2}{\sqrt{1-h^2}}) \right]^i \\ &\left[\Phi(\tau)^{k-2} \Phi(\tau - \frac{\beta g_1}{\sqrt{1-h^2}}) \Phi(\tau - \frac{\beta g_2}{\sqrt{1-h^2}}) \right]^{1-i} \end{aligned} \quad (7.9)$$

In a balanced study, with equal number of cases and controls, the above two tables change.

$$p_{ij_1j_2}^{(A_\Delta)} = \frac{p_{\mu,ij_1j_2}^{(A_\Delta)}}{2\mu^i(1-\mu)^{1-i}}; \quad p_{ij_1j_2}^{(LP)} = \frac{p_{\mu,ij_1j_2}^{(LP)}}{2\mu^i(1-\mu)^{1-i}} \quad (7.10)$$

The non-centrality parameter is,

$$NCP_2(n, f, \eta) = n \sum_{i,j_1,j_2} \frac{(p_{ij_1j_2}^{(LP)} - p_{ij_1j_2}^{(A_\Delta)})^2}{p_{ij_1j_2}^{(A_\Delta)}} \quad (7.11)$$

and power is given via the χ^2 approximation (in similar to eq. (7.7)),

$$Power_2(n, f, \eta, \alpha) = 1 - F_{\chi^2}^{-1}(1 - \alpha; 1; NCP_2(n, f, \eta)) \quad (7.12)$$

We used a significance level α that accounts for the multiplicity testing among all pairs of loci, $\alpha = 0.01 / \binom{km}{2}$.

7.5 Detecting interaction between two pathways

In principle, the power to detect genetic interactions might be increased by looking at the aggregate effects of sets of genes. One possibility which we describe below would be to place genes into relevant sets (for example, common pathways) and test for “meta-interactions” between these sets. Substantial biological knowledge about the underlying physiology might be required to organize the genes into pathways and infer key aspects of the genetic architecture.

Nevertheless, we devised a test to detect interactions between the two pathways, under the assumption that a subset of the loci in the two pathways are known and can be correctly assigned to the two pathways. We assume that in each pathway Ψ_i multiple loci with small effects were detected. We denote the set of detected loci as S_i . Thus, in similar to eq. (3) in the main text, the i -th pathway can be partitioned as:

$$\Psi_i = x_i + y_i + \epsilon_R + \epsilon_u \quad (7.13)$$

where $x_i = \sum_{j \in S_i} \beta_j g_{i,j}$ and $y_i = \sum_{j \in \bar{S}_i} \beta_j g_{i,j}$ denote the additive contribution of the detected and undetected loci in pathway i , respectively.

We model the additive contributions of detected loci as a Gaussian $x_i \sim N(0, h_{i,known}^2)$ that explains $h_{i,known}^2$ of the total variance of the pathway Ψ_i . We test for an interaction between the detected loci in two pathways. For simplicity we assume these are (x_1, x_2) , representing interaction between the first two pathways. In a balanced case-control study, the available data are a collection of n triplets (x_1, x_2, z) for each individual. x_1 and x_2 are two real numbers, representing the additive contribution of all loci in a given pathway, and z is a binary variable representing disease state (with $z=1$ or $z=0$ in equal numbers of individuals). Under the null hypothesis, the A_Δ model is correct, and the probability of disease is $Pr(Z = 1|x_1, x_2) = \Phi(\beta_0 + \beta_1 x_1 + \beta_2 x_2)$. Since the correct architecture would not be known in advance, we performed a goodness-of-fit test for the A_Δ model. We divided the (x_1, x_2) plane into L^2 equi-probable regions R_{ij} . To avoid bins with few counts, we chose the value of L such that on average, each bin will have at least 50 data points,

$$L = \lfloor \sqrt{n/50} \rfloor \quad (7.14)$$

We then computed the bin boundaries as the quantiles of the standard Gaussian distribution function,

$$b_0 = -\infty, b_L = \infty, \quad b_i = \Phi^{-1}(i/L) \quad \forall i = 1, \dots, L-1 \quad (7.15)$$

In each such region, we compared the observed number of diseased individuals O_{ij} , to the expected number under the A_Δ model, $E_{ij}^{(A_\Delta)}$. The goodness-of-fit test statistic measures the deviations of O_{ij} from $E_{ij}^{(A_\Delta)}$,

$$S = \sum_{ij} \frac{(O_{ij} - E_{ij}^{(A_\Delta)})^2}{E_{ij}^{(A_\Delta)}} \quad (7.16)$$

We compute the observed value O_{ij} in each bin as,

$$O_{ij} = \sum_l z_l \cdot 1_{\{x_{1,l} \in [b_{i-1}, b_i], x_{2,l} \in [b_{j-1}, b_j]\}} \quad (7.17)$$

where the sum is on affected individuals ($z_l = 1$) whose known liabilities $x_{1,l}, x_{2,l}$ are in the i th and j th bins, respectively. We compute the expected number of affected individuals $E_{ij}^{(A_\Delta)}$ in the bin by integrating over the densities of each x_i , and for each (x_1, x_2) pair writing the expected value of the disease status variable z ,

$$\begin{aligned} E_{ij}^{(A_\Delta)} &= \frac{\int_{x_1=b_{i-1}}^{b_i} \int_{x_2=b_{j-1}}^{b_j} Pr(x_1, x_2, z=1) dx_1 dx_2}{\int_{x_1=b_{i-1}}^{b_i} \int_{x_2=b_{j-1}}^{b_j} Pr(x_1, x_2) dx_1 dx_2} = \\ &L^2 \int_{x_1=b_i}^{b_{i+1}} \int_{x_2=b_j}^{b_{j+1}} \varphi(x_1) \varphi(x_2) \Phi\left(\tau - \frac{(x_1 + x_2) h_{i,known}}{\sqrt{1 - 2h_{i,known}^2}}\right) dx_1 dx_2 \end{aligned} \quad (7.18)$$

Under the null-hypothesis, S has an approximate chi-square distribution, $S \sim \chi^2(L^2)$. Under the alternative, S has a non-central chi-square distribution $S \sim \chi^2(L^2, NCP)$. The non-centrality parameter NCP , measuring the (expected) deviation of O_{ij} from its expectation under the (wrong) A_Δ null model, $E_{ij}^{(A_\Delta)}$, is given by the formula,

$$NCP_{path} = \sum_{i,j} \frac{(E_{ij}^{(LP)} - E_{ij}^{(A_\Delta)})^2}{E_{ij}^{(A_\Delta)}(1 - E_{ij}^{(A_\Delta)})} \quad (7.19)$$

where $E_{ij}^{(LP)} = E[O_{ij}]$ is the expected number of disease individuals in bin (i, j) under the alternative (true) LP model. The formula for $E_{ij}^{(LP)}$ under the alternative LP model is (compare to eq. (7.18)),

$$E_{ij}^{(LP)} = L^2 \int_{x_1=b_{i-1}}^{b_i} \varphi(x_1) \Phi\left(\tau - \frac{x_1 h_{i,known}}{\sqrt{1 - h_{i,known}^2}}\right) dx_1 \int_{x_2=b_{j-1}}^{b_j} \varphi(x_2) \Phi\left(\tau - \frac{x_2 h_{i,known}}{\sqrt{1 - h_{i,known}^2}}\right) dx_2 \quad (7.20)$$

Using this approximation, we computed power as the tail probability under the non-central chi-square distribution, in similar to eq. (7.7):

$$Power_{path}(n, h_{i,known}^2, \alpha) = 1 - F_{\chi^2}(F_{\chi^2}^{-1}(1 - \alpha; L^2); L^2, NCP_{path}(n, h_{i,known}^2)) \quad (7.21)$$

We used a significance level α accounting just for multiplicity in testing all pairs of *pathways*, $\alpha = 0.01/\binom{k}{2}$.

8 Consistent estimator $h_{\text{slope}(\kappa_0)}^2$: Proof of Theorem 1

In the main text, we describe a top-down estimator $h_{\text{slope}(\kappa_0)}^2$ for h_{all}^2 that is provably consistent even in the presence of genetic interactions. In this section, we provide the proof. Our estimator is based on observing how the phenotypic correlation between individuals varies with the proportion of their genomes in large IBD segments. A few important definitions and comments:

- By a “large IBD segment”, we mean a segment that is identical-by-descent (having descended from a recent common ancestor) and exceeds a specified threshold L in length (measured in centimorgans). The threshold L determines the expected number N_g of generations to the common ancestor.
- By the IBD-sharing level between two individuals, we mean the probability that a randomly chosen genomic position on homologous chromosomes from each of the individuals lies in a large IBD segment shared by the two individuals. Thus IBD sharing takes values between 0 and 1.
- Large IBD segments can be readily recognized by virtue of two individuals sharing alleles at a large number of consecutive markers across a region. Several algorithms for detecting large IBD segments have been described recently.^{29,30,31} By focusing on large IBD segments, we ensure that the segments have a recent common ancestor. This avoids the issues with defining and identifying small IBD segments discussed by Powell et al.³¹
- We will assume that large IBD segments are genetically identical at the causal loci within the segment. Rarely, apparently IBD segments will have different alleles at a causal locus if a new mutation has occurred since the common ancestor. Our estimate of h_{all}^2 will therefore exclude heritability due to such extremely recent mutations. In practice, the probability-per-generation of new mutations is extremely low ($\sim 2 \times 10^{-8}$), and the total probability of new mutations since the common ancestor can be bounded (as noted above, the length threshold L sets the expected number N_g of generations to the common threshold). Extremely new mutations could play a significant role only if the alleles responsible for a trait (i) largely act dominantly and (ii) have extremely high selective coefficients, so that they are eliminated extremely rapidly from the population.

8.1 Heritability on the observed scale

We now turn to the proof of Theorem 1. The theorem applies to both quantitative traits and to disease traits, when measured on the observed (0,1) scale.

Theorem 1 *Consider a population in which one can detect large segments shared IBD between individuals. Given individuals I_1 and I_2 , let $\kappa = \kappa(I_1, I_2)$ denote the proportion of their genomes shared in large IBD segments. Let κ_0 denote the average value of κ across the pairs in the population. For a trait $Z = \Psi(G, E)$, let $\rho(\kappa)$ denote the average phenotypic correlation between pairs of*

individuals who share proportion κ of their genomes in large IBD blocks. Define the “heritability at unrelatedness”, $h_{slope(\kappa_0)}^2 = (1 - \kappa_0)\rho'(\kappa_0)$.

Then, regardless of the genetic architecture of the trait,

$$h_{slope(\kappa_0)}^2 = h_{all}^2 \quad (8.1)$$

In other words, the true heritability, h_{all}^2 , equals $(1 - \kappa_0)$ times the rate of change of phenotypic correlation around the average level of IBD-segment sharing, $\rho'(\kappa_0)$.

Thus, if $\widehat{\rho'(\kappa_0)}$ is a consistent estimator of $\rho'(\kappa_0)$, obtained from pairwise genotypic and phenotypic similarities in a population sample, then $\widehat{h_{slope(\kappa_0)}^2} = (1 - \kappa_0)\widehat{\rho'(\kappa_0)}$ is a consistent estimator of h_{all}^2 .

Proof: We will consider the distribution of genotypes and phenotypes for pairs (I_1, I_2) of individuals in the population, conditional on their degree of IBD sharing. For individual I_j (for $j = 1, 2$), we will denote the genotype by $G_j = (g_{j1}, g_{j2}, \dots, g_{jn})$ and the phenotype by $Z_j = \Psi(G_j, E_j)$. To simplify the proof, we will write the variant loci on the maternally and paternally inherited genomes separately, so that each genotype g_{ji} is a binary variable.

i. **Genotypic correlation.** Let $\vartheta(\kappa)$ denote the conditional probability distribution on pairs (G_1, G_2) of genotypes, conditional on the individuals having average IBD sharing level κ . (That is, $\vartheta(\kappa)[(G_1, G_2)]$ denotes the conditional probability of the genotype (G_1, G_2) .) In particular, $\vartheta(\kappa_0)$ is the background distribution for the whole population, in which G_1 and G_2 are independent. We similarly let $\vartheta_i(\kappa)$ denote the conditional probability distribution over pairs (g_{1i}, g_{2i}) of genotypes at the i -th locus, conditional on the individuals having average IBD sharing level κ .

Because the variant sites are assumed to be in linkage equilibrium, $\vartheta(\kappa)$ is the product of the distributions $\vartheta_i(\kappa)$:

$$\vartheta(\kappa)[(G_1, G_2)] = \prod_{i=1}^n \vartheta_i(\kappa)[(g_{1i}, g_{2i})] \quad (8.2)$$

We can express $\vartheta_i(\kappa)$ as a mixture of the distribution $\vartheta_i(1)$, conditional on IBD-sharing at the i -th locus and the distribution $\vartheta_i(0)$, conditional on non-IBD-sharing at the i -th locus:

$$\vartheta_i(\kappa) = \kappa\vartheta_i(1) + (1 - \kappa)\vartheta_i(0). \quad (8.3)$$

One can then show that,

$$\vartheta_i(\kappa_0 + \epsilon) = \frac{\epsilon}{1 - \kappa_0}\vartheta_i(1) + \left(1 - \frac{\epsilon}{1 - \kappa_0}\right)\vartheta_i(\kappa_0). \quad (8.4)$$

(To see this, write eq. (8.3) for $\vartheta_i(\kappa_0)$ and for $\vartheta_i(\kappa_0 + \epsilon)$. Solve for $\vartheta_i(0)$ in eq. (8.3) for $\vartheta_i(\kappa_0)$ and substitute it in eq. (8.3) for $\vartheta_i(\kappa_0 + \epsilon)$.) For notational convenience below, we will rewrite eq. (8.4) as

$$\vartheta_i(\kappa_0 + \epsilon) = \frac{\epsilon}{1 - \kappa_0}\vartheta_i^*(1) + \left(1 - \frac{\epsilon}{1 - \kappa_0}\right)\vartheta_i^*(0) \quad (8.5)$$

where $\vartheta_i^*(1) = \vartheta_i(1)$ and $\vartheta_i^*(0) = \vartheta_i(\kappa_0)$. Using the equations above, we have:

$$\begin{aligned} \vartheta(\kappa_0 + \epsilon) &= \prod_{i=1}^n \vartheta_i(\kappa_0 + \epsilon) = \\ &\prod_{i=1}^n \left[\frac{\epsilon}{1 - \kappa_0} \vartheta_i^*(1) + \left(1 - \frac{\epsilon}{1 - \kappa_0}\right) \vartheta_i^*(0) \right] = \\ &\sum_{T=(t_1, t_2, \dots, t_n) \in \mathbb{Z}_2^n} \left[\frac{\epsilon}{1 - \kappa_0} \right]^{w(T)} \left[1 - \frac{\epsilon}{1 - \kappa_0} \right]^{n-w(T)} \prod_{i=1}^n \vartheta_i^*(t_i) \end{aligned} \quad (8.6)$$

where \mathbb{Z}_2^n is the set of binary vectors of length n and $w(T)$ is the number of non-zero entries in the vector T .

ii. Phenotypic correlation. Consider the phenotypic correlation for individuals with IBD sharing level κ . Because Z_1 and Z_2 have expected value 0, we have:

$$\rho(\kappa) = E_{\vartheta(\kappa)}[Z_1 Z_2] = \sum_{(G_1, G_2)} \vartheta(\kappa)[(G_1, G_2)] E[Z_1 Z_2 | G_1, G_2]. \quad (8.7)$$

where E_D denotes the expectation under the distribution D . We want to calculate the derivative $\rho'(\kappa_0)$. To calculate $\rho'(\kappa_0) = \frac{d}{d\epsilon} \vartheta(\kappa_0 + \epsilon)|_{\epsilon=0}$, we examine eq. (8.6) as $\epsilon \rightarrow 0$. Because all terms corresponding to vectors T with $w(T) > 1$ have derivative 0 at κ_0 , we have:

$$\rho'(\kappa_0) = \frac{1}{1 - \kappa_0} \left[-n\vartheta(\kappa_0) + \sum_{i=1}^n \vartheta(T_i) \right] \quad (8.8)$$

where T_i is the vector that is all zero except at position i . We thus have

$$\rho'(\kappa_0) = \frac{1}{1 - \kappa_0} \left[-nE_{\vartheta(\kappa_0)}[Z_1 Z_2] + \sum_{i=1}^n E_{\vartheta(T_i)}[Z_1 Z_2] \right] \quad (8.9)$$

We need two facts. First, we have $E_{\vartheta(\kappa_0)}[Z_1 Z_2] = 0$. This holds because Z_1 and Z_2 are independent under $\vartheta(\kappa_0)$, which is the unconditional background distribution for the population. Second, $E_{\vartheta(T_i)}[Z_1 Z_2] = V_i$, where V_i is the additive variance explained by the i -th variant. This follows because

$$E_{\vartheta(T_i)}[Z_1 Z_2] = E[Z_1 Z_2 | g_{1i} = g_{2i}] = \sum_j Pr(g_{1i} = j) E[Z_1 | g_{1i} = j]^2 = E[Z^2] - Var[Z | g_i] = V_i. \quad (8.10)$$

where we have used the facts that (i) when the two individuals share only the i -th variant by descent, Z_1 and Z_2 are conditionally independent given the value of g_i , and (ii) $E[y]^2 = E[y^2] - Var[Y]$ for any random variable y . Finally, we have:

$$\rho'(\kappa_0) = \frac{1}{1 - \kappa_0} [0 + \sum_{i=1}^n V_i] = \frac{1}{1 - \kappa_0} V_A = \frac{1}{1 - \kappa_0} h_{all}^2. \quad (8.11)$$

■

Some notes concerning Theorem 1:

- The proof makes no assumption on the genetic architecture of the trait: it may involve dominance at a locus or genetic interactions among loci. (By denoting maternal and paternal alleles separately, dominance is simply a special case of a genetic interaction - that is, between the maternal and paternal alleles at a locus.)
- The proof makes no assumption that IBD blocks contain only a single causal variant.
- The proof assumes that the proportion of genome shared in large IBD blocks can be measured accurately. Because we restrict attention to “large” IBD blocks (exceeding a specified threshold length L), identity-by-descent can be reliably detected by virtue of allele sharing at a large number of consecutive genetic loci. The precise boundaries of the IBD block may not be measured perfectly, because small regions of IBS sharing at the edge of the block may be inaccurately scored as IBD. This will introduce some noise in the estimate. However, the proportional impact on the overall estimate of IBD sharing is expected to be small for large IBD blocks and could be eliminated by using complete genome sequence information.

8.2 Ascertainment bias in Case-Control studies

Theorem 1 provides a consistent estimator of the heritability for both quantitative and disease traits, provided that the slope is measured in a representative sample from the population. For disease traits, it is typical to use case-control studies, where the proportion of cases is larger than the proportion in the population. Using a non-representative sample creates a bias in the derivative ρ' that must be corrected. Suppose that a disease has prevalence μ , and we use a case-control study in which the proportion of affected individuals is μ_{cc} . As shown in ref.³², the derivative in a representative sample, $\rho'(\kappa)$, is related to the derivative calculated in the case-control study, $\rho'_{cc}(\kappa)$, by the following formula:

$$\rho'(\kappa) = \frac{\mu(1 - \mu)}{\mu_{cc}(1 - \mu_{cc})} \rho'_{cc}(\kappa) \quad (8.12)$$

8.3 Heritability on a hidden liability scale

As discussed in Section 2, geneticists often assume that disease traits arise from a liability threshold model. They typically compute heritability not on the observed disease scale, but rather with respect to the unseen liability scale. In the special case in which the liability is a strictly additive function of the genotypes that has a normal distribution, there is a simple conversion between the heritability on the disease and liability scales:⁴

$$h_S^2 = \frac{\mu(1 - \mu)}{\varphi(x_\mu)^2} h_{S,\Delta}^2 \quad (8.13)$$

where S is a set of variants, h_S^2 is the heritability on the liability scale attributable to the variants in S , $h_{S,\Delta}^2$ is the heritability on the disease scale attributable to the variants in S , μ is the disease prevalence, $x_\mu = \Phi^{-1}(1 - \mu)$ is the threshold and φ is the standard Gaussian density function.

Geneticists like to use the liability scale when estimating the total additive heritability, because calculations on the liability scale tend to be less sensitive to uncertainty about the precise prevalence. However, the choice of scale is irrelevant when calculating the fraction $\frac{h_{known}^2}{h_{all}^2}$ of the total additive heritability explained by a set of known loci (inasmuch as the formula above involves multiplying the numerator and denominator by the same constant).

Importantly, the formula above does not hold in general when the liability function is not additive and normal. When considering traits that may involve additive interactions, it thus makes sense to calculate $\pi_{explained} = \frac{h_{known}^2}{h_{all}^2}$ on the disease scale.

9 Applying the theorem in practice

To apply the theorem in practice, we would proceed as follows:

- i. For each pair of individuals in a sample of size n , calculate the pairwise phenotypic product matrix $\rho(i, j)$ (defined as the product $Z_1 \times Z_2$ of the (normalized) phenotypes) and the pairwise IBD-sharing matrix $B(i, j)$ (defined as the proportion of the genotype inferred to be in “large” segments, based on dense genotype information and an appropriate definition of “large”).
- ii. For a window size ϵ , regress the values of $\rho(i, j)$ on $B(i, j)$ for those pairs (i, j) of individuals with IBD sharing in the interval $[\kappa_0 - \epsilon, \kappa_0 + \epsilon]$. (Ideally, one should use a weighted generalized least-square regression so that (i) equal weight is attached to each value of κ , and (ii) correlations in the $\rho(i, j)$ values for different pairs are taken into account.)
- iii. Determine the slope β and set $h_{all}^2 = (1 - \kappa_0)\beta$. While Theorem 1 applies to the limit as $\epsilon \rightarrow 0$, two considerations must be balanced in practice: On the one hand, if ϵ is too small, there will be too few pairs to obtain a good estimate. On the other hand, if ϵ is too large, the value may not agree with the limit as $\epsilon \rightarrow 0$. In fact, the error in the slope is $O(\epsilon^2)$ and thus is not overly sensitive to ϵ . In practice, one would examine multiple values of ϵ .

9.1 Heuristic formula for variance of slope

We give a heuristic formula for the variance of our estimate of the slope β , as a function of the number of individuals n . We first recall standard facts on slope estimation in linear regression. Consider the linear model

$$Y = \beta_0 + \beta_1 X + \xi \quad (9.1)$$

where $\xi \sim N(0, \sigma_\xi^2)$ is a noise variable, and the error variables ξ are independent Gaussian random variables. Under this model, one can obtain an estimator $\hat{\beta}$ for the slope β_1 using standard least squares. The distribution of the estimator $\hat{\beta}$ when observing m independent observations (x_i, y_i) can be explicitly written as,

$$\hat{\beta} \sim N\left(\beta_1, \frac{\sigma_\xi^2}{\sum_{i=1}^m (x_i - \bar{x})^2}\right) \quad (9.2)$$

When m is large, the variance is approximately

$$Var[\hat{\beta}] = \frac{\sigma_\xi^2}{m\sigma_x^2} \quad (9.3)$$

We can apply the approximate formula in eq. (9.3) to our situation of regressing $\rho(i, j)$ on $B(i, j)$. First, we estimate the variance of $Z_1 Z_2$ for individuals with a given IBD sharing level near κ_0 to be similar to the variance of $Z_1 Z_2$ for individuals whose expected IBD sharing level is κ_0 , which is equal to 1 (since Z_1 and Z_2 are independent in this case). Second, we define $\alpha(\epsilon)$ to be the proportion of pairs with IBD sharing in the interval $[\kappa_0 - \epsilon, \kappa_0 + \epsilon]$. Since we have n individuals,

the number of pairs of individuals with IBD in the interval is $M(\epsilon) = \alpha(\epsilon) \binom{n}{2}$. Third, we define $\sigma_{IBD}(\epsilon)$ to be the standard deviation of IBD sharing for pairs of individuals with IBD sharing in the interval $[\kappa_0 - \epsilon, \kappa_0 + \epsilon]$. With these definitions, the variance of $\hat{\beta}$ should be approximately

$$Var[\hat{\beta}] = \frac{1}{\alpha(\epsilon) \binom{n}{2} \sigma_{IBD}(\epsilon)^2} \quad (9.4)$$

And

$$\sigma[\hat{\beta}] \sim \frac{\sqrt{2}}{\sqrt{\alpha(\epsilon)} n \sigma_{IBD}(\epsilon)} \quad (9.5)$$

Since our estimate for h_{all}^2 is $(1 - \kappa_0)\hat{\beta}$, the variance of our estimate is $(1 - \kappa_0)\sigma[\hat{\beta}]$.

9.2 Simulation

We applied the theorem to simulated data to examine its performance. We did not attempt to create a fully realistic model of IBD relationships in an isolated population, but instead used a simple model as follows:

We assume a current population of n individuals originated from a founding population of n_F different founders, who themselves did not share any large IBD blocks. We thus mark each of the founding genomes with a distinct “color”. We designate n_c causal variant sites in the genome and designate certain colors at each site to indicate the presence of a risk allele (with the choice made so as to achieve a specified risk-allele frequency.) We generate modern genomes as a mosaic of the founding genomes, with an average of n_b recombination events. We generate a phenotype for each individual based on the genotype at the causal variants and on the phenotype function Ψ . We calculate the IBD relationships between individuals based on their genotypes, where IBD blocks are regions with the same color.

We generated data for a quantitative trait following the P^* model ($= LP(4, 50\%)$), with 1000 causal variants with risk-allele frequency $f = 50\%$. We assumed a founding population of 28 individuals and a recombination density of 23 events. These values were chosen such that the mean and standard deviation of the resulting IBD distribution (3.6% and 4.0%) are roughly similar to that observed in the Qatari population (3.6% and 4.0%) (data kindly provided by Haley Hunter-Zinck and Andrew Clark³³). The true heritability for the P^* model is $h_{all}^2 = 25.4\%$. When we performed 100 simulations with samples of 1000 individuals, the estimated values in various windows around the mean were very close to the true values (for example, 0.258 ± 0.082 for $\epsilon = 0.036$). Estimates were similar for values of ϵ that cover more than $\sim 20\%$ of the pairs.

We also performed simulations for other population parameters, which were consistent with the result in Theorem 1.

Detailed simulations to study the performance characteristics of the estimate would best be performed using actual genotype data from real populations.

10 Estimator based on slope of variation in IBD sharing among sibs

Visscher et al.³⁴ proposed estimating heritability by regressing phenotypic correlation between sibs on their level of IBD sharing. The notion is premised on the fact that the level of IBD sharing varies around the mean of 50%, with a standard deviation of $\sim 4\%$. The estimator has the attraction that it compares pairs of individuals of the same familial relationships (that is, sibs) and thus, unlike estimates based on comparisons among different types of relatives, is not confounded by differences in shared-environment components among relative types. We will refer to this estimator as $h_{\text{slope(sib)}}^2$.

The problem with the estimator $h_{\text{slope(sib)}}^2$ is that it is not consistent. One can see this in two ways:

- i. Mathematically, one can see by examining the proof of Theorem 1 that the value of $\rho'(\kappa)$ for $\kappa > \kappa_0$ has additional positive terms (arising from interactions) and thus over-estimates h_{all}^2 .
- ii. Empirically, one can simply calculate the value of $h_{\text{slope(sib)}}^2$ for a specific model and show that $h_{\text{slope(sib)}}^2 > h_{\text{all}}^2$. For P^* (the $LP(4)$ model discussed above), we can calculate that $h_{\text{pop}}^2(ADE) = 79.2\%$, $h_{\text{pop}}^2(PO) = 70.9\%$, $h_{\text{pop}}^2(ACE) = 54.0\%$, $h_{\text{slope(sib)}}^2 = 30.5\%$ and $h_{\text{all}}^2 = 25.4\%$. The phantom heritability associated with $h_{\text{slope(sib)}}^2$ is thus lower than the phantom heritability associated with the traditional estimators, it is still $16.7\% = (30.5 - 25.4)/25.4$.

11 Arguments advanced in support of additivity

Various authors (such as Hill et al.⁹) have proposed arguments in support of the notion that genetic interactions play little role in complex traits. We briefly discuss these arguments, pointing out the flaws.

11.1 Allele frequencies

Hill et al.⁹ assert that genetic theory implies that complex traits will have largely additive variance. Specifically, they state that (a) most variants in a large population will have extremely low minor allele frequency and (b) traits caused by low-frequency alleles will not have substantial variance due to interactions.

Their claim is wrong, because the LP models (a) can have substantial variance due to interactions (indeed, the majority) and yet (b) can involve any class of allele frequencies. (Specifically, LP models are defined as the minimum value of a set of traits, each of which is additive and normally distributed. There is no constraint on the allele frequencies of the variants that sum to yield these additive and normally distributed traits.)

What then is the flaw in Hill et al.'s argument?

- i. Hill et al.⁹ consider only two-locus models - rather than multi-locus models. (They examine a 10-locus model, but 8 of the loci are monomorphic, so the model is equivalent to a two-locus model.) Multi-locus models have much greater opportunity for genetic interactions, because n loci have $n(n - 1)/2$ potential interactions. (Hill et al. actually discuss a single multi-locus model: their "duplicate factor" model. Notably, this model shows huge (100%) interaction variance, but they argue that "such extreme models" are not compatible with observed data.)
- ii. The main problem with the argument, however, is more fundamental. We discuss it for their two-locus models (although the reasoning applies to multi-locus models as well). Hill et al.⁹ carry out detailed calculations for various two-locus models, calculating the expected values of the interaction variance V_{AA} , under the "U"-shaped allele-frequency distribution expected in large populations. Their argument boils down to the following:
 - Consider two loci with alleles A, a and B, b , where the first allele is the major allele.
 - As the population grows, the allele frequencies of a and b tend to zero. (That is, the loci tend toward monomorphism.)
 - As the allele frequencies of a and b tend to zero, three (of the nine possible) genotypes dominate the population ($AABB, AABb, AaBB$).
 - As these three genotypes dominate the population, the ratio of the interaction variance to the total genetic variance V_{AA}/V_G tends to zero (since there can be no interaction terms with only three states and two variables).

The problem with this reasoning is: As the population grows (and the typical locus tends toward monomorphism), typical traits involving typical loci become very boring! They not only have low interaction variance V_{AA} , they also have very low total genetic variance V_G . That is, the typical trait doesn't vary much in the population! In effect, Hill et al.'s theory thus actually describes what happens for *rare* traits caused by a few *rare* variants. Not surprisingly, interactions account for a small proportion of the variance for such traits.

Hill et al.'s model, however, is not pertinent to common traits. The *interesting* complex traits are those that have significant genetic variance in the population: these traits necessarily have higher allele frequencies (assuming they depend only on a few, e.g. two loci) and thus, under Hill et al.'s analysis, can involve larger interaction variance and a higher ratio V_{AA}/V_G . (We illustrate this point in Supp. Fig. 9, where we analyze the first two-locus model in Hill et al.⁹ In the example, we have $V_{AA}/V_G > 50\%, 20\%$ and 10% for minor allele frequencies $> 27\%, 14\%$ and 8% , respectively. The cases with very low interaction variance have much lower-than-average genetic variance.)

11.2 Breeder's equation

Breeders have long successfully employed the so-called “breeder’s equation”, which states that the *response* to selection scales *linearly* with the *strength* of selection, over generations. Some authors appear to believe that a roughly linear response to selection implies that the trait itself has an additive architecture. However, this is false. The breeder’s equation¹ is

$$\Delta\mu = A\Delta s \tag{11.1}$$

where Δs denotes the average phenotypic shift of the parents selected for breeding (relative to the population mean) and $\Delta\mu$ denotes the average phenotypic shift of the resulting offspring. The coefficient A is determined by the correlation between mid-parents and offspring phenotypes - that is, by the slope of the regression line for these quantities. It is frequently referred to as the “heritability”. More precisely, A is the top-down quantity $h_{pop}^2(PO)$, which does not necessarily equal the narrow-sense heritability h_{all}^2 .

The equation can be mathematically proven to hold exactly in the case of a strictly additive trait. However, importantly, it also holds approximately for a wide range of non-additive traits.

Specifically, the equation will hold whenever the mid-parent and offspring phenotypes are linearly related across a wide range of values. (That is, they are distributed along a regression line - whose slope is, by definition, $h_{pop}^2(PO)$.) If we select parents with an average phenotypic shift of Δs , then their offspring will have an average phenotypic shift of $h_{pop}^2(PO)\Delta s$. This relationship will continue to hold across generations of selection, provided that the points largely lie in the linear range of parent-offspring correlation.

For typical *LP* traits, parent-offspring values fall along a regression line despite the fact that the LP models involve interactions. The case of $P^* = LP(4, 50\%, 50\%)$ model is illustrated in Supp.

Fig. 10. The model itself is highly non-linear ($h_{all}^2 = 25.4\%$, $h_{pop}^2(PO) = 70.8\%$), yet the relation between the mid-parent value and the offspring value is very close to linear.

We performed a computer simulation on this trait (Supp. Fig. 11). For various selection cutoffs T , we randomly selected genotypes for parents conditional on both having phenotype $> T$ and calculated the value of the phenotype for an offspring. We confirmed that (i) the response to selection is indeed very nearly linear in the strength of selection and (ii) the slope is very close to the apparent heritability $h_{pop}^2(PO) = 70.8\%$, but far from the true heritability $h_{all}^2 = 25.4\%$.

11.3 Observed sibling correlations

As evidence that quantitative traits fit an additive model, some authors have cited the observation that the observed median value of $r_{MZ} - 2r_{DZ}$ across traits is centered around zero. For example, Hill et al.⁹ note that the median value of $(r_{MZ} - 2r_{DZ})$ for 86 quantitative traits is close to zero. They suggest that this observation provides support for an additive model.

We do not find this argument persuasive for two reasons. First, the observed value of $(r_{MZ} - 2r_{DZ})$ actually varies widely (from -0.50 to $+0.30$) - much more widely than appears to be consistent with sampling error. Second, shared environment is known to be important for many traits. For a strictly additive trait, shared environment will cause $(r_{MZ} - 2r_{DZ})$ to be negative. The fact that $(r_{MZ} - 2r_{DZ})$ is observed to be centered around zero could thus be taken as a case for the presence of genetic interactions, because genetic interactions would increase $(r_{MZ} - 2r_{DZ})$ and thus offset the effects of shared environment. In short, the empirical data are not compelling.

12 Supplementary code

We have implemented the calculations used in the paper in a Matlab software package. The package provides functions for computing heritability for non-additive models (e.g. the LP models), functions for computing detection power for different tests for epistasis, functions for simulating populations with IBD structure and for computing our estimator $h_{\text{slope}(\kappa_0)}^2$, and many additional utilities. The package is available at www.broadinstitute.org/mpg/hc, with a readme file providing explanations for the different functions. Please refer any questions to orzuk@broadinstitute.org.

References

1. M. Lynch and B. Walsh. *Genetics and Analysis of Quantitative Traits*. Sinauer Associates, Inc., 1998.
2. D.S. Falconer and T.F.C. Mackay. Introduction to quantitative genetics (4th edn.).
3. F. Galton. Regression towards mediocrity in hereditary stature. *The Journal of the Anthropological Institute of Great Britain and Ireland*, 15:246–263, 1886.
4. E.R. Dempster and I.M. Lerner. Heritability of threshold characters. *Genetics*, 35(2):212, 1950.
5. D.S. Falconer. The inheritance of liability to certain diseases, estimated from the incidence among relatives. *Annals of Human Genetics*, 29(1):51–76, 1965.
6. P.D. Sasieni. From genotypes to genes: doubling the sample size. *Biometrics*, 53(4):1253–1261, 1997.
7. S.M. Berman. Limit theorems for the maximum term in stationary sequences. *The Annals of Mathematical Statistics*, 35(2):502–516, 1964.
8. E.L. Ferguson and H.R. Horvitz. The multivulva phenotype of certain *caenorhabditis elegans* mutants results from defects in two functionally redundant pathways. *Genetics*, 123(1):109–121, 1989.
9. W.G. Hill, M.E. Goddard, and P.M. Visscher. Data and theory point to mainly additive genetic variance for complex traits. *PLoS Genetics*, 4(2):e1000008, 2008.
10. N.R. Wray and M.E. Goddard. Multi-locus models of genetic risk of disease. *Genome Medicine*, 2(2):1–13, 2010.
11. A. Franke, D.P.B. McGovern, J.C. Barrett, K. Wang, G.L. Radford-Smith, T. Ahmad, C.W. Lees, T. Balschun, J. Lee, R. Roberts, et al. Genome-wide meta-analysis increases to 71 the number of confirmed Crohn’s disease susceptibility loci. *Nature Genetics*, 42(12):1118–1125, 2010.
12. C.M. Lewis, S.C.L. Whitwell, A. Forbes, J. Sanderson, C.G. Mathew, and T.M. Marteau. Estimating risks of common complex diseases across genetic and environmental factors: the example of crohn disease. *Journal of Medical Genetics*, 44(11):689–694, 2007.
13. M.D. Kappelman, S.L. Rifas-Shiman, K. Kleinman, D. Ollendorf, A. Bousvaros, R.J. Grand, and J.A. Finkelstein. The prevalence and geographic distribution of crohn’s disease and ulcerative colitis in the united states. *Clinical Gastroenterology and Hepatology*, 5(12):1424–1429, 2007.
14. J.F. Fielding. The relative risk of inflammatory bowel disease among parents and siblings of Crohn’s disease patients. *Journal of clinical gastroenterology*, 8(6):655, 1986.

15. M. McGue, I.I. Gottesman, and D.C. Rao. The transmission of schizophrenia under a multi-factorial threshold model. *American Journal of Human Genetics*, 35(6):1161–1178, 1983.
16. N. Risch. Linkage strategies for genetically complex traits. I. Multilocus models. *American Journal of Human Genetics*, 46(2):222–228, 1990.
17. P. Lichtenstein, C. Björk, C.M. Hultman, E. Scolnick, P. Sklar, and P.F. Sullivan. Recurrence risks for schizophrenia in a swedish national cohort. *Psychological Medicine*, 36(10):1417–1426, 2006.
18. G. Galarneau, C.D. Palmer, V.G. Sankaran, S.H. Orkin, J.N. Hirschhorn, and G. Lettre. Fine-mapping at three loci known to affect fetal hemoglobin levels explains additional genetic variation. *Nature Genetics*, 42(12):1049–1051, 2010.
19. E.K. Speliotes, C.J. Willer, S.I. Berndt, K.L. Monda, G. Thorleifsson, A.U. Jackson, H.L. Allen, C.M. Lindgren, J. Luan, R. Mgi, et al. Association analyses of 249,796 individuals reveal 18 new loci associated with body mass index. *Nature Genetics*, 42(11):937–948, 2010.
20. C.E. Elks, J.R.B. Perry, P. Sulem, D.I. Chasman, N. Franceschini, C. He, K.L. Lunetta, J.A. Visser, E.M. Byrne, D.L. Cousminer, et al. Thirty new loci for age at menarche identified by a meta-analysis of genome-wide association studies. *Nature Genetics*, 42(12):1077–1085, 2010.
21. D.M. Evans, C.C.A. Spencer, J.J. Pointon, Z. Su, D. Harvey, G. Kochan, U. Opperman, A. Dilthey, M. Pirinen, M.A. Stone, et al. Interaction between ERAP1 and HLA-B27 in ankylosing spondylitis implicates peptide handling in the mechanism for HLA-B27 in disease susceptibility. *Nature Genetics*, 43(8):761–767, 2011.
22. A. Strange, F. Capon, C.C.A. Spencer, J. Knight, M.E. Weale, M.H. Allen, A. Barton, G. Band, C. Bellenguez, J.G.M. Bergboer, et al. A genome-wide association study identifies new psoriasis susceptibility loci and an interaction between HLA-C and ERAP1. *Nature Genetics*, 42(11):985–990, 2010.
23. J.C. Barrett, D. Clayton, P. Concannon, B. Akolkar, J.D. Cooper, H.A. Erlich, C. Julier, G. Morahan, J. Nerup, C. Nierras, et al. Genome-wide association study and meta-analysis finds over 40 loci affect risk of type 1 diabetes. *Nature Genetics*, 41(6):703–707, 2009.
24. M.M. Carrasquillo, A.S. McCallion, E.G. Puffenberger, C.S. Kashuk, N. Nouri, and A. Chakravarti. Genome-wide association study and mouse model identify interaction between RET and EDNRB pathways in hirschsprung disease. *Nature Genetics*, 32(2):237–244, 2002.
25. W.G. Cochran. Some methods for strengthening the common χ^2 tests. *Biometrics*, 10(4):417–451, 1954.
26. P. Armitage. Tests for linear trends in proportions and frequencies. *Biometrics*, 11(3):375–386, 1955.

27. D.G. Chapman and J.M. Nam. Asymptotic power of chi square tests for linear trends in proportions. *Biometrics*, 24(2):315–327, 1968.
28. D. Gordon, S.J. Finch, M. Nothnagel, and J. Ott. Power and sample size calculations for case-control genetic association tests when errors are present: application to single nucleotide polymorphisms. *Human Heredity*, 54(1):22–33, 2002.
29. S. Purcell, B. Neale, K. Todd-Brown, L. Thomas, M.A.R. Ferreira, D. Bender, J. Maller, P. Sklar, P.I.W. de Bakker, M.J. Daly, et al. PLINK: a tool set for whole-genome association and population-based linkage analyses. *The American Journal of Human Genetics*, 81(3):559–575, 2007.
30. S.R. Browning and B.L. Browning. High-resolution detection of identity by descent in unrelated individuals. *The American Journal of Human Genetics*, 86(4):526–539, 2010.
31. J.E. Powell, P.M. Visscher, and M.E. Goddard. Reconciling the analysis of IBD and IBS in complex trait studies. *Nature Reviews Genetics*, 11(11):800–805, 2010.
32. S.H. Lee, N.R. Wray, M.E. Goddard, and P.M. Visscher. Estimating missing heritability for disease from genome-wide association studies. *The American Journal of Human Genetics*, 88(3):294–305, 2011.
33. H. Hunter-Zinck, S. Musharoff, J. Salit, K.A. Al-Ali, L. Chouchane, A. Gohar, R. Matthews, M.W. Butler, J. Fuller, N.R. Hackett, et al. Population genetic structure of the people of qatar. *The American Journal of Human Genetics*, 87(1):17–25, 2010.
34. P.M. Visscher, S.E. Medland, MA Ferreira, K.I. Morley, G. Zhu, B.K. Cornes, G.W. Montgomery, and N.G. Martin. Assumption-free estimation of heritability from genome-wide identity-by-descent sharing between full siblings. *PLoS Genetics*, 2(3):e41, 2006.

13 Supplementary figures

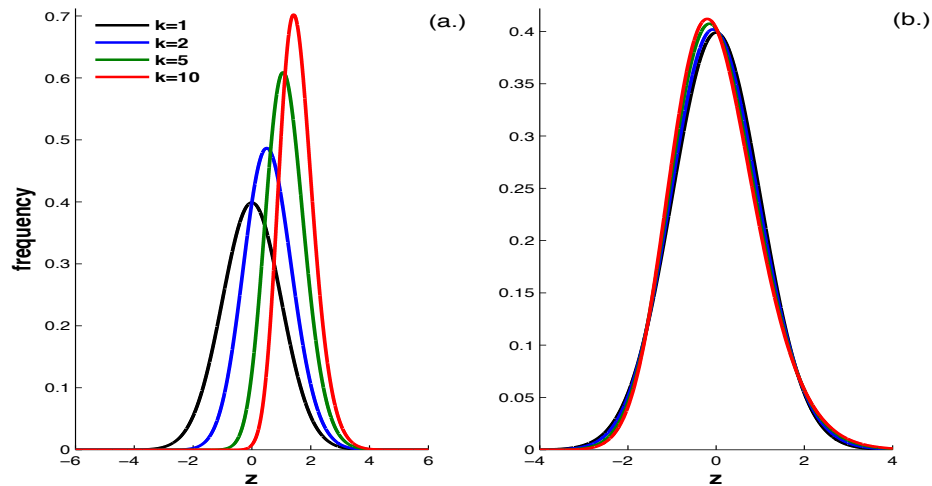


Figure 1: (a.) The distribution of the maximum of k standard Gaussian random variables, for different values of k . For $k = 1$ (black), the distribution is the standard Gaussian distribution. (b.) The (normalized) distribution of quantitative traits under the Limiting Pathway model $LP(k, h_{pathway}^2, 0)$ for different values of k . These are the same distributions as in (a.), scaled to have mean zero and variance one. For $k \leq 10$, the deviations are small and would not be taken as meaningful evidence of non-linearity. Even for somewhat larger k , human geneticists would tend to ignore the deviations or apply a modest transformation.

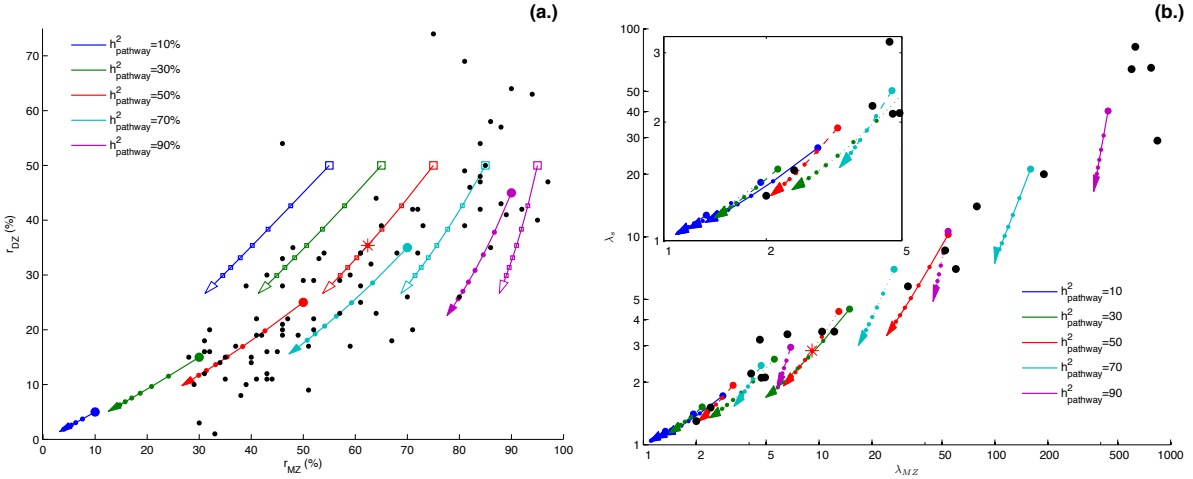


Figure 2: (a.) Phenotypic correlation of monozygotic twins (r_{MZ}) and dizygotic twins (r_{DZ}) for quantitative traits under the same LP models as in Fig. 1a (main text). The curves connect points with various values of k (1, 2, 3, 4, 5, 6, 7, 10 with the tip of the arrow corresponding to $k = 10$) for particular values of $h^2_{pathway}$ (10, 30, 50, 70 and 90%, indicated by color of the curve). Red star indicates the example referred to in the text. Black points show the values of (r_{MZ}, r_{DZ}) for 86 actual quantitative traits reported by Hill et al.⁹ (Supp. Table 6). Under a purely additive model with no shared environment, the expectation is $r_{DZ} = r_{MZ}/2$. The values under the LP models, including as a special case the additive model ($k = 1$), are largely similar to the values seen for the actual traits. (For raw data, see Supp. Table 7.) (b.) Relative risk to monozygotic twins (λ_{MZ}) and siblings (λ_s) for the same LP models as in Fig. 1b (main text). The curves connect points with various values of k (1, 2, 3, 4, 5, 6, 7, 10 with the tip of the arrow corresponding to $k = 10$) for particular values of $h^2_{pathway}$ (10, 30, 50, 70 and 90%, indicated by color of the curve) and prevalence (solid 0.1%, dotted 1%, dashed 10%). Red star indicates the example referred to in the text. Black points show the values of (λ_{MZ}, λ_s) for 15 actual diseases, reported by Wray et al.¹⁰ (Supp. Table 2). The values of (λ_{MZ}, λ_s) observed under the LP models show largely similar relationships to those observed for the actual traits. (Interestingly, the median value of λ_s observed for real diseases is $\sim 11\%$ smaller than the value expected under a strictly additive model, although the variance is large $\sim 32.3\%$.) Inset shows a zoomed-in view for $\lambda_{MZ} < 5$. (For raw data, see Supp. Table 2.)

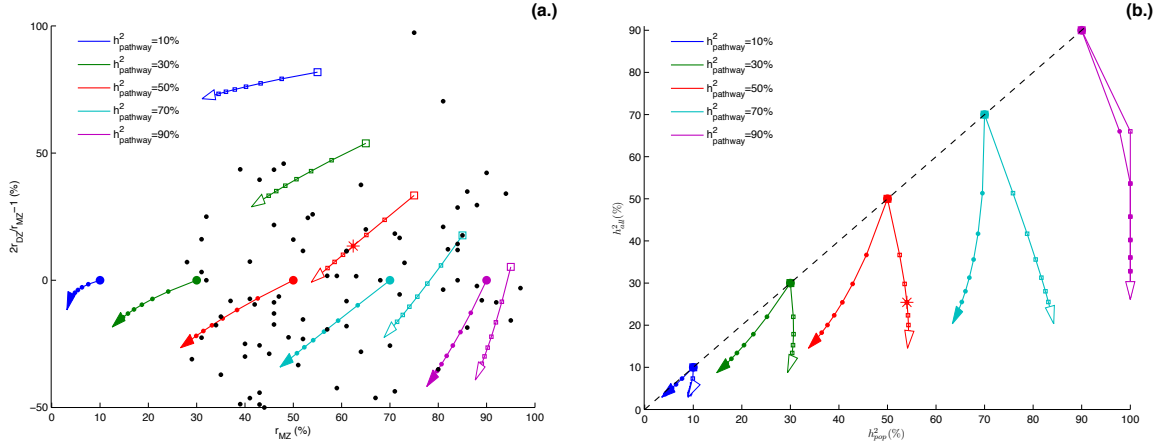


Figure 3: (a.) Deviation between the values of r_{DZ} observed under the Limiting Pathway model, and the values expected under the (incorrect) assumption that the trait follows an A_Δ model, for various parameters. The curves connect points with various values of k (1, 2, 3, 4, 5, 6, 7, 10, with the tip of the arrow corresponding to $k = 10$) for particular values of $h^2_{pathway}$ (10, 30, 50, 70 and 90%), indicated by color of the curve) and c_R (0% filled circles and arrows, 50% open boxes and arrows). Red star indicates the example referred to in the main text. The deviations are largely similar to the values seen for actual traits.

(b.) The apparent heritability h^2_{pop} (y-axis) plotted against the heritability h^2_{all} (x-axis), under the same Limiting Pathway models as in (a). For $k = 1$, the points lie on the diagonal dashed black line $h^2_{all} = h^2_{pop}$, indicating that the phantom heritability is zero. As k increases, the true heritability h^2_{all} drops rapidly, but the top-down estimate h^2_{pop} either decreases at a slower rate (for $c_R = 0\%$), or even increases ($c_R = 50\%$). In both cases the gap between the two quantities increases, resulting in an increase in phantom heritability.

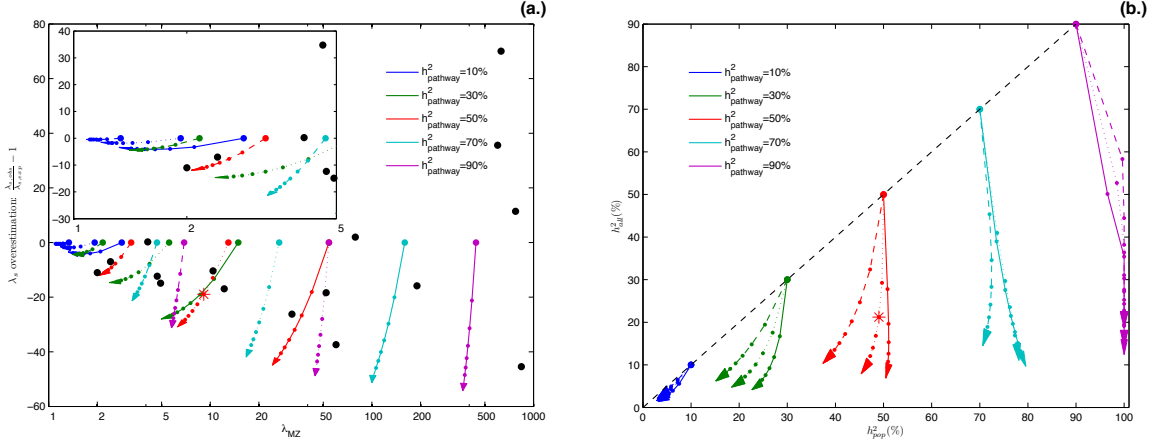


Figure 4: (a.) Deviation between the value of λ_s observed under the Limiting Pathway model and the value expected under the (incorrect) assumption that the trait follows an A_Δ model, for various parameters. The curves connect points with various values of k (1, 2, 3, 4, 5, 6, 7, 10) with the tip of the arrow corresponding to $k = 10$ for particular values of $h^2_{pathway}$ (10, 30, 50, 70 and 90%, indicated by color of the curve) and prevalence (solid 0.1%, dotted 1%, dashed 10%). We assume no shared environmental variance ($c_R = 0$). Red star indicates the example referred to in the main text. The deviations are largely similar to the values seen for actual traits, except for traits where the observed λ_s is much bigger than the expected λ_s .

(b.) The apparent heritability h^2_{pop} (y-axis) plotted against the true heritability h^2_{all} (x-axis) under the same Limiting Pathway models as in (a). For $k = 1$, the points lie on the diagonal dashed black line $h^2_{all} = h^2_{pop}$, indicating that the phantom heritability is zero. As k increases, the true heritability h^2_{all} drops rapidly, but the top-down estimate either decreases at a slower rate or even increases, depending on $h^2_{pathway}$ and μ . The gap between the two quantities increases, resulting in an increase in phantom heritability.

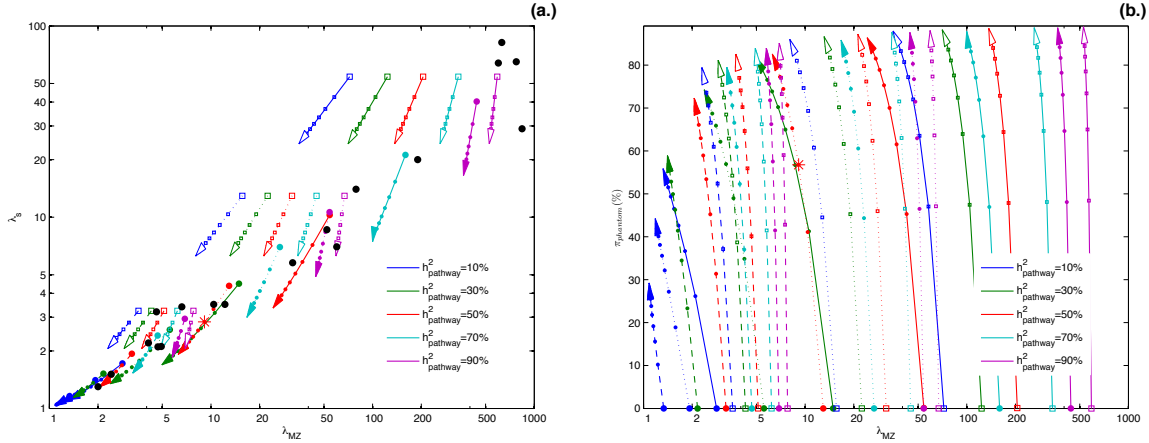


Figure 5: (a.) Relative risk to monozygotic twins (λ_{MZ}) and siblings (λ_s) for disease traits under the Limiting Pathway model $LP_\Delta(k, h_{pathway}^2, c_R, \mu)$ for various parameters. The curves connect points with various values of k (1, 2, 3, 4, 5, 6, 7, 10 with the tip of the arrow corresponding to $k = 10$) for particular values of $h_{pathway}^2$ (10, 30, 50, 70 and 90%, indicated by color of the curve), prevalence (solid 0.1%, dotted 1%, dashed 10%), and shared environment (0% filled circles and arrows, 50% open boxes and arrows). Red star indicates the example referred to in the main text. Black points show the values of $(\lambda_{MZ}, \lambda_s)$ for 15 actual diseases, reported by Wray et al.¹⁰ Supp. Fig. 2b includes only the case of no shared environment ($c_R = 0$). The inclusion of shared environment further increases λ_s relative to λ_{MZ} (and to the expected λ_s) and provides a better fit for some of the observed epidemiological parameters. (b.) Phantom heritability $\pi_{phantom}$ (y-axis) plotted against the monozygotic twin relative risk λ_{MZ} (x-axis) under the same Limiting Pathway models as in (a). The phantom heritability increases with k . Shared environment increases the monozygotic risk λ_{MZ} substantially, and also slightly increases the phantom heritability.

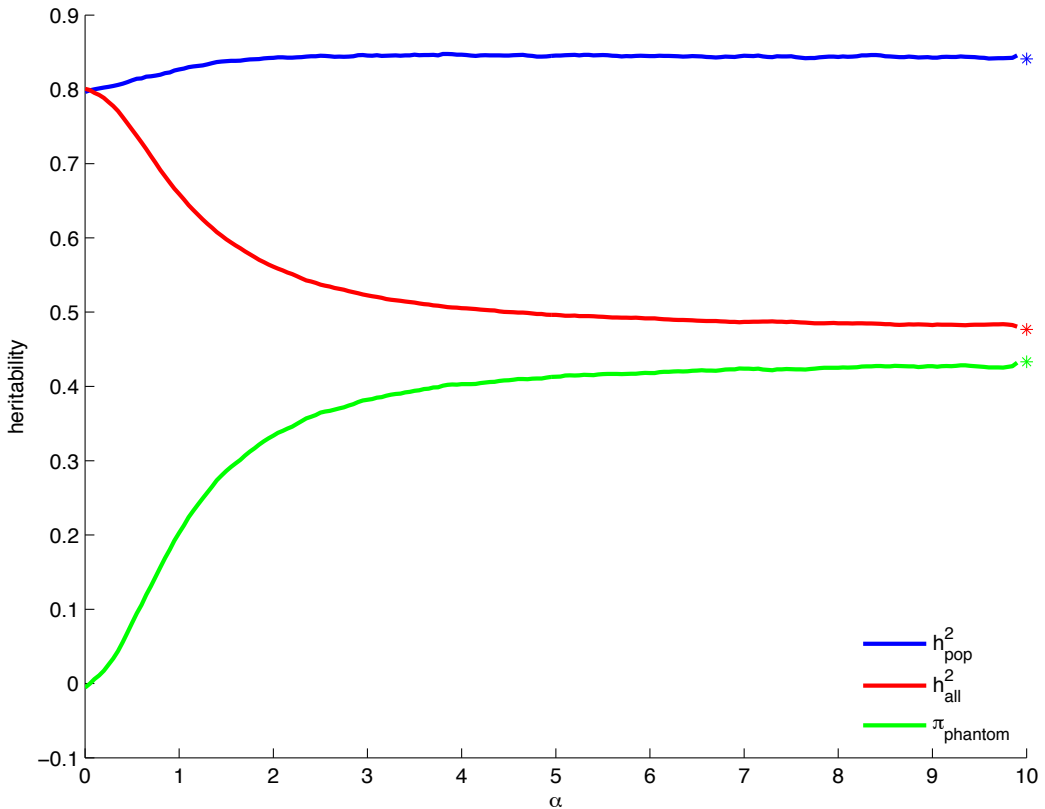


Figure 6: (a.) Heritability for the generalized LP model $\Psi = \log[\sum_i e^{\alpha\Psi^{(i)}}]$ for different values of α . Shown are the top-down heritability h_{pop}^2 (blue), bottom-up heritability h_{all}^2 (red), and the resulting phantom heritability $\pi_{phantom}$ (green) for α in the range $[0, 10]$, for a model with $k = 3$ pathways and $h_{pathway}^2 = 80\%$ heritability in each pathway. For each value of α , the heritabilities were computed by simulating 10^6 families and computing the familial correlation (for h_{pop}^2) and the correlation between genotypes and phenotypes (for h_{all}^2). For $\alpha \rightarrow 0$ the model is additive, with $h_{all}^2 = h_{pop}^2 = 80\%$ and $\pi_{phantom} = 0\%$. As α increases, the model becomes more and more non-linear and the phantom heritability increases. At $\alpha = 10$, the model is already very close to the LP model $LP(k = 3, h_{pathway}^2 = 80\%)$ (denoted in stars).

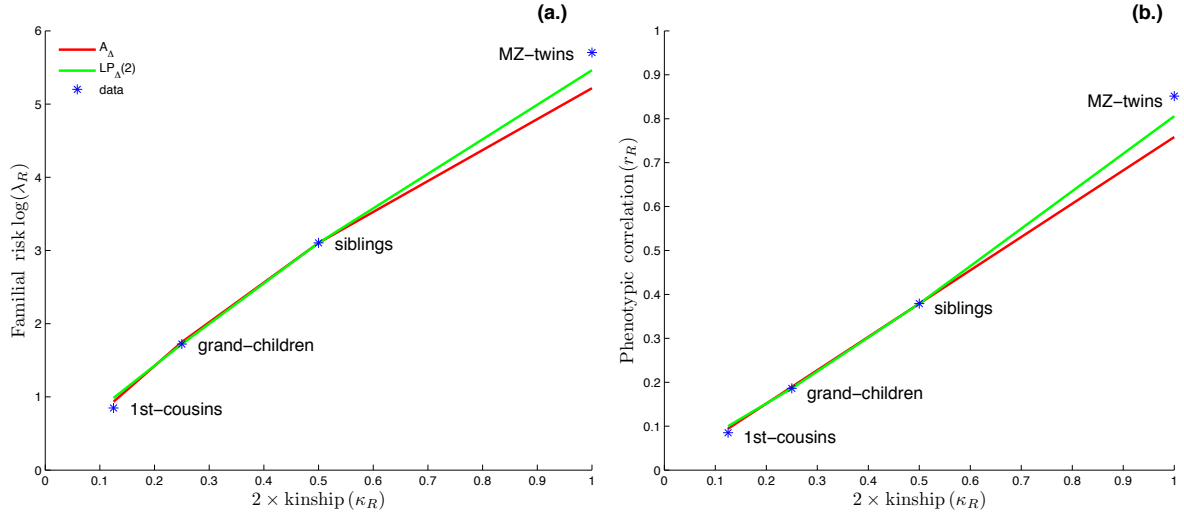


Figure 7: (a.) Curves show log of relative risk (λ_R) for schizophrenia to relatives of an affected individual, as a function of twice the kinship coefficient (κ_R) (for MZ twins, DZ twins, grandchildren and cousins). Blue stars show data from Risch et al.¹⁶ Red curve shows the fit to an additive A_Δ model. Green curve shows the fit to the $LP_\Delta(2)$ model. Both models provide similar fit to the empirical data. (b.) Curves are as in (a), except that the y-axis is correlation (r_R) among family members, as a function of twice the kinship coefficient (for MZ twins, DZ twins, grandchildren and cousins). To obtain the data, the relative risk (λ_R) was transformed to correlation the liability scale (r_R), by fitting a A_Δ model with prevalence $\mu = 0.85\%$ (see Supp. Table 5). Under the additive model, the correlations are proportional to the kinship - that is fall on a straight line (shown in red). The deviations from the red line for both the empirical data and the $LP_\Delta(2)$ model are small. While both the additive and non-additive models fit the data, the phantom heritability according the additive model is 0% and under the $LP_\Delta(2)$ model is large (46%).

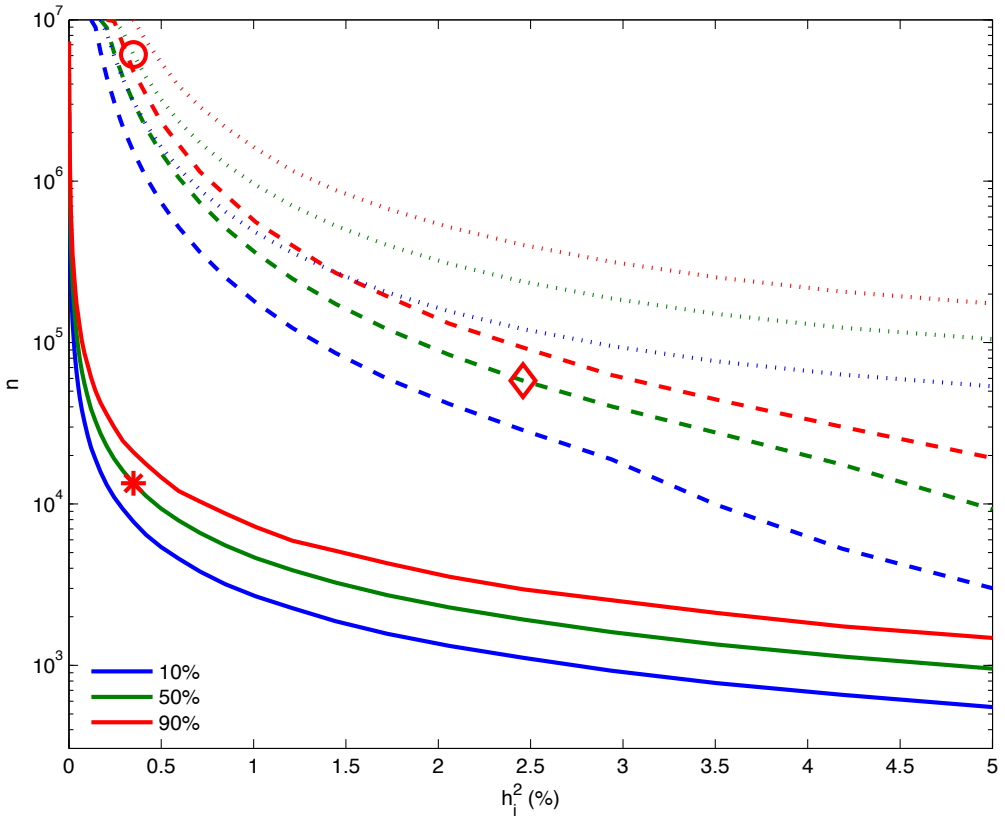


Figure 8: Curves show sample size required to detect individual loci (solid curves), pairwise interactions between two loci (dotted curves) and meta-interactions (dashed curves), at indicated power levels (10% (blue), 50% (green) and 90% (red)) for a disease with prevalence corresponding to the model LP_Δ ($k = 3, h_{pathway}^2 = 50\%, c_R, \mu = 0.01\%$). For the calculations here, each locus g_i is assumed to have minor allele frequency $f_i = 0.2$. For detecting individual loci, the x-axis refers to the fraction ϕ_i of the apparent heritability that a geneticist would attribute to a locus given the effect size η_i observed in a GWAS and the (incorrect) assumption that the trait follows an A_Δ model. (Specifically, the variance attributed to the locus is $h_i^2 = \beta_i^2 f_i(1 - f_i)$, and the fraction of the apparent heritability explained is $\phi_i = h_i^2/h_{pop}^2$). For detecting pairwise interactions, the x-axis refers to the fraction ϕ_i of the apparent heritability that would be attributed to each of the two loci being tested for interaction. For detecting meta-interactions between pathways, the x-axis refers to the fraction h_i^2 of the apparent heritability that would be attributed to a set of loci in each of two pathways (See Section 7 for a description of power calculations). Red star indicates the example referred to in the text. Compared to the sample size required to detect the individual loci, the sample size required to detect the pairwise interactions among the loci is roughly 8-fold larger. This is due to both the greater statistical power obtained by combining the signal from multiple loci, as well as to the lower burden of multiple hypothesis testing.

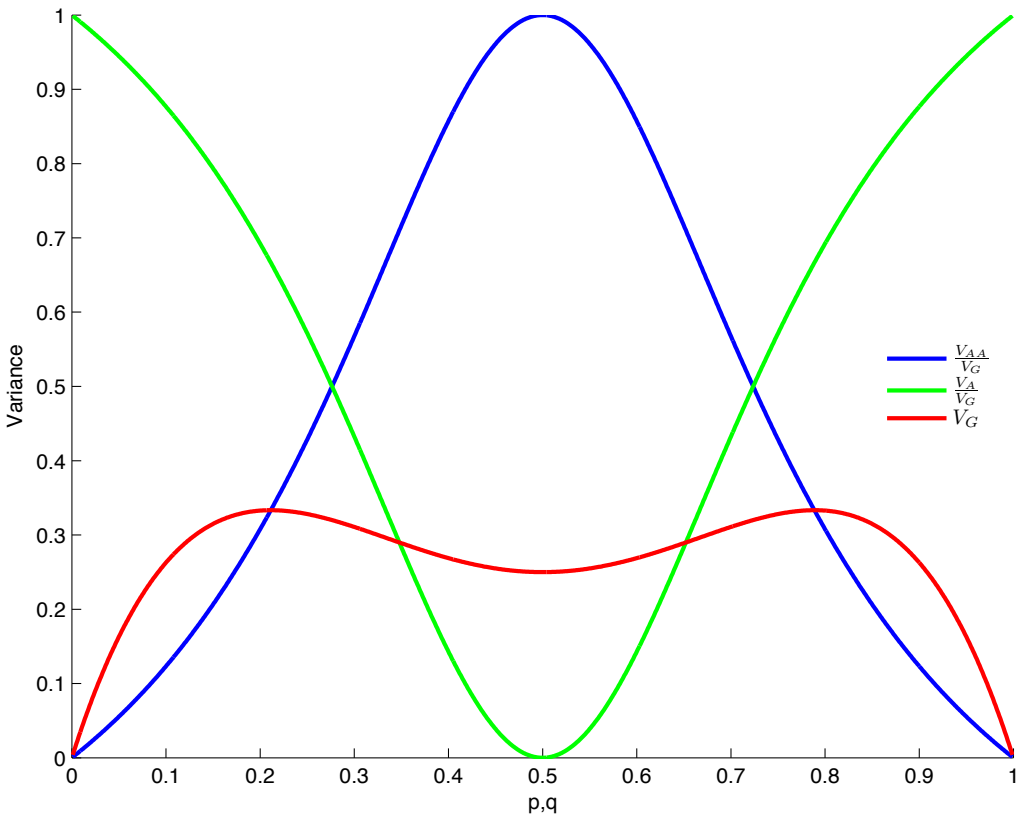


Figure 9: The graph shows the different variance components for a two-locus model from Hill et al.⁹ The model specifies the value of a quantitative trait as a function of genotype according to the following table (for some constant $c > 0$):

	AA	Aa	aa	
BB	$2c$	c	0	
Bb	c	c	c	
bb	0	c	$2c$	

(13.1)

The variance components for this model are plotted as a function of the allele frequencies, where we assume both variants have the same minor allele frequency, $Pr(a) = Pr(b) = p$. The curves show the total genetic variance V_G (red), the fraction of additive variance V_A/V_G (green) and the fraction of interaction variance V_{AA}/V_G (blue). As the allele frequency p approaches zero, the fraction of interaction variance, V_{AA}/V_G , approaches zero, but the total genetic variance V_G also approaches zero and the trait becomes a rare trait.

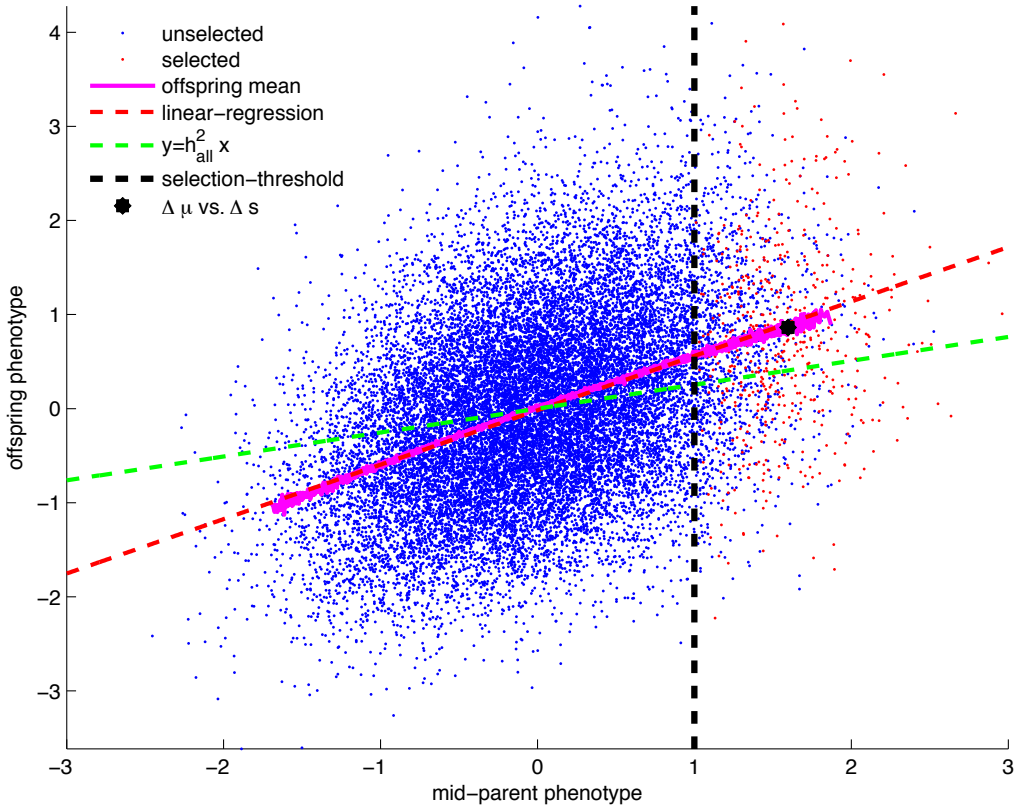


Figure 10: The graph shows the relation between the response to selection, $\frac{\Delta\mu}{\Delta s}$, and the apparent heritability $h_{pop}^2(PO)$. We studied the $P^* = LP(4, 50\%, 50\%)$ model, for which the true narrow sense heritability is $h_{all}^2 = 25.4\%$ and the population estimate $h_{pop}^2(PO) = 70.8\%$. For 50,000 simulated trios we plotted the mid-parent phenotype (x-axis) vs. offspring phenotype (y-axis). Blue points represent unselected trios. Red points represent selected trios. Parents were required to have phenotype ≥ 1 to reproduce (dashed vertical black line denotes mid-parent value = 1). Not all points with mid-parent value ≥ 1 are selected (red), since selection requires *both* parent's phenotype to exceed the threshold (not merely their average). The magenta curve shows, for each value of the mid-parent phenotype (x-axis), the mean value of the offspring phenotype (y-axis). The mean value of the offspring phenotype is roughly linearly proportional to the mid-parent phenotype, as can be seen by comparing it to the linear regression line over all points (dashed red). The black star denotes the average mid-parent phenotype in the selected parents (Δs) vs. the expected offspring phenotype for these parents ($\Delta\mu$). It is obtained by averaging over all values of parent phenotypes above the threshold 1. Since the black star lies roughly on the line connecting mid-parent phenotype and expected offspring phenotype, the value $\frac{\Delta s}{\Delta\mu}$ (the response to selection) is roughly equal to the slope of this line ($h_{pop}^2(PO)$). Both values exceed h_{all}^2 , as can be seen by plotting the line $y = h_{all}^2 x$ (shown in dashed green), which has a lower slope.

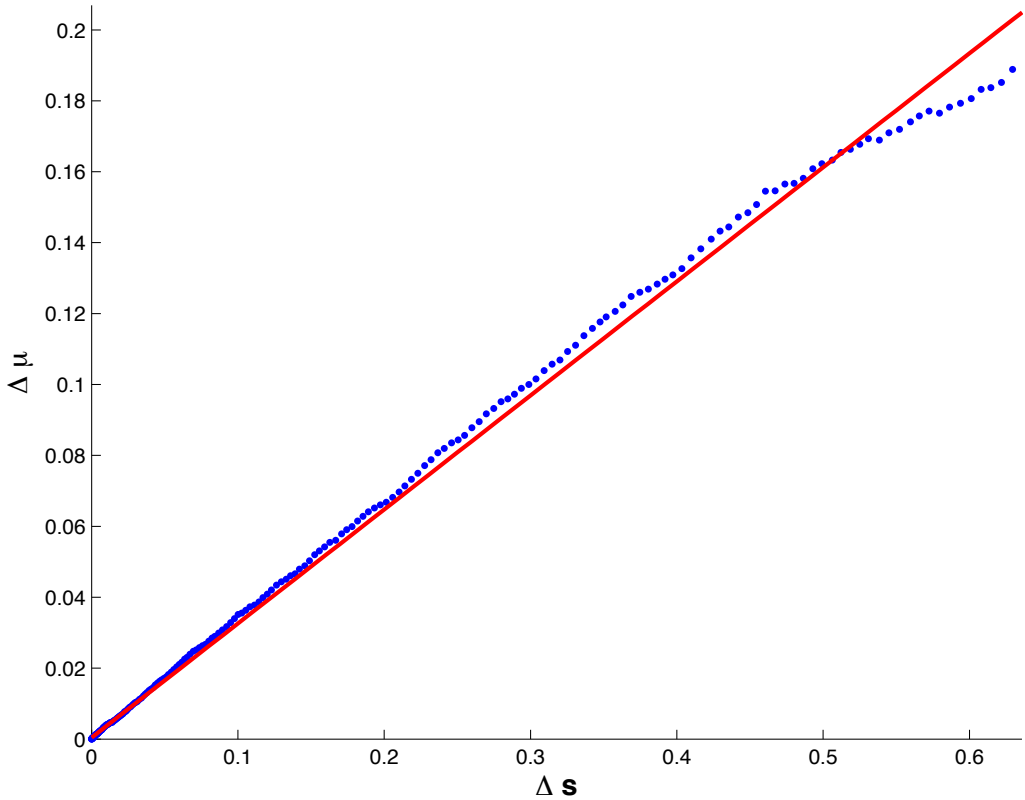


Figure 11: The graph shows how the average phenotypic deviation in a set of selected parents (x-axis) corresponds to the average phenotypic deviation in the resulting offspring. We studied the $LP(4, 50\%, 50\%)$ model, for which the true narrow sense heritability is $h_{all}^2 = 25.4\%$ and the apparent heritability based on parent-offspring calculation $h_{pop}^2(PO) = 70.8\%$. Selection was performed by taking the parents to be individuals with phenotype $Z > \tau$, for a given threshold τ , and then simulating 50,000 parent-offspring trios. For various thresholds τ , we calculated: the value of Δs , the average value of $\Delta \mu$ across the offspring and the average ratio $\frac{\Delta \mu}{\Delta s}$ (by regressing $\Delta \mu$ on Δs .) We repeated the simulation 100 times, to find average regression coefficient as an estimator for heritability. The mean slope of the regression line is ~ 0.071 , which is very close to $h_{pop}^2(PO)$. Thus, the breeder's equation $\frac{\Delta \mu}{\Delta s} = h_{pop}^2(PO)$ still holds to a good approximation, even though the trait is highly non-additive.

14 Supplementary tables

Table 6: The table shows reported values of r_{MZ} and r_{DZ} for different traits. Under an additive model with no shared environment we expect $r_{MZ} - 2r_{DZ} = 0$. While observed values of $r_{MZ} - 2r_{DZ}$ have a median around zero, they display wide deviations.

Trait	$r_{MZ}(\%)$	$r_{DZ}(\%)$	$r_{MZ} - 2r_{DZ}(\%)$
Age at first reproduction	39	28	-17
Age at menarche	51	17	17
Age at menopause	52	29	-6
Airway histamine responsiveness	63	32	-1
Alanine aminotransferase	49	19	10
Alcohol consumption	68	34	1
Alcohol dependence	61	34	-6
ApoE	61	28	5
Aspartate aminotransferase	32	16	0
Birth weight	75	74	-73
Blood: CD4/CD8 ratio	85	50	-15
Blood: Lymphocytes	72	42	-12
Blood: Mean corpuscular volume	97	47	3
Blood: Platelets	82	46	-11
Blood: White blood cells	71	42	-14
BMI, age 20-29	70	26	18
BMI, age 30-39	73	39	-4
Cannabis dependence	64	44	-25
Carabelli trait in teeth (right side)	89	41	6
Chronic pelvic pain	43	11	21
Cloninger: Harm avoidance	44	11	21
Cloninger: Novelty seeking	41	11	18
Cloninger: Persistence	35	11	13
Cloninger: Reward dependence	38	8	22
Coffee consumption	52	20	12
DSVIV Major depressive disorder	31	12	6
Depth of sleep	33	1	31
Diastolic blood pressure	53	33	-13
Disordered eating in women (Wave 2)	29	10	9
Endometriosis	46	28	-10
Eosinophils	59	17	25
Exercise participation	46	21	5
Fainting because of blood	43	30	-16
Fainting non-blood	46	54	-63
Fatigue	43	16	11
Fear of blood	71	20	31
Female orgasm	31	16	-1
Finger ridge count	95	40	15
Fitness	42	19	4
Forced expiratory volume	90	64	-38
Haemoglobin age 12	84	54	-24
Hay fever	61	25	10
Height (clinically measured)	92	42	7
IQ	84	47	-10
Immunoglobulin E	67	18	31

Table 6: Epidemiological parameters for a list of quantitative traits. (Source: Hill et al.⁹) (cont.)

Trait	r_{MZ} (%)	r_{DZ} (%)	$r_{MZ} - 2r_{DZ}$ (%)
Incisor dimension: Lower-right-2	84	42	0
Incisor dimension: Upper-left-1	88	43	2
Individual Alpha frequency (EEG)	86	35	16
Inspection Time	41	19	3
Insulin concentration	32	20	-8
Liability to appendectomy	48	35	-23
Liability to asthma	64	23	18
Liability to tonsillectomy: Cohort 1	86	58	-29
Male baldness	81	39	3
Melanocytic naevi size (area)	65	39	-12
Mouth ulcers	57	29	-1
Neuroticism	37	17	3
Neuroticism	40	14	12
Nevus (mole) count	94	63	-32
Osteoarthritis in women	41	22	-3
Parietal P300 latency	47	22	3
Parietal slow wave amplitude	46	33	-20
Performance IQ	72	34	5
Prefrontal P300 latency	46	19	8
Prefrontal slow wave amplitude	40	15	10
Premature parturition for any birth	30	3	24
Premenstrual Symptoms (factor score)	45	16	13
Psychosis proneness Scale 1	34	14	6
Psychosis proneness Scale 2	28	15	-2
Psychosis proneness Scale 3	51	9	33
Psychosis proneness Scale 4	39	10	19
Quality of sleep	31	18	-4
Red blood cell folate	46	20	6
Red cell count age 12	88	57	-25
Serum dehydroepiandrosterone sulfate	59	30	0
Serum gamma-glutamyltransferase	52	22	9
Smoking initiation (younger cohort)	84	48	-13
Stuttering	43	12	19
Susceptibility to Migraine	35	15	5
Systolic blood pressure	57	23	11
Tea consumption	50	29	-9
Teenage acne severity, age 14	80	26	28
Total cholesterol	61	34	-7
Triglycerides	54	34	-14
Verbal IQ	81	49	-18
Voting behavior	81	69	-57

Table 7:

For each choice of the model parameters (k , $h_{pathway}^2$ and c_R) we calculated relevant genetic and population parameters.

- V_c is the fraction of total *phenotypic* variance for the trait attributable to shared environment. (Recall that c_R is the fraction of the *environmental* variance for each pathway attributable to shared environment.)
- r_{MZ} and r_{DZ} are the monozygotic and dizygotic twin correlations in phenotype, respectively.
- h_{all}^2 is the true narrow sense heritability (fraction of phenotypic variance explained by an additive model including all genetic variants).
- $h_{pop}^2(ACE)$, $h_{pop}^2(ADE)$ and $h_{pop}^2(PO)$ are the apparent heritabilities calculated using the three population estimators (See Section 1).
- $\pi_{phan}(ACE)$, $\pi_{phan}(ADE)$ and $\pi_{phan}(PO)$ are the missing heritabilities associated with each of the apparent heritabilities. (See Section 1).

Table 7: Model parameters for the LP model $LP(k, h_{pathway}^2, c_R)$ for quantitative traits. (cont.)

k	$h_{path}^2(\%)$	$c_R(\%)$	$r_{MZ}(\%)$	$r_{DZ}(\%)$	$h_{all}^2(\%)$	$V_c(\%)$	$h_{pop}^{2(ACE)}(\%)$	$\pi_{phan}^{(ACE)}(\%)$	$h_{pop}^{2(ADE)}(\%)$	$\pi_{phan}^{(ADE)}(\%)$	$h_{pop}^{2(PO)}(\%)$	$\pi_{phan}^{(PO)}(\%)$
10	10	0	3.1	1.4	2.9	0.0	3.5	17.1	2.4	0.0	2.8	0.0
10	30	0	12.5	5.1	8.7	0.0	14.8	41.2	7.9	0.0	10.2	14.8
10	50	0	26.6	9.8	14.5	0.0	33.7	56.9	12.5	0.0	19.6	25.8
10	70	0	47.2	15.6	20.3	0.0	63.4	67.9	15.0	0.0	31.1	34.7
10	90	0	77.6	22.6	26.1	0.0	100.0	76.2	12.8	0.0	45.2	42.1
10	10	25	14.0	11.1	2.9	10.9	5.8	49.6	30.5	90.5	22.2	86.9
10	30	25	24.6	14.0	8.7	12.0	21.1	58.8	31.4	72.3	28.0	68.9
10	50	25	38.6	17.2	14.5	12.0	42.8	66.1	30.1	51.8	34.4	57.8
10	70	25	57.2	20.7	20.3	10.0	73.0	72.1	25.6	20.7	41.4	50.9
10	90	25	82.5	24.6	26.1	4.8	100.0	77.4	15.8	0.0	49.1	46.8
10	10	50	31.1	26.6	2.9	28.0	8.9	67.4	75.5	96.2	53.3	94.6
10	30	50	41.3	26.6	8.7	28.8	29.4	70.4	65.2	86.6	53.3	83.7
10	50	50	53.7	26.6	14.5	27.1	54.1	73.2	52.9	72.5	53.3	72.8
10	70	50	68.8	26.6	20.3	21.5	84.2	75.9	37.8	46.3	53.3	61.9
10	90	50	87.7	26.6	26.1	10.1	100.0	78.6	18.9	0.0	53.3	51.0
10	10	75	57.2	50.4	2.9	54.0	13.6	78.6	100.0	98.0	100.0	97.1
10	30	75	64.7	44.2	8.7	52.2	41.0	78.7	100.0	92.2	88.4	90.1
10	50	75	73.1	38.6	14.5	46.4	68.9	78.9	81.4	82.2	77.2	81.2
10	70	75	82.5	33.5	20.3	35.2	97.9	79.2	51.5	60.5	67.0	69.6
10	90	75	93.3	28.8	26.1	15.7	100.0	79.7	22.0	0.0	57.6	54.7

Table 8:

For each choice of the model parameters (k , $h_{pathway}^2$, c_R and μ), we calculated relevant genetic and population parameters.

- V_c is the fraction of total *phenotypic* variance for the trait attributable to shared environment. (Recall that c_R is the fraction of the *environmental* variance for each pathway attributable to shared environment.)
- λ_{MZ} and λ_s are the monozygotic twin and sibling relative risks for disease, respectively.
- h_{all}^2 is the true narrow-sense heritability (fraction of phenotypic variance explained by an additive model including all genetic variants) on the liability scale.
- $h_{pop}^{2(ACE)}$, $h_{pop}^{2(ADE)}$ and $h_{pop}^{2(PO)}$ are the apparent heritabilities on the liability scale, calculated using these estimators. (See Section 1).
- $\pi_{phan}^{(ACE)}$, $\pi_{phan}^{(ADE)}$ and $\pi_{phan}^{(PO)}$ are the missing heritabilities associated with each of the apparent heritabilities. (See Section 1).

Table 9:

For each of the 74 loci associated with Crohn's disease, we display the reported SNP-ID, nearest gene reported, Risk-Allele-Frequency (RAF) and Genetic-Relative-Risk (GRR).

- $V_i(\%)$ is the fraction of variance explained (on the liability scale).
- $h_{all}^2 \text{expl.}(A_\Delta)$ is the fraction of the true narrow sense heritability explained under the additive A_Δ model
- $h_{all}^2 \text{expl.}(LP_\Delta)$ is the fraction of the true narrow sense heritability explained under the alternative $LP_\Delta(3)$ model.
- Pathway denotes are random assignment of the known SNPs to the three notional pathways in the $LP_\Delta(3)$ model. Different pathway assignments did not affect the heritability results.

Table 9: Assumed and actual variance explained by associated SNPs for Crohn's disease. (Source: Franke et al.¹¹). Epidemiological Parameters: $\mu = 0.2\%$, $h_{pop}^2 = 83\%$, $\lambda_{MZ} = 250$, $\lambda_s = 35$. (cont.)

#	SNP-ID	Gene	RAF	GRR	$V_i(\%)$	$\%h_{all}^2$ expl. (A_Δ)	$\%h_{all}^2$ expl. (LP_Δ)	Pathway
51	rs10495903	THADA	0.13	1.14	0.04	0.05	0.13	3
52	rs2062305	TNFSF11	0.35	1.10	0.04	0.05	0.13	3
53	rs7423615	SP140	0.19	1.12	0.04	0.04	0.13	3
54	rs694739	PRDX5	0.63	1.10	0.04	0.04	0.13	2
55	rs17309827	C6orf85	0.64	1.10	0.04	0.04	0.12	1
56	rs3024505	IL10	0.16	1.12	0.03	0.04	0.11	1
57	rs181359	YDJC	0.20	1.10	0.03	0.03	0.09	3
58	rs713875	MTMR3	0.47	1.08	0.03	0.03	0.09	2
59	rs359457	CPEB4	0.57	1.08	0.03	0.03	0.09	1
60	rs102275	FADS1	0.34	1.08	0.02	0.03	0.08	1
61	rs13073817		0.32	1.08	0.02	0.03	0.08	3
62	rs12722489	IL2RA	0.85	1.11	0.02	0.03	0.08	1
63	rs281379	FUT2	0.49	1.07	0.02	0.02	0.07	1
64	rs151181	APOB48R	0.39	1.07	0.02	0.02	0.07	2
65	rs4902642	ZFP36L1	0.58	1.07	0.02	0.02	0.07	3
66	rs12720356	TYK2	0.08	1.12	0.02	0.02	0.07	3
67	rs1847472	BACH2	0.66	1.07	0.02	0.02	0.06	1
68	rs6738825	PLCL1	0.47	1.06	0.01	0.02	0.05	1
69	rs736289		0.61	1.06	0.01	0.02	0.05	3
70	rs13428812	DNMT3A	0.33	1.06	0.01	0.02	0.05	1
71	rs2549794	ERAP2	0.41	1.05	0.01	0.01	0.04	2
72	rs11167764	NDFIP1	0.80	1.06	0.01	0.01	0.03	2
73	rs2797685	VAMP3	0.19	1.05	0.01	0.01	0.02	3
74	rs1998598	DENND1B	0.30	1.04	0.01	0.01	0.02	1
Total (%):					10.8	21.5	57.5	